2016

Temporal Dynamics Of The Skin Microbiome In Disease

Michael Austin Loesche
University of Pennsylvania, loesche@upenn.edu

Temporal Dynamics Of The Skin Microbiome In Disease

Abstract

The skin is colonized by communities of bacteria, fungi, and viruses, collectively referred to as the skin microbiome. These microbial communities are shaped by the topology and diseases of the skin. Dysbiosis of the cutaneous microbiome has been associated with several ailments of the skin including atopic dermatitis, acne, rosacea, psoriasis, and chronic wounds. However, our understandings of the processes by which these microbes initiate, maintain, or modulate skin diseases is lacking. Moreover, previous research on the topic has largely been limited by cross-sectional study designs, neglecting the natural dynamism of microbial communities. Here we present a comprehensive analysis of the temporal dynamics of the skin microbiome in various diseases. In the first section, we characterize the diversity and dynamics of both bacterial and fungal communities colonizing chronic wounds and its associations with clinical outcomes. In a study of 100 subjects with diabetic foot ulcers, we sampled the wound microbiota in 2-week intervals until healing, amputation of 26 weeks of follow-up. We demonstrate the high levels of community instability in chronic wounds and expose the positive association between wound healing community instability. We also reveal the effect of antibiotic perturbation on the microbiota. The fungal component was found to have associations with various bacteria and clinical outcomes. Our results should inform the design of future studies and provides evidence that microbial dynamics may be an effective biomarker for identifying high-risk ulcers. The second section investigates the body-site specific effects of psoriasis on the skin microbiome and how it responds to therapy. We reveal these patterns in a study of 114 subjects, across 6 body sites, and over 112 weeks of follow-up. The effect of psoriatic lesions was found to be mild and body-site specific. In contrast, ustekinumab treatment was found to induce moderate shifts in microbial composition, including an increase in atypical skin bacteria and inter-individual heterogeneity. These results suggest that the effect of psoriasis lesions is secondary to the effect the broad effects of the immune environment. Together the work presented in this thesis represents a significant advancement in our understanding of the microbial dynamics of the skin and their associations with human health.

Degree Type
Dissertation

Degree Name
Doctor of Philosophy (PhD)

Graduate Group
Cell & Molecular Biology

First Advisor
Elizabeth A. Grice

Second Advisor
Frederic D. Bushman

Keywords

Chronic Wounds, Foot Ulcer, Microbiology, Microbiome, Psoriasis, Skin

Subject Categories

Microbiology

TEMPORAL DYNAMICS OF THE SKIN MICROBIOME IN DISEASE

Michael Austin Loesche

A DISSERTATION

in

Cell and Molecular Biology

Presented to the Faculties of the University of Pennsylvania

in

Partial Fulfillment of the Requirements for the

Degree of Doctor of Philosophy

2016

Supervisor of Dissertation

_____
Elizabeth A. Grice, PhD
Assistant Professor in Dermatology

Co-Supervisor of Dissertation

_____
Frederic D. Bushman, PhD
William Maul Measey Professor
in Microbiology

Graduate Group Chairperson

_____
Daniel S. Kessler
Associate Professor of Cell and
Developmental Biology

Dissertation Committee

Aimee Payne, MD, PhD
Albert M. Kligman Associate
Professor of Dermatology

David Margolis, MD, PhD
Professor of Dermatology

Phillip Scott, PhD
Professor of Microbiology and
Immunulogy

Hongzhe Li, PhD
Professor of Biostatistics and
Statistics

DEDICATION

For my mentor Elizabeth Grice, members of Club Grice, my family, and friends… and Texas.

ACKNOWLEDGMENT

ABSTRACT

TEMPORAL DYNAMICS OF THE SKIN MICROBIOME IN DISEASE

Michael A Loesche

Elizabeth A Grice, PhD

The skin is colonized by communities of bacteria, fungi, and viruses, collectively referred to as the skin microbiome. These microbial communities are shaped by the topology and diseases of the skin. Dysbiosis of the cutaneous microbiome has been associated with several ailments of the skin including atopic dermatitis, acne, rosacea, psoriasis, and chronic wounds. However, our understandings of the processes by which these microbes initiate, maintain, or modulate skin diseases is lacking. Moreover, previous research on the topic has largely been limited by cross-sectional study designs, neglecting the natural dynamism of microbial communities. Here we present a comprehensive analysis of the temporal dynamics of the skin microbiome in various diseases. In the first section, we characterize the diversity and dynamics of both bacterial and fungal communities colonizing chronic wounds and its associations with clinical outcomes. In a study of 100 subjects with diabetic foot ulcers, we sampled the wound microbiota in 2-week intervals until healing, amputation of 26 weeks of follow-up. We demonstrate the high levels of community instability in chronic wounds and expose the positive association between wound healing community instability. We also reveal the effect of antibiotic perturbation on the microbiota. The fungal component was found to have associations with various bacteria and clinical outcomes. Our results should inform the design of future studies and provides evidence that microbial dynamics may be an effective biomarker for identifying high-risk ulcers. The

second section investigates the body-site specific effects of psoriasis on the skin microbiome and how it responds to therapy. We reveal these patterns in a study of 114 subjects, across 6 body sites, and over 112 weeks of follow-up. The effect of psoriatic lesions was found to be mild and body-site specific. In contrast, ustekinumab treatment was found to induce moderate shifts in microbial composition, including an increase in atypical skin bacteria and inter-individual heterogeneity. These results suggest that the effect of psoriasis lesions is secondary to the effect the broad effects of the immune environment. Together the work presented in this thesis represents a significant advancement in our understanding of the microbial dynamics of the skin and their associations with human health.

TABLE OF CONTENTS

LIST OF TABLES

LIST OF FIGURES

xi

1.1 From Microscopes to Microbiomes

It was advancements in the field of microscopy that led to the discovery of bacteria and other microbes inhabiting our world in 1676 by Antonie van Leeuwenhoek (Dobell 1960), ushering in an era of awe and fascination with the microscopic world that persists to this day. It did not take long before many noticed large discrepancies between numbers of bacteria visible under a microscope and the number of colonies they could culture on a plate. In some cases the difference between the two was several orders of magnitude, a phenomenon known as the *great plate count anomaly* (Staley & Konopka 1985). Bacteria, such as *E. coli,* that are easily cultured have fueled decades of discovery in genetics, molecular biology, and modern medicine. However, the fastidious and oligotrophic bacteria that have eluded being cultured greatly outnumber those that have. It is now estimated that 95-99% of bacteria are not readily culturable, though focused efforts to improve culturing surveys are changing this number (Browne et al. 2016).

It was the development of next-generation sequencing technology that facilitated the study of entire microbial communities or *microbiomes*, overcoming the biases and limitations of culturing techniques. The term microbiome refers to the community of bacteria, fungi, viruses and other microbes occupying an ecological niche. Microbiome studies have revealed rich and complex communities inhabiting nearly all surfaces of the environment, including the human body (Gevers et al. 2012). They have led to significant increases in our understanding of microbial ecology, host-microbe interactions, and microbe-microbe interactions. To manage the massive amounts of data generated by microbiome studies, the field of microbiology has become the recipient of a rapid infusion of bioinformatics and computational biology. The rich data sets

have also attracted inter-disciplinary collaborations resulting in the adoption of theories and methodologies from many fields including ecology, multivariate statistical modeling, machine-learning, evolution, phylogenetics, and network analysis.

The study of the world's microbiomes is still in its infancy, though rapid progress is being made. Studies characterizing microbial communities and documenting ecological phenomenon are being published at an ever-increasing rate. Standards for sample collection, processing, and analysis are beginning to become formalized; and tools to manipulate the microbiome, experimentally and medically, are being developed. After more than a century of mechanistic and hypothesis driven work, microbiology has returned to the stage of observation. Like the naturalists of the past, we have been give a new lens to discover a world previously unknown.

1.2 The Human Microbiome

The human microbiome is the collection of ecological communities of bacteria, fungi, viruses, and other microbes that colonize our bodies. The commensal bacteria perform a variety of beneficial roles including immune system education, vitamin production, and protection form invading pathogens. They inhabit nearly every surface of the human body exposed to the external environment including the skin, gut, vagina, oral cavity, and even the upper airways of the lung (Grice & Segre 2012; Charlson et al. 2012). While some constituents are conserved, the structure, composition, and biomass of the human microbiome vary greatly between body sites and are exquisitely sensitive to variation in their microenvironment. As such, the microbiome often

reflects the health of its host, and in many cases may be a driving factor in the initiation or persistence of disease (Cho & Blaser 2012).

The complexity of human-microbe interactions is staggering in its breath and depth. Even the bacterial component alone, by far the best studied, is unfathomable in its scale. The average human body is composed of 30 trillion cells, but it is colonized by approximately 39 trillion bacterial cells (Sender et al. 2016). These commensal bacteria interact with their human host via a wealth of secreted compounds, metabolites, antigens, and occasionally toxins. They also interact with each other by competing for nutrients, producing antibiotics and bacteriocins, facilitating horizontal gene transfer, and myriad other antagonistic and mutualistic interactions. Nowhere is this more apparent than in the gut, where the microbiome has been shown to contribute to disease, modulate physiologic responses to diet, and provide protection from invading pathogens (Shreiner et al. 2015). There is mounting evidence for the role of the gut microbiome in inflammatory bowel diseases (Morgan et al. 2012), coronary artery disease (Koeth et al. 2013), obesity (Turnbaugh et al. 2006), insulin resistance (Suez et al. 2014), depression (Foster & McVey Neufeld 2013), hepatic encephalopathy (Bajaj et al. 2012), and differential drug absorption (Clayton et al. 2009). Moreover, it is well established that antibiotic perturbations of the gut microbiota leads to *dysbiotic* states (Modi et al. 2014), which increase the risk of developing *Clostridium difficile* infections (Buffie et al. 2014), which can be successfully treated with fecal microbiota transplantation (Kassam et al. 2013).

The centrality of the gut microbiome in many ailments has raised the possibility that the microbiome of other body sites may hold similar promise as driving determinants of health and disease. Indeed studies of the human microbiome across the body have borne out this belief.

Alterations in the vaginal microbiome have been linked to bacterial vaginosis (Mayer et al. 2015), chronic yeast infections (Liu et al. 2013), and preterm delivery (DiGiulio et al. 2015). The oral microbiome may contribute to periodontal disease and dental caries (Wade 2013). Even the lung, which is generally thought to be a sterile site, has been shown to have a microbiome that can reflect the immunity status of its host (Charlson et al. 2012; Wang et al. 2016; Young et al. 2014; Quinn et al. 2014).

Seminal work put forth by Grice *et al* characterized the healthy skin microbiome and how it varies spatially across the body(Grice et al. 2009). Subsequent studies have since linked dysbiosis of the skin microbiome with psoriasis (Takemoto et al. 2014; Alekseyenko et al. 2013; Ganju et al. 2016), chronic wounds (Grice et al. 2010; Gardner et al. 2013), acne (Fitz-Gibbon et al. 2013), and atopic dermatitis (Kong et al. 2012); however, whether the skin microbiome plays a causative or reactive role remains to be established. The majority of these studies implemented cross-sectional study designs, and those with longitudinal analyses have been limited by sample number. Consequently, the temporal dynamics of the skin microbiome in disease are poorly understood and may yield better understanding and potential therapeutic targets for diseases of the skin. The work presented here endeavors to advance our understanding in this regard by characterizing the microbial dynamics of chronic wounds and psoriasis and their associations with clinically meaningful outcomes.

1.3 Microbiome Workflow

Microbiome studies can be broadly classified into metataxonomic and metagenomic analyses. Metataxonomic studies, the focus of this work, involve the sequencing of evolutionarily

conserved marker genes, which serve as a proxy for taxonomic classification. The 16S rRNA gene has been extensively used to characterize prokaryotic communities, whereas the 18S rRNA gene and the internal transcribed spacer (ITS) regions are used for fungal communities. Bacteriophage and other viruses do not possess universally conserved genes, making metataxonomic analyses impossible to perform. These marker genes contain conserved and hypervariable regions, which allow for universal primer annealing and taxonomic classification respectively. The 16S rRNA gene is approximately 1.5 kilobases in length and contains 9 hypervariable regions, denoted V1 through V9. Because of the current limitations in sequence lengths generated by next-generation sequencing technologies, specific sub-regions must be chosen for amplification and sequencing. The most commonly used sub-regions are V1-V3 and V4, however, resident evidence suggests that the V1-V3 region introduces less bias for skin communities (Meisel et al. 2016). In contrast, metagenomic studies involve shotgun sequencing the combined genomic content of the entire community. Metagenomic studies provide both a taxonomic and functional perspective of the community, but require much greater sequencing depth, computational resources, and controlling for human contamination.

Metaxonomic studies begin with the aggregation of similar sequences into clusters, termed *operational taxonomic units* (OTU), which serve as proxies for species (Kopylova et al. 2016). OTUs are taxonomically identified and are then used to estimate *alpha* and *beta* diversity by a variety of metrics. Alpha metrics measure the diversity intrinsic to a sample by quantifying the richness (number of observed OTUs) and evenness of the community. Beta metrics measure the amount of shared diversity between samples. Diversity metrics differ in how abundance or phylogenetic relationships are weighted, which reveal different components of the community structure. While there is considerable diversity in specific algorithms or metrics applied, the

popular adoption of software packages such as QIIME and MOTHUR has partially standardized these analyses (Caporaso et al. 2010; Schloss et al. 2009).

1.4 The Structure and Function of Human Skin

The skin is one of the most exposed organs of the body and serves a critical role as the primary interface between the external environment and the underlying tissues. The skin provides a barrier against constant physical, chemical, and immunological insults. It also performs key homeostatic functions in regulating body temperature, fluid balance, and production of vitamin D (Telofski et al. 2012). The skin covers approximately 1.8 m^2 with multiple microenvironments created by variation in exposure (folds, invaginations, and clothing), sweat and sebum production, and hair distribution. The diversity of skin microenvironments is reflected by the rich and complex communities of microbes that colonize the skin. Thus, to fully understand the skin microbiome and its interactions with the skin, we must be familiar with the biology and topology of the skin.

The skin is composed of two layers, the dermis and epidermis, which rest above a layer of subcutaneous fat (Simpson et al. 2011). The deeper of the two, the dermis is composed of dense, irregular connective tissue and contains a variety of receptors, vessels, and glands involved in maintenance of epidermal integrity. Superficial to the dermis is the epidermis, which itself is composed of four layers of keratinocytes various stages of development. The stratum basale, as the name implies, is the basal layer, which is separated from the dermis by the epidermal basement membrane (Fuchs & Raghavan 2002). This layer contains the undifferentiated stem cells that undergo asymmetric division to give rise to the stratum spinosum. In this layer, the

6

immature keratinocytes begin to flatten and develop lamellar bodies and keratin fibrils. As keratinocytes continue to mature, they develop into the stratum granulosum, characterized by abundant keratohyalin granules. The granules contain filagrin, keratin, loricin, and involucrin, which are critical for the proper barrier function of the epidermis. To complete the differentiation process, the keratinocytes then anucleate and fully flatten forming the stratum corneum. Cells at this stage are termed corneocytes for their highly cornified envelope (Candi et al. 2005).

The orderly layers of the epidermis are regularly interrupted by hair follicles and glands that extend into the dermis. Sebaceous glands specialized in the secretion of a lipid-rich substance termed sebum, which contributes to the waterproofing of the skin (Zouboulis & Boschnakow 2001). The glands are often associated with hair follicles forming pilosebacious units, particularly prevalent on the face and scalp. These units provide an ideal environment for anaerobic bacteria that metabolize the secreted lipids into free fatty acids, contributing to the relatively acidic pH of the skin (Puhvel et al. 1975). Sweat glands in contrast are distributed throughout the body, though they are particularly concentrated in the axillae, palms, soles, and forehead (Lu & Fuchs 2014). The eccrine sweat glands produce a salty solution primarily composed of sodium-chloride and water, which is critical to their role in thermoregulation. The apocrine sweat glands secrete a more specialized solution including steroids, proteins, and lipids, which are thought to be involved in pheromone production and are particularly active during puberty. The apocrine secretions, initially odorless, are metabolized by microbes into volatile compounds associated with body odor.

Critical to the barrier function of the skin is its role in protection again invading pathogens. Skin immunity is mediated primarily by keratinocytes and cells of both the adaptive

and innate immune system (Pasparakis et al. 2014). As part of its immunological role, keratinocytes produce a variety of antimicrobial peptides, which function as broad antibiotics. Keratinocytes express Toll- and Nod-like receptors, which are activated by conserved molecules produced by commensals and pathogens alike (Heath & Carbone 2013). When activated, keratinocytes are prolific producers of proinflammatory cytokines and chemokines, which recruit nearby cells of the immune system. Langerhans cells, a dendritic cell subset, monitor the dermis and epidermis for microbial antigens, though they are also involved in promoting tolerance to self-antigens. When activated by foreign antigen, Langerhans cells will migrate to the skin-draining lymph nodes and present the offending antigen to naïve T-cells. Differentiated effector and memory T-cells then migrate to the skin to address the potential pathogen.

1.5 The Healthy Skin Microbiome

The skin features rich and complex communities of microbes, which reflect the diversity of microenvironments of the body. Body sites may be sebaceous, moist, or dry; haired or glabrous; exposed or occluded. They vary in humidity, pH, temperature, and level of antimicrobial peptides. These features define the microenvironments that microbes interact with and are major determinants of the community composition and structure. In general, the skin is dominated by four major taxa – *Propionibacterium, Staphylococcus, Corynebacterium*, and Proteobacteria – though the relative abundances of each vary with body site (Grice & Segre 2011). Foundational work by Grice *et al* revealed the topographical diversity of the bacterial microbiome at 20 distinct body sites, characterized as moist, sebaceous, or dry (Grice et al. 2009). Sebaceous sites were dominated by *Propionibacterium* species, with some contributions of *Staphylococcus* species. The moist sites were dominated by a combination of *Corynebacterium,*

β-Proteobacteria, and *Staphylococcus* species, though the distribution between these three varied considerably. The dry sites in contrast are more diverse, with no taxa being particularly dominant, however, increased prevalence of *β-Proteobacteria* and *Flavobacteriaceae* species were apparent. Sebaceous sites exhibited low levels of community diversity, whereas the dry sites exhibited the highest levels. This was found to be true for both the number of observed OTUs (richness) and Shannon Diversity Index (evenness).

Body sites have been shown to be the greatest determinants of community structure in healthy individuals. Community differences between body sites of the same individual are significantly larger than those between individuals of the same body site (Costello et al. 2009). Even so, differences between individuals at the same body site are greater than those between contralateral samples of the same subject and body site. Similarly, individuals are more similar to themselves over time (1-3 months), than between individuals at the same time point (Grice et al. 2009; Costello et al. 2009). Importantly, skin microbiome was shown to be less stable than communities of the gut or mouth (Costello et al. 2009), however, a recent metagenomic analysis found the skin to be more stable than previously reported (Oh et al. 2016).

Body sites also vary in the permissiveness of accepting microbiome transplants from other body sites. Costello *et al* found that the microbiome of the forehead, a sebaceous site, was significantly more resistant to microbiome transplants than the forearm, a dry site (Costello et al. 2009). The forehead also regained its original community structure faster than the forearm. This suggests that sebaceous sites exert more selective pressures on the microbiota than dry sites.

9

Fungal communities colonizing the skin have not been as extensively studied, but are beginning to emerge (Findley et al. 2013). *Malassezia* species were found to dominate fungal communities at most body sites, though species level signatures could be detected. In contrast, the fungal communities of the foot exhibited much greater levels of diversity and had significant contributions from *Aspergillus* and *Epicoccum*. Interestingly, community types clustered by body site geography rather than physiologic niche (sebaceous, moist, dry). This suggests that the fungal communities are less sensitive to these selective pressures.

The microbiota of the skin develops with age, beginning with birth and normalizing with the completion of puberty. Neonatal skin is markedly different from that of adults – the stratum corneum is thinner and composed of smaller corneocytes (Stamatas et al. 2010), the epidermal barrier is more permeable as a result of lower lipid content (Nikolovski et al. 2008), and the skin pH is more alkaline (Giusti et al. 2001). The cutaneous microbiome of neonates is marked by high levels of *Staphylococcus* and *Streptococcus*, but body-site specific patterns begin to emerge by six months of age (Capone et al. 2011). Using Tanner stages to distinguish between children and adults, a study found that subjects in late puberty had developed the adult-like dominances of *Propionibacterium* and *Corynebacterium* (Oh et al. 2012). Even whether a neonate is born vaginally or via Caesarean section has profound differences on the composition of the skin microbiota (Dominguez-Bello et al. 2010); however, it is unclear what impact this has on health outcomes. In contrast to age, the effect of gender on the skin microbiome is less clear and likely dwarfed by individual-specific forces (SanMiguel & Grice 2014).

The interactions between the immune system and the cutaneous microbiome are of critical importance in determining the efficacy of the former and the composition of the latter

10

(Belkaid & Tamoutounour 2016). There is a growing appreciation for the role of the skin

microbiota in educating the immune system. One study compared the cutaneous immunity

profiles of germ-free (GF) and specific pathogen-free (SPF) mice (Naik et al. 2012). This study

documented significant decreases in the production of IFN-γ and IL-17A and increased presence

of Foxp3$^+$ regulatory T-cells in GF mice. When mono-colonized by the human commensal

Staphylococcus epidermids, the IL-17A deficiency was abrogated. When applied to GF mice

infected with *Leishmania major*, *S. epidermidis* mono-colonization was enough to correct the

defective immune response normally mounted by GF mice. *S. epidermidis* has also been shown to

increase the production of antimicrobial peptides and proinflammatory cytokines, through its

activation of TLR2, leading to improved responses to infection with the bacteria Group A

Streptococcus and human papilloma virus (HPV) (Lai et al. 2010; Wanke et al. 2011; Percoco et

al. 2013). Lipoteichoic acid, a component of gram-positive cell walls, may also modulate TLR3-

mediated inflammation in keratinocytes during acute injury (Lai et al. 2009). The immune system

also shapes the cutaneous microbiome as demonstrated by studies in humans with primary

immunodeficiencies (Oh et al. 2013). Immunocompromised subjects' skin was marked by

increased permissiveness to the opportunistic pathogen, *Serratia marcesens,* and other atypical

bacteria. Longitudinal stability and site specificity were also noted to be less pronounced in these

subjects, suggesting that the immune system plays an active role in defining the cutaneous

microbiome.

1.6 Wound Healing and Chronic Wounds

On occasion the integrity of the skin may be compromised by traumatic injury or some

other insult to the skin resulting in a wound. The wounded skin then commences a series of

organized and well-characterized processes collectively referred to as wound healing. Wound healing can be divided into four phases with considerable overlap: hemostasis, inflammation, proliferation, and remodeling; however, some include hemostasis as a part of the inflammation phase (Velnar et al. 2009). The process begins with coagulation and the formation of a fibrin-rich clot, ensuring hemostasis and additionally providing a matrix for tissue regeneration. Platelets, embedded in the clot, degranulate, releasing chemokines and growth factors critical for facilitating keratinocyte and leukocyte migration to the wound and cellular proliferation (Gurtner et al. 2008).

Soon after, the early inflammation phase commences with the infiltration of neutrophils into the wounded tissue (Hart 2002). Their primary purpose is to prevent infection by phagocytosing bacteria and cellular debris. Neutrophils also produce elastases and collagenases that assist in degrading the extracellular matrix, facilitating migration of other cells. The late inflammatory phase begins 48-72 hours after injury and is characterized by the migration of macrophages to the wound, which continue the process of phagocytosis and crucially, produce copious amounts of additional growth factors promoting wound healing.

The proliferative phase begins at approximately the third day following injury and may persist for two weeks or more depending on the extent of injury (Velnar et al. 2009). Fibroblasts migrate into the wound and produce hyaluronan, proteoglycans, fibronectin, and pro-collagen, which replace the makeshift fibrin-matrix created during the coagulation phase. After the first week, fibroblasts mature into myofibroblasts, adhere to the extracellular matrix and contract, pulling the edges of the wound closer together. During this phase, new blood vessels develop to perfuse the regenerating tissue with a process termed angiogenesis. Endothelial cells proliferate

12

and migrate into the wound following chemotactic and proliferative signals. Together these processes lead to the creation of vasculature, connective tissue, and extracellular matrix that collective is termed granulation tissue. Re-epithelialization, the migration and proliferation of the epithelial keratinocytes, begins as early as the first day of wounding but is most pronounced during the proliferative phase.

Finally, the wound undergoes the remodeling phase, during which the healing tissue is remodeled into mature, healthy skin. This includes thickening, organizing, and cross-linking of collagen bundles and degradation of hyaluronic acid and fibronectin fibers. This process develops the tensile strength of the wound and may take weeks to years to finish, depending on the size and location of the injury.

In chronic wounds, this process is delayed or halted in the inflammatory phase. In the case of diabetic foot ulcers, a common and costly complication of diabetes, these wounds may persist for months to years before healing or in many cases terminating in amputation (Wolcott 2015). Chronic diabetes results in significant impairments of upwards of 100 physiologic factors, dramatically increasing the risk of foot ulceration and impeding nearly all aspects of wound healing (Brem & Tomic-Canic 2007). The hyperglycemic state of subjects with diabetes results in the development of distal neuropathies and peripheral vascular disease. The severity of these defects is a function of distance, which is why the distal extremity of the foot is the first and most affected.

Diabetic distal neuropathy is manifested in autonomic, motor, and sensory deficits (Falanga 2005). Autonomic dysfunction leads to decreased sweat and sebum production resulting

13

in dry skin prone cracking, injury, and infection. Foot deformities may develop as a consequence of motor defects, creating bony protuberances and other sites vulnerable to mechanical stress. Sensory deficits exacerbate the situation, by increasing the risk of injury due to repetitive or acute trauma. More importantly, diabetics with distal neuropathy are often unaware their injury, thus foot ulcers continue to be exposed to trauma and infection before receiving any medical intervention. All of this is compounded by deficiencies in phagocytic activity, growth factor production, cellular migration, angiogenesis, and extracellular matrix accumulation, which impede effective wound healing (Brem & Tomic-Canic 2007).

1.7 A Note on Terminology

The study of the human microbiome is relatively new and its vocabulary is rapidly evolving and often ambiguous. The word *microbiome* is used generally to describe all microbes and their genomes inhabiting a niche, however, it is can also be used to describe the bacterial component specifically, with *mycome* and *virome* referring to the fungal and viral components respectively. For the remainder of the text, I will use distinguish between the bacterial, fungal, and viral components using these terms and adopt the convention of distinguishing between the actual cells, *microbiota/mycobiota*, and the collective genetic content, *microbiome/mycome*.

1.8 References

Alekseyenko, A.V. et al., 2013. Community differentiation of the cutaneous microbiota in
    psoriasis. *Microbiome*, 1(1), p.31.

Bajaj, J.S., et al., 2012. Linkage of gut microbiome with cognition in hepatic encephalopathy.
    American Journal of Physiology. Gastrointestinal and Liver Physiology, 302(1), pp.G168-75

Belkaid, Y. & Tamoutounour, S., 2016. The influence of skin microorganisms on cutaneous immunity. *Nature Reviews Immunology*, 16(6), pp.353–366.

Brem, H. & Tomic-Canic, M., 2007. Cellular and molecular basis of wound healing in diabetes. *The Journal of clinical investigation*, 117(5), pp.1219–1222.

Browne, H.P. et al., 2016. Culturing of "unculturable" human microbiota reveals novel taxa and extensive sporulation. *Nature*, 533(7604), pp.543–546.

Buffie, C.G. et al., 2014. Precision microbiome reconstitution restores bile acid mediated resistance to Clostridium difficile. *Nature*, 517(7533), pp.205–208.

Candi, E., Schmidt, R. & Melino, G., 2005. The cornified envelope: a model of cell death in the skin. *Nature Reviews Molecular Cell Biology*, 6(4), pp.328–340.

Capone, K.A. et al., 2011. Diversity of the Human Skin Microbiome Early in Life. *Journal of Investigative Dermatology*, 131(10), pp.2026–2032.

Caporaso, J.G. et al., 2010. QIIME allows analysis of high-throughput community sequencing data. *Nature Methods*, 7(5), pp.335–336.

Charlson, E.S. et al., 2012. Lung-enriched Organisms and Aberrant Bacterial and Fungal Respiratory Microbiota after Lung Transplant. *American Journal of Respiratory and Critical Care Medicine*, 186(6), pp.536–545.

Cho, I. & Blaser, M.J., 2012. The human microbiome: at the interface of health and disease. *Nature Reviews Genetics*, 13(4), pp.260–270.

Clayton, T.A. et al., 2009. Pharmacometabonomic identification of a significant host-microbiome metabolic interaction affecting human drug metabolism. *Proceedings of the National Academy of Sciences*, 106(34), pp.14728–14733.

Costello, E.K. et al., 2009. Bacterial community variation in human body habitats across space and time. *Science*, 326(5960), pp.1694–1697.

15

DiGiulio, D.B. et al., 2015. Temporal and spatial variation of the human microbiota during

    pregnancy. *Proceedings of the National Academy of Sciences*, 112(35), pp.201502875–

    11065.

Dobell, C., 1960. *Antony Van Leeuwenhoek and His "Little Animals,"* New York: Harcourt,

    Brace, and Co.

Dominguez-Bello, M.G. et al., 2010. Delivery mode shapes the acquisition and structure of the

    initial microbiota across multiple body habitats in newborns. *Proceedings of the National*

    Academy of Sciences, 107(26), pp.11971–11975.

Falanga, V., 2005. Wound healing and its impairment in the diabetic foot. *The Lancet*, 366(9498),

    pp.1736–1743.

Findley, K. et al., 2013. Topographic diversity of fungal and bacterial communities in human

    skin. *Nature*, 498(7454), pp.367–370.

Fitz-Gibbon, S. et al., 2013. Propionibacterium acnes Strain Populations in the Human Skin

    Microbiome Associated with Acne. *Journal of Investigative Dermatology*, 133(9), pp.2152–

    2160.

Foster, J.A. & McVey Neufeld, K.-A., 2013. Gut–brain axis: how the microbiome influences

    anxiety and depression. *Trends in neurosciences*, 36(5), pp.305–312.

Fuchs, E. & Raghavan, S., 2002. Getting under the skin of epidermal morphogenesis. *Nature*

    Reviews Genetics, 3(3), pp.199–209.

Ganju, P. et al., 2016. Microbial community profiling shows dysbiosis in the lesional skin of

    Vitiligo subjects. *Scientific reports*, 6, p.18761.

Gardner, S.E. et al., 2013. The neuropathic diabetic foot ulcer microbiome is associated with

    clinical factors. *Diabetes*, 62(3), pp.923–930.

Gevers, D. et al., 2012. The Human Microbiome Project: a community resource for the healthy

human microbiome. *PLoS biology*, 10(8), p.e1001377.

Giusti, F. et al., 2001. Skin barrier, hydration, and pH of the skin of infants under 2 years of age. *Pediatric dermatology,* 18(2), pp.93-96.

Grice, E.A. & Segre, J.A., 2012. The human microbiome: our second genome. *Annual review of genomics and human genetics*, 13(1), pp.151–170.

Grice, E.A. & Segre, J.A., 2011. The skin microbiome. *Nature reviews. Microbiology*, 9(4), pp.244–253.

Grice, E.A. et al., 2010. Longitudinal shift in diabetic wound microbiota correlates with prolonged skin defense response. *Proceedings of the National Academy of Sciences*, 107(33), pp.14799–14804.

Grice, E.A. et al., 2009. Topographical and Temporal Diversity of the Human Skin Microbiome. *Science (New York, N.Y.)*, 324(5931), pp.1190–1192.

Gurtner, G.C. et al., 2008. Wound repair and regeneration. *Nature*, 453(7193), pp.314–321.

Hart, J., 2002. Inflammation. 1: Its role in the healing of acute wounds. *Journal of Wound Care*, 11(6), pp.205–209.

Heath, W.R. & Carbone, F.R., 2013. The skin-resident and migratory immune system in steady state and memory: innate lymphocytes, dendritic cells and T cells. *Nature immunology*, 14(10), pp.978–985.

Kassam, Z. et al., 2013. Fecal Microbiota Transplantation for Clostridium difficile Infection: Systematic Review and Meta-Analysis. *The American journal of gastroenterology*, 108(4), pp.500–508.

Koeth, R.A. et al., 2013. Intestinal microbiota metabolism of l-carnitine, a nutrient in red meat, promotes atherosclerosis. *Nature Medicine*, 19(5), pp.576–585.

Kong, H.H. et al., 2012. Temporal shifts in the skin microbiome associated with disease flares

and treatment in children with atopic dermatitis. *Genome research*, 22(5), pp.850–859.

Kopylova, E. et al., 2016. Open-Source Sequence Clustering Methods Improve the State Of the Art N. Segata, ed. *mSystems*, 1(1), pp.e00003–15.

Lai, Y. et al., 2010. Activation of TLR2 by a small molecule produced by Staphylococcus epidermidis increases antimicrobial defense against bacterial skin infections. *The Journal of investigative dermatology*, 130(9), pp.2211–2221.

Lai, Y. et al., 2009. Commensal bacteria regulate Toll-like receptor 3-dependent inflammation after skin injury. *Nature Medicine*, 15(12), pp.1377–1382.

Liu, M.-B. et al., 2013. Diverse Vaginal Microbiomes in Reproductive-Age Women with Vulvovaginal Candidiasis J. Ravel, ed. *PLoS ONE*, 8(11), p.e79812.

Lu, C. & Fuchs, E., 2014. Sweat Gland Progenitors in Development, Homeostasis, and Wound Repair. *Cold Spring Harbor perspectives in medicine*, 4(2), pp.a015222–a015222.

Mayer, B.T. et al., 2015. Rapid and Profound Shifts in the Vaginal Microbiota Following Antibiotic Treatment for Bacterial Vaginosis. *Journal of Infectious Diseases*, 212(5), pp.793–802.

Meisel, J.S. et al., 2016. Skin Microbiome Surveys Are Strongly Influenced by Experimental Design. *The Journal of investigative dermatology*, 136(5), pp.947–956.

Modi, S.R., Collins, J.J. & Relman, D.A., 2014. Antibiotics and the gut microbiota. *The Journal of clinical investigation*, 124(10), pp.4212–4218.

Morgan, X.C. et al., 2012. Dysfunction of the intestinal microbiome in inflammatory bowel disease and treatment. *Genome biology*, 13(9), p.1.

Naik, S. et al., 2012. Compartmentalized Control of Skin Immunity by Resident Commensals. *Science (New York, N.Y.)*, 337(6098), pp.1115–1119.

Nikolovski, J., Stamatas, G.N. & Kollias, N., 2008. Barrier function and water-holding and

transport properties of infant stratum corneum are different from adult and continue to
develop through the first year of life. *Journal of Investigative …*.

Oh, J. et al., 2012. Shifts in human skin and nares microbiota of healthy children and adults.
Genome Medicine, 4(10), p.77.

Oh, J. et al., 2016. Temporal Stability of the Human Skin Microbiome. *Cell*, pp.1–14.

Oh, J. et al., 2013. The altered landscape of the human skin microbiome in patients with primary
immunodeficiencies. *Genome research*, 23(12), pp.2103–2114.

Pasparakis, M., Haase, I. & Nestle, F.O., 2014. Mechanisms regulating skin immunity and
inflammation. *Nature Reviews Immunology*, 14(5), pp.289–301.

Percoco, G. et al., 2013. Antimicrobial peptides and pro-inflammatory cytokines are differentially
regulated across epidermal layers following bacterial stimuli. *Experimental Dermatology*,
22(12), pp.800–806.

Puhvel, S.M., Reisner, R.M. & Sakamoto, M., 1975. Analysis of Lipid Composition of Isolated
Human Sebaceous Gland Homogenates After Incubation with Cutaneous Bacteria. Thin-
Layer Chromatography. *Journal of Investigative Dermatology*, 64(6), pp.406–411.

Quinn, R.A. et al., 2014. Biogeochemical Forces Shape the Composition and Physiology of
Polymicrobial Communities in the Cystic Fibrosis Lung. *mBio*, 5(2), pp.e00956–13–e00956–
13.

SanMiguel, A. & Grice, E.A., 2014. Interactions between host factors and the skin microbiome.
Cellular and Molecular Life Sciences, 72(8), pp.1499–1515.

Schloss, P.D., Westcott, S.L. & Ryabin, T., 2009. Introducing mothur: open-source, platform-
independent, community-supported software for describing and comparing microbial
communities. *Applied and …*.

Sender, R., Fuchs, S. & Milo, R., 2016. *Revised estimates for the number of human and bacteria*

cells in the body,

Shreiner, A.B., Kao, J.Y. & Young, V.B., 2015. The gut microbiome in health and in disease. *Current opinion in gastroenterology*, 31(1), pp.69–75.

Simpson, C.L., Patel, D.M. & Green, K.J., 2011. Deconstructing the skin: cytoarchitectural determinants of epidermal morphogenesis. *Nature Reviews Molecular Cell Biology*, 12(9), pp.565–580.

Staley, J.T. & Konopka, A., 1985. Measurement of in Situ Activities of Nonphotosynthetic Microorganisms in Aquatic and Terrestrial Habitats. *Annual Review of Microbiology*, 39(1), pp.321–346.

Stamatas, G.N., Nikolovski, J. & Luedtke, M.A., 2010. Infant skin microstructure assessed in vivo differs from adult skin in organization and at the cellular level. *Pediatric ….*

Suez, J. et al., 2014. Artificial sweeteners induce glucose intolerance by altering the gut microbiota. *Nature*.

Takemoto, A. et al., 2014. Molecular characterization of the skin fungal microbiome in patients with psoriasis. *The Journal of Dermatology*, 42(2), pp.166–170.

Telofski, L.S. et al., 2012. The Infant Skin Barrier: Can We Preserve, Protect, and Enhance the Barrier? *Dermatology Research and Practice*, 2012(1, part 1), pp.1–18.

Turnbaugh, P.J. et al., 2006. An obesity-associated gut microbiome with increased capacity for energy harvest. *Nature*, 444(7122), pp.1027–131.

Velnar, T., Bailey, T. & Smrkolj, V., 2009. The Wound Healing Process: An Overview of the Cellular and Molecular Mechanisms. *Journal of International Medical Research*, 37(5), pp.1528–1542.

Wade, W.G., 2013. The oral microbiome in health and disease. *Pharmacological research*, 69(1), pp.137–143.

Wang, Z. et al., 2016. Lung microbiome dynamics in chronic obstructive pulmonary disease exacerbations. pp.1–11.

Wanke, I. et al., 2011. Skin commensals amplify the innate immune response to pathogens by activation of distinct signaling pathways. *The Journal of investigative dermatology*, 131(2), pp.382–390.

Wolcott, R., 2015. Economic aspects of biofilm-based wound care in diabetic foot ulcers. *Journal of Wound Care*, 24(5), pp.189–90– 192–4.

Young, J.C. et al., 2014. Viral Metagenomics Reveal Blooms of Anelloviruses in the Respiratory Tract of Lung Transplant Recipients. *American Journal of Transplantation*, 15(1), pp.200–209.

Zouboulis, C.C. & Boschnakow, A., 2001. Chronological ageing and photoageing of the human sebaceous gland. *Clinical and Experimental Dermatology*, 26(7), pp.600–607.

CHAPTER 2 – Temporal Stability In Chronic Wound Microbiota Is Associated

With Poor Healing

The contents of this chapter are accepted for publication as:

Michael Loesche*, Sue E. Gardner*, Lindsay Kalan, Joseph Horwinski, Qi Zheng,

Brendan P. Hodkinson, Amanda S. Tyldsley, Carrie L. Franciscus, Stephen L. Hillis,

Samir Mehta, David J. Margolis, Elizabeth A. Grice. Temporal Stability In Chronic

Wound Microbiota Is Associated With Poor Healing. *J. Inv. Dermatol*. (In Press)

2.1 Abstract

Microbial burden of chronic wounds is believed to play an important role in impaired

healing and development of infection-related complications. However, clinical cultures have little

predictive value of wound outcomes, and culture-independent studies have been limited by cross-

sectional design and small cohort size. We systematically evaluated the temporal dynamics of the

microbiota colonizing diabetic foot ulcers, a common and costly complication of diabetes, and its

association with healing and clinical complications. Dirichlet multinomial mixture modeling,

Markov chain analysis, and mixed-effect models were used to investigate shifts in the microbiota

over time and its associations with healing. Here we show for the first time the temporal

dynamics of the chronic wound microbiome. Microbiota community instability was associated

with faster healing and improved outcomes. DFU microbiota were found to exist in one of four

community types that experienced frequent and non-random transitions, which corresponded to

the healing time. Exposure to systemic antibiotics destabilized the wound microbiota, rather than

altering overall diversity or relative abundance of specific taxa. This study provides the first

evidence that the dynamic wound microbiome is indicative of clinical outcomes and may be a valuable guide for personalized management and treatment of chronic wounds.

2.2 Introduction

Chronic, non-healing wounds affect 6.5 million patients annually in the US and are an increasing public health and economic threat, exceeding estimated annual treatment costs of $9.7 billion (Bickers et al. 2006). Chronic wounds almost always affect individuals with an underlying predisposition (e.g. obesity, advanced age, diabetes) and are often disguised as a comorbid condition. A major type of chronic wound is the diabetic foot ulcer (DFU), a common complication of diabetes that results from neuropathy coupled with mechanical stress and tissue breakdown. Those with diabetes have a 15-25% lifetime incidence of DFU (Valensi et al. 2005) and result in amputation in 15.6% of cases (Ramsey et al. 1999). Projections estimate that diabetes will continue to increase in prevalence (Guariguata et al. 2014); thus addressing management and treatment strategies for this complication is critical.

Microbial bioburden is believed to contribute to impaired healing of chronic wounds and it is estimated that over 50% of DFUs are infected upon presentation (Prompers et al. 2007); however, infections are difficult to diagnose due to the diminished or absent clinical signs in DFUs (Glaudemans et al. 2015). Without clinical suspicion, wound cultures provide little diagnostic value, as bacteria colonize all open wounds. Our previous work demonstrated that clinical cultures underestimate bacterial diversity and load when compared to culture-independent techniques, based on the prokaryote-specific 16S ribosomal RNA (rRNA) gene. Multiple dimensions of the microbiota may be important, including microbial diversity, microbial load,

23

and abundance of potential pathogens (Gardner and Frantz 2008). Although other studies have used culture-independent methods to examine DFUs and other chronic wound microbiomes, these studies employed cross-sectional designs (Dowd et al. 2008; Price et al. 2009; Gontcharova 2010; Gardner et al. 2013; Wittebole et al. 2014; Wolcott et al. 2015) and the relationship between the wound microbiome and outcomes has not been rigorously examined.

Microbial communities exhibit a wide range of stabilities across the human body (Ding and Schloss 2014; Flores et al. 2014); however, what these differing stabilities mean for the health of the community or the host remain poorly understood. Very little is known about the dynamics of the wound microbiota during healing, deterioration, or exposure to antibiotics. To date, no study has investigated the microbial dynamics of chronic wounds. These dynamics may contain information about the vulnerability of the wound to opportunistic infections or provide insight as to the origin of stalled wound healing. It is critical to study these dynamics to enhance our understanding of chronic wounds and improve our ability to effectively treat them.

We address several important limitations of previous studies by performing a study designed to capture the longitudinal dynamics of microbiota colonizing DFUs and examining the association between the DFU microbiome and clinical outcomes. Microbiota were sampled from DFUs every two weeks for 26 weeks or until healed. We employed high throughput sequencing of the 16S rRNA gene to define multiple metrics of the microbiome, including diversity, stability, and relative abundance of potential pathogens and identified microbiomic features associated with DFU clinical outcomes. Though our study was focused on the microbiota in DFU, many of these findings may be true of other chronic wounds and should be considered in future studies and treatments of chronic wounds.

24

2.3 Results

We enrolled 100 subjects into a prospective, longitudinal cohort study to analyze temporal dynamics of DFU microbiota and association with outcomes using culture-independent approaches. DFU microbiota was collected at initial presentation (baseline) and resampled every two weeks until: 1) DFU healed; 2) lower extremity amputation; or 3) the conclusion of 26 weeks of follow up. All subject received standardized treatment of surgical debridement and offloading. Of the 100 enrolled subjects, 31 experienced an infection-related complication, defined as: 1) amputation; 2) wound deterioration, or 3) development of osteomyelitis. **Table S1** summarizes clinical factors by complication status.

2.3.1 Characterization of the DFU microbiota at baseline

DFU microbiomes were determined by sequencing of hypervariable regions V1 through V3 of the 16S ribosomal RNA (rRNA) gene. The most abundant genus identified was *Staphylococcus*, present in 345 of the 349 samples, with an average relative abundance of 22.77%. The second, third, and fourth most abundant genera were *Streptococcus* (11.98%; 318 of 349 samples), *Corynebacterium* (11.46%; 346 of 349 samples), and *Anaerococcus* (7%; 300 of 349 samples), respectively. All other genera represented <5% of bacterial relative abundance in this dataset. A more detailed characterization can be found in **Table S2**. We further classified *Staphylococcus* operational taxonomic units (OTUs) to species level for 79.5% of the OTUs. Of the 22.77% attributed to *Staphylococcus*, 13.3% was classified as *S. aureus*, 5.3% was *S. pettenkoferi*, and 4% was not further classified. While *S. aureus* is a common DFU isolate, the high abundance of *S. pettenkoferi* was surprising as this species was only recently characterized

in 2007 (Trülzsch et al. 2007), though it was identified as the cause of osteomyelitis in patient with a chronic DFU in France (Loïez et al. 2007).

2.3.2 DFU microbiota can be partitioned into four community types

We assigned DFUs to community types with the Dirichlet multinomial mixture (DMM) model-based approach (Holmes et al. 2012). The DMM model supposes a more biologically relevant distribution of data, which overcomes limitations of alternative methods such as k-means (Holmes et al. 2012) and PAM clustering (Ding and Schloss 2014). The DFU microbiomes were clustered into 4 groups, or Community Types (CT), by minimizing the Laplace approximation (**Fig. S1**). The top five differentiating taxa contributed 48.9% of the total difference between a one and four component model, though the major distinguishing taxa were *Streptococcus* (25.6%) and *S. aureus* (11.8%) (**Fig. 1A**). CT3 DFUs were characterized by high relative abundances of *Streptococcus* (median = 64.0%). CT4 DFUs were comprised of relatively high levels of *S. aureus* (median=23.8%). CT1 and CT2 were highly heterogeneous with no dominant taxa contributing more than a median of 5% of total relative abundance. This was also reflected by Theta values, a measure of cluster variability with smaller values corresponding to highly variable communities, which were 3.7 and 6.9, for the CT1 and CT2 compared to 16.4 and 10.5 for CT3 and CT4, respectively. Community type summaries are described in greater detail in **Supplemental Table 3**.

To better visualize how CTs were associated with microbiota composition and clinical features, we generated a biplot depicting these relationships (**Fig. 1B**). As would be expected, the taxa vectors for *Streptococcus* and *S. aureus* are closely associated with the CT3 and CT4, respectively. Interestingly, the samples with the highest proportion of *S. aureus* are not included

in CT4, demonstrating the importance of the whole community in distinguishing clusters. *Streptococcus* was closely associated with HbA1C levels and anaerobe levels with ulcer depth. Serum C-reactive protein levels (CRP) and white blood cell counts (WBC), both measures of inflammation used to inform the diagnosis of infections, localized separately with CT4 and CT3, respectively. Subject outcomes also contributed to data separation, with amputation localizing with CT1 and CT2, and unhealed subjects localizing with CT4.

2.3.3 The frequency of Community Type transitions in DFU are associated with clinical outcomes

We next investigated the stability of the CTs by exploring the frequency and type of CT transitions. The DFU microbiota was highly dynamic with CT transitions occurring every 1.76 study visits (approximately 3.52 weeks) on average (**Fig. 2A**). Transition frequencies were significantly associated with subject outcomes (healed = 1.60, unhealed = 2.04, amputation = 3.08 study visits/CT-transition). We further subdivided healed subjects into those whose ulcers closed in <12 weeks and those closed in >12 weeks. Consistent with our analysis, the faster healing subjects experienced greater transition frequencies (<12 weeks = 1.45, >12 weeks 2.11 study visits/CT-transition, Wilcoxon p-value = 0.011).

We then questioned whether transition patterns between CTs were related to ulcer outcomes. By quantifying transitions between CTs we could represent the data as a Markov chain, with nodes representing CTs and edges representing transition frequencies by their weight (**Fig. 2B**). The transition patterns between those that healed in <12 weeks and those that healed in >12 weeks were significantly different (p-value < 0.0001). In those who healed in <12 weeks, CT1 and CT2 dominated the transitions and were noted to have high self-transition rates of 0.74

27

and 0.53, respectively. In contrast CT3 and CT4 experienced lower self-transition rates of 0.23

and 0.29, and had a predilection for transitioning to CT2. For subjects that took >12 weeks to

heal, there is a marked increase in self-transitions, with ulcers stalling in CT3 and CT4 at rates of

0.45 and 0.84, respectively, indicating that the stability of these CTs may be detrimental to wound

healing. Analysis of the stationary distribution and expected recurrence time revealed similar

trends **(Table S4)**. The presence or absence of transitions between CT3 and CT4 also

differentiated the two groups, with no recorded instances in wounds healing in <12 weeks.

Together these findings suggest that community stability reflects a delayed healing phenotype.

2.3.4 DFU with more dynamic microbiota heal faster than those with less dynamic microbiota

To address more subtle patterns of variation, which may not be apparent when examining

broad community types, we used the inter-visit weighted UniFrac (WUF) distance as a proxy of

stability. The weighted UniFrac metric measures the proportion of shared OTUs, their

phylogenetic relationships, and their relative distributions on a scale of 0 to 1, with higher values

indicating greater instability. We generated mixed-effect linear regressions to model the

relationship between microbiota instability and time required to heal in those that healed within

24 weeks. This model suggests that all ulcers are slowly stabilizing at a rate of -0.024/visit;

however, slow healing ulcers begin in a more stable state (-0.036 per visit required to heal) **(Fig.**

3A). Because mixed-effect models do not allow generation of a traditional R^2 value, we

calculated marginal and conditional pseudo-R^2 values, which reveals an estimate of the variance

due to the fixed effects alone and the combined model of fixed and random effects respectively.

The marginal R^2 was estimated to be 0.201 and the conditional to be 0.280, indicating that our

model explains a moderate amount of the variation.

The first inter-visit distance, between the baseline study visit and following visit, includes the effect of the initial surgical debridement. Thus it was possible that the high instability in faster healing wounds was an artifact of the first study visit being weighted more. To address this concern, we investigated the relationship between healing time and the amount of change between baseline and the following visit (2 weeks' time) using a traditional linear model. We found the same negative association between healing time and the inter-visit distance ($R^2 = 0.16$, p<0.0001) **(Fig. 3B)**, suggesting the effect is independent of debridement.

2.3.5 Effect of antibiotics on temporal stability in DFU microbiota

During the course of the study, 32 subjects required the administration of antibiotics, which afforded us the opportunity to glean the effects of antibiotics on ulcer microbiomes. Antibiotic exposure did not drive microbiota variation in our samples (**Fig 1B**). Furthermore, we did not detect any significant changes in community diversity as measured by the Shannon index or OTU richness, perhaps due to unique interactions between specific antibiotic classes and personal microbial communities. We assessed the potential for antibiotics to disrupt microbial communities using the inter-visit WUF distances as before and by binning antibiotics into distinct categories based on their class and mechanism of action. We did not detect significant differences in microbial stability due to antibiotic class. However, in half of the cases, the antibiotics were prescribed to treat infections not involving the studied ulcer (e.g. other ulcers, urinary tract infection, upper respiratory infection, sinus infection). When we examined the subjects treated specifically for the study ulcer, we found that antibiotics administered produced significantly higher community disruption than if the antibiotic was given for a different indication **(Fig. 4A)**.

In some cases, during the same time period that antibiotics were administered, the ulcer was designated as having a complication (wound deterioration or osteomyelitis). We modeled how these complications interacted with the antibiotics using mixed-effect linear regressions as before **(Fig. 4B)**. We found that both complications and antibiotics contributed to community disruption, though the larger effect was noted for antibiotics (WUF = 0.084 and 0.140 respectively). Furthermore, targeted antibiotics and complications had an additive effect on the amount of community disruption (WUF = 0.201).

2.4 Discussion

Ours is the first study to explore the temporal dynamics of the human chronic wound microbiota. Microbiome studies in other body sites have shown that disease states are associated with less stability (Martinez et al. 2008; Jenq et al. 2012; DiGiulio et al. 2015). Surprisingly, DFUs that experienced delayed healing or resulted in amputation were associated with increased stability, while the inverse was true for faster healing wounds. One way of interpreting these findings is to conclude that there is no "normal" DFU community. A wound is by definition an abnormal and transient state in physiology. As such, colonizing bacteria should be considered opportunistic and unlikely to have evolved harmonious methods of existing with the host. From this perspective, instability in the microbiome is a reflection of effective control of wound bacteria, which prevents any community structure from stabilizing. In contrast, a DFU with a stable outgrowth of certain bacteria reflects a stalled healing state where the colonizing bacteria have overridden the host's defenses.

We found that the DFU microbiome can be partitioned into 4 community types. Increased community type transitions were associated with improved healing rates; however, these

30

community type transitions were not random. In quickly healing ulcers, CT1 and CT2 were substantially more likely to remain unchanged, whereas CT3 and CT4 were more likely to transition to CT2. In slow or unhealing wounds, we found that CT3 and CT4 became much more resilient. These findings suggest that the prognostic capacity of transition frequencies would be augmented by information of community structure. Further studies are needed to delineate cause and effect relationships of the microbiota with the wound environment.

Despite the regular use of antibiotics to treat infections, little is known about their impact on microbial communities in chronic wounds. We did not detect any differences in community diversity or composition due to antibiotic exposure, unlike the gut where exposure to certain antibiotics is known to decrease diversity levels, predisposing to infection by *Clostridium difficile* (Dethlefsen and Relman 2011; Stein et al. 2013). Instead, as in other body sites (Keeney et al. 2014; Modi et al. 2014; Zhang et al. 2014; Mayer et al. 2015), antibiotics disrupted the microbiota. The extent of community disruption was not dependent on the class of antibiotic; rather it was whether the antibiotic was targeted towards the ulcer being studied. However, our analysis is limited by the biweekly sampling frequency, limiting the detection of short-lived changes.

In some reports, over half of DFUs are infected at the time of presentation (Prompers et al. 2007); however, identifying reliable criteria to diagnose an infection is complicated by the attenuated response to infections in diabetic persons (Brem and Tomic-Canic 2007). While our results would benefit from validation in larger cohorts, and their applicability to other types of chronic wounds needs to be tested, we provide evidence that the temporal dynamics of the wound microbiome may be useful for identifying stalled wounds requiring antibiotic treatment. We

31

envision that these findings will ultimately guide clinicians in the management of chronic wounds in a personalized manner.

2.5 Materials and Methods

2.5.1 Study Design

A prospective, longitudinal cohort design was used to examine DFU microbiota and outcomes in 100 subjects. DFU microbiota was collected at initial presentation (baseline) and resampled every two weeks until: 1) DFU healed; 2) lower extremity amputation; or 3) the conclusion of 26 weeks of follow up. The Institutional Review Boards at the University of Iowa and the University of Pennsylvania approved all study procedures.

2.5.2 Setting and Sample

Subjects were enrolled from September 2008 through October 2012 at the University of Iowa Hospitals and Clinics (UIHC) and the Iowa City Veteran's Affairs Medical Center (VA). Subjects were recruited through local media advertisements and from outpatient clinics at UIHC and the VA. The target population was diabetic adults (i.e., 18 years of age or older) with a DFU on the plantar surface of the foot. Individuals meeting these criteria were enrolled after providing informed written consent.

We standardized the management of the study DFUs after enrollment, including ulcer dressings (i.e., Lyofoam®, Molnlycke Health Care), devices used for offloading (i.e., total contact casts were used for 87 subjects; DH boots for 13 subjects), and ulcer debridement (i.e.,

aggressive sharp debridement of necrotic tissue in the wound bed was completed at baseline and callus on the wound edge was removed every two weeks), in order to minimize the number of factors unrelated to ulcer bioburden that could impact DFU outcomes. DFU management did not include antimicrobial dressings, topical antimicrobials, and/or systemic antibiotics, unless an infection-related complication was present at enrollment or occurred during follow-up. Baseline data were collected immediately after enrollment. Study data were collected every two weeks until one of the study endpoints was reached.

2.5.3 Study Variables

Clinical factors: The research team measured a set of clinical factors in order to identify pertinent co-variates for the analyses and to comprehensively describe the study sample. At baseline, demographic data, diabetes type and duration, and duration of study ulcer were collected using subject self-report and medical records. Standard laboratory tests were used to measure baseline glycemic control (haemoglobin A1c levels), as well as immune (White blood cell count) and inflammatory markers (C reactive protein). The research team assessed each subject for ischemia using toe-brachial index and for neuropathy using 5.07 Semmes-Weinstein monofilament. Transcutaneous oxygen pressure was measured at baseline and at each follow-up visit, using a transcutaneous oxygen monitor (Novametrix 840®, Novametrix Medical Systems Inc.). Ulcer location was categorized as forefoot, midfoot, or heel.

Microbiome: Ulcer specimens were collected using the Levine technique. After cleansing with non-bacteriostatic saline, an Amies swab (Copan, Italy) was rotated over a 1-cm^2 area of viable wound tissue in the center of the wound bed for five seconds, using sufficient pressure to extract wound-tissue fluid, DNA was isolated from swab specimens as previously described

(Gardner et al. 2013). Amplification of the 16S V1-V3 region was performed as described previously (Meisel et al. 2016), using the Illumina MiSeq platform with 300 bp paired-end 'V3' chemistry. This resulted in a dataset of 7,702,607 high quality, classifiable sequences used in the final analysis, with a mean of 22,070 (range 1,206-69,167) sequences per sample.16S rRNA sequence pre-processing followed methods described previously (Meisel et al. 2016), modified by performing *denovo* OTU clustering via UCLUST, assigning taxonomy with BLAST, and subsampling at 1200 sequences per sample. Sequences corresponding to the taxa "Geobacillus", "Bacillus", and "Lactococcus" were removed as these were identified as contaminants in the negative controls. QIIME 1.9.0 (Caporaso et al. 2010) was used for initial stages of sequence analysis. Sequences were clustered into OTUs (operational taxonomic units, a proxy for 'species') using UCLUST(Edgar 2010) at 97% sequence similarity. Microbial diversity was calculated using the following alpha diversity indices: 1) Shannon diversity index; 2) Faith's phylogenetic distance (PD); and 3) number of observed OTUs. Taxonomic classification of sequences were made using BLAST, as implemented in QIIME.

Outcomes: Members of the research team, who were blinded to the microbiota status, assessed healing and infection-related complications every two weeks. Ulcer closure was assessed using the Wound Healing Society's definition of "an acceptably healed wound," a valid and reliable definition (Margolis et al. 1996). The outcome "healed by 12 weeks" was defined as wound closure before or at 12 weeks of follow-up. "Development of infection-related complications" was defined as wound deterioration, new osteomyelitis, and/or amputations due to DFU infections.

Wound deterioration was defined as the new development of frank erythema and heat, and an increase in size > 50% over baseline. Two members of the research team independently assessed each DFU for erythema and heat. Two members of the research team independently assessed size using the VeVMD® digital software system (Vista Medical, Winnipeg, Manitoba, Canada), which was loaded on a Dell Latitude D630 laptop computer (Dell, Round Rock, Texas). Digital images were taken that contained the ulcer, a 3x3 square-centimeter image orientation card, and a single-point wound-depth indicator (i.e. A cotton-tipped swab that had been placed in the deepest aspect of the DFU and marked where the swab intersected with the plane of the peri-wound skin) and uploaded into the VeVMD program. VevMD tools were used to trace the ulcer outline and a line along the wound depth indicator to generate measures of depth and surface area.

Osteomyelitis was assessed using radiographs and MRI at baseline and during follow-up visits when subjects presented with new tracts to bone, wound deterioration, elevated temperature, elevated white count, elevated erythrocyte sedimentation rate, or elevated C-reactive protein. If these indicators were absent at follow-up, radiographs were not retaken. Subjects experiencing lower limb amputations had their medical records reviewed by the research team to ensure amputations were due to DFU infection, and not some other reason.

2.5.4 Data Analyses

The R Statistical Package ({R Core Team} 2016) was used for all computations. Non-parametric Wilcoxon rank-sum tests were used to compare differences between groups. Spearman correlations were used to correlate continuous variables. Kruskal-Wallis tests, followed by Wilcoxon rank sum post-hoc tests, were used for categorical variables. Linear models were calculated in base R; mixed-effect regressions were generated using the NLME package(Pinheiro

et al. 2007). Partial and conditional pseudo-R2 values were calculated using the piecewiseSEM

package (Lefcheck 2015). Sample biplot was generated using the Breadcrumbs package as done

in (Morgan et al. 2015). Differences in Markov chain transition frequencies were tested with a

Fisher's test and simulated p-value. Dirichlet multinomial mixture modeling was performed using

the R package Dirichlet Multinomial (v1.10.0). Counts were calculated at the highest level of

taxonomic classification. The number of community types was determined by selecting the

number of Dirichlet components that minimized the Laplace approximation of the model

evidence (Holmes et al. 2012). Each sample was assigned to the community type that had the

largest posterior probability. Inter-visit distances were calculated using the weighted UniFrac

distance between consecutive visits. If visits were discontinuous (i.e. missing sample) no

distances were reported.

3.6 Author Contributions

Conceptualization, Supervision, and Funding Acquisition: SEG and EAG; Methodology:

MAL, SEG, DJM, EAG; Formal Analysis: MAL, LK, SLH, DJM; Investigation: MAL, LK, JH,

AST, BPH; Data Curation: QZ, CLF; Resources: SEG, SM, DJM, EAG; Visualization: MAL;

Writing-Original Draft: MAL, SEG, EAG; Writing-Review and Editing: All authors

3.7 Acknowledgements

Figure 1

The DFU microbiome clusters into four Community Types. (A) DFU samples partitioned into four clusters by Dirichlet multinomial mixture model. Mean relative abundances of bacterial taxa in DFU samples assigned to each Community Type. Relative abundance is shown on the Y-axis. Taxa are filtered to those with a mean abundance greater than 1%. (B) Sample similarity between DFU microbial communities were calculated using the Bray-Curtis distance and these distances were ordinated via non-metric multidimensional scaling. Each taxonomic contribution to community differentiation is overlaid with black text and "x" indicating the exact location. The impacts of various metadata are depicted as vectors labeled with gray text. Samples, taxa, and metadata that are closer together are more related. Samples are color-coded based on community type.
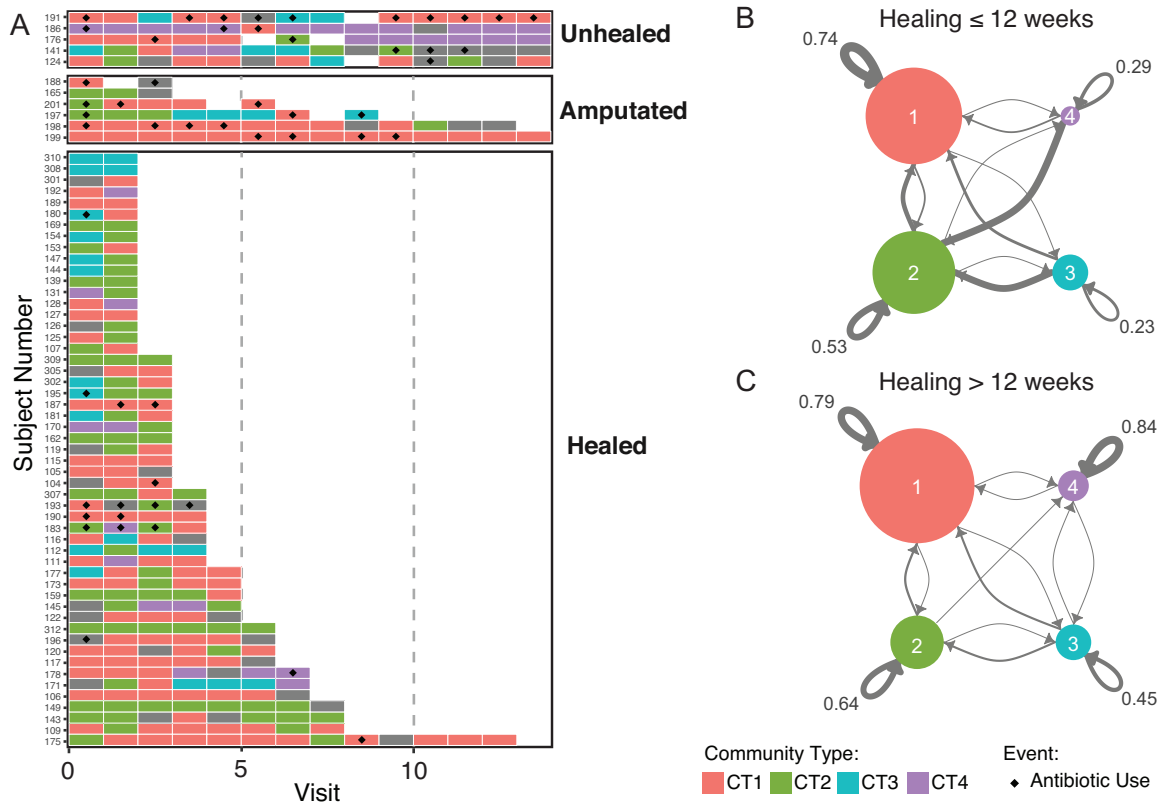
Figure 2.

DFU Community Types are dynamic. (A) Per patient illustration of Community Type switching grouped by outcome. Depicted on the X-axis is visit number. Each row on the Y-axis represents a subject with a DFU. Colored boxes illustrate which Community Type was colonizing the DFU at the indicated visit number. Empty tiles represent a missed visit, whereas gray tiles indicate that a sample was not collected or available for analysis at that time point. The black diamonds indicate that the patient received antibiotics since the last visit. Only subjects that participated in >1 study visit are shown. (B) Markov chain visualization depicting the differential transition probabilities between community types of DFUs that healed in 12 weeks or did not. Each node represents a Community Type, arrows indicate the transition direction and probability (thickness), node-size represents number of samples. Annotated are the self-transition probabilities.
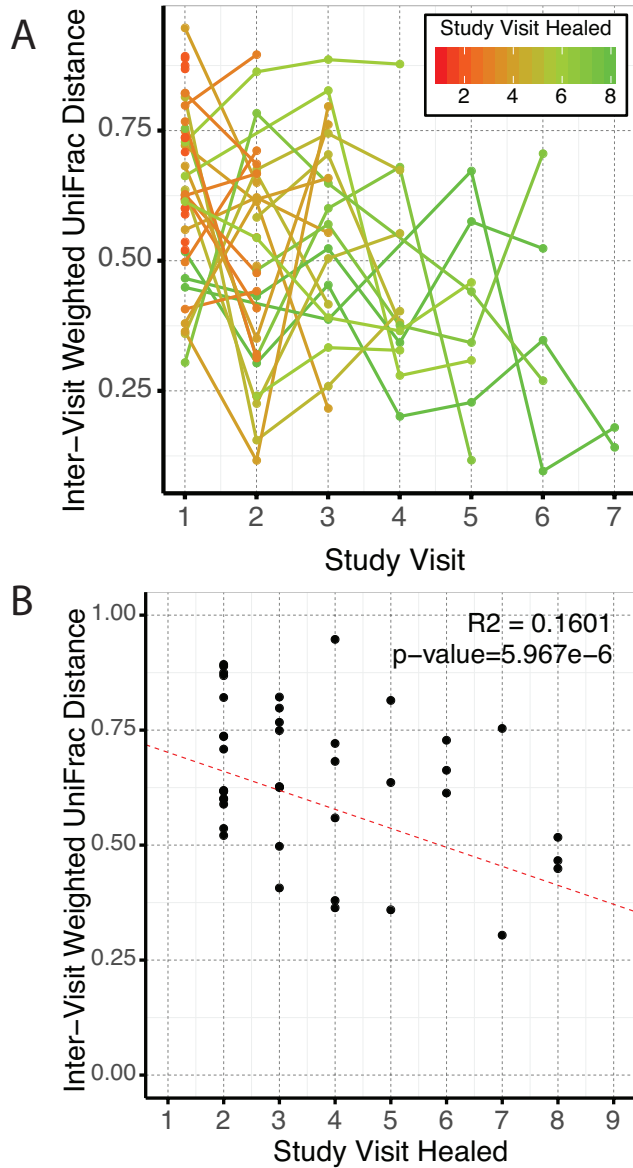
Figure 3

Inter-visit Weighted UniFrac distances associations with healing time for subjects that healed within 24 weeks. (A) Inter-visit distances are shown for each subject and depict a negative trend over time. Line and point colors represent the number of study visits that the ulcer persisted (red = 1, green = 8). Ulcers stabilize at a rate of -0.024/visit, but start at a lower rate in those ulcers that require more time to heal (-0.036 per visit required to heal). (B) Inter-visit distances between

baseline and first study visit as a function of number of visits until healing. A negative correlation

is found even within this initial comparison ($R^2 = 0.1601$, p<0.0001).
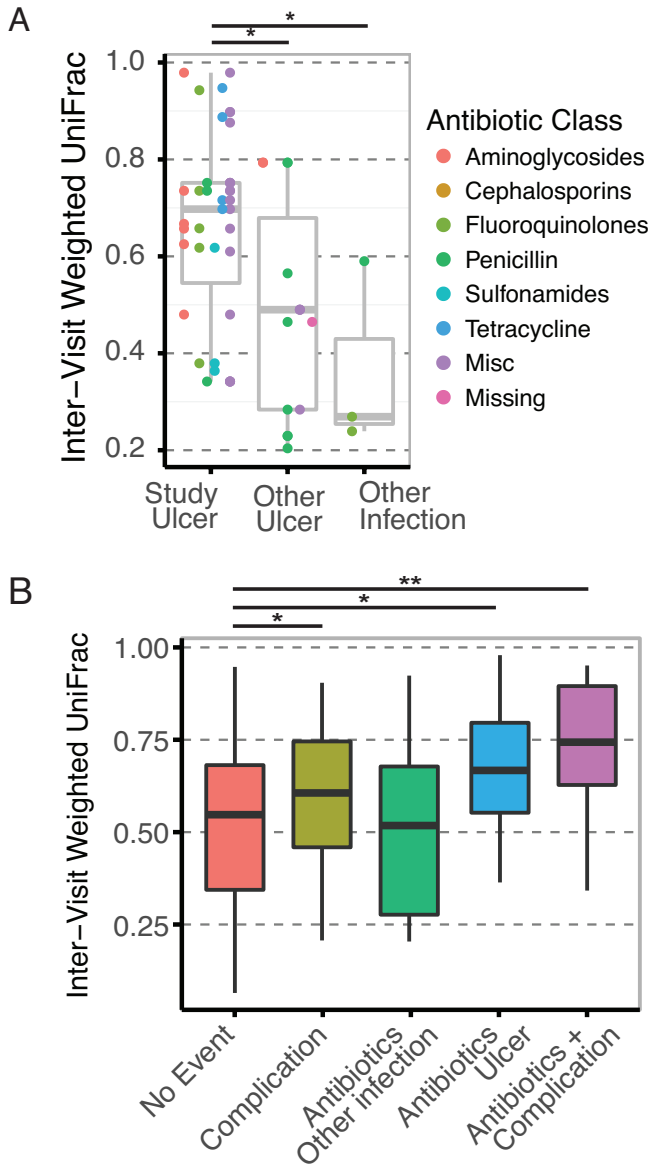
Figure 4

Effects of antibiotics on microbial communities in DFUs. (A) Boxplot showing the inter-visit Weighted UniFrac distances of subjects during exposure to antibiotics split by indication. Antibiotics given for the ulcer being studied produces greater community disruption than antibiotics given for other ulcers or other infections. Antibiotic class did not yield more information. (B) Boxplot showing the inter-visit distances of all samples binned by event type

42

(complication, antibiotics, both, or none). Antibiotics and ulcer complications both disrupt the microbiota, and their combined effect is additive.
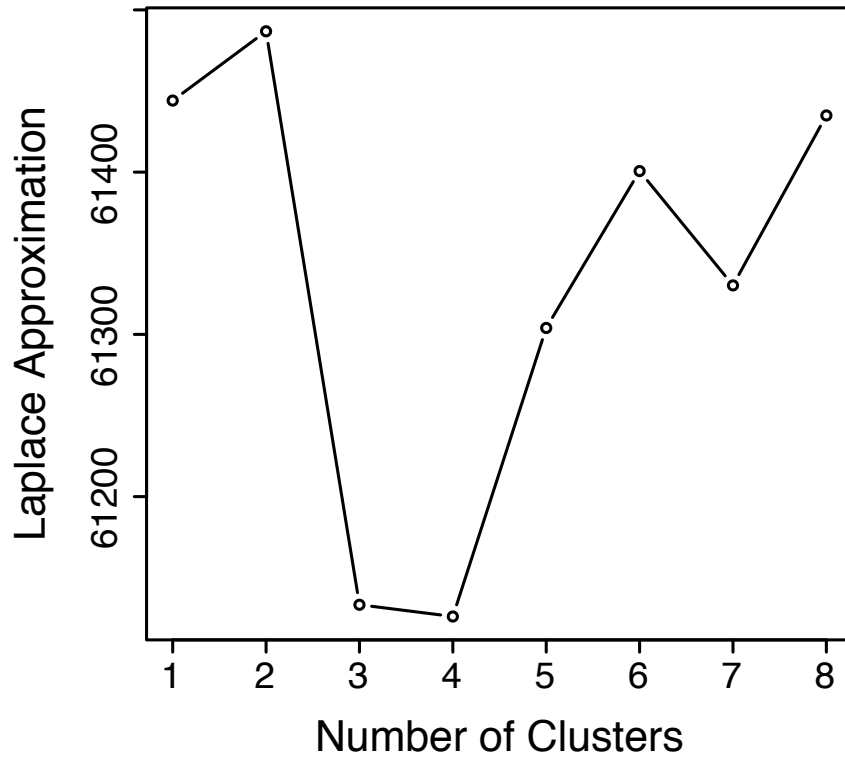
Figure S1

Laplace approximation predicts 4 clusters as optimal. The Laplace approximation of model evidence is a measure of the model fit. Lower values indicate better fits.

3.9 Tables

Characteristic	Total Sample (N=100)	Did not develop infection-related complication (n=69)	Developed infection-related complication (n=31)	‡p-value
Age (years), mean (SD)	54.1 (11.29)	55.4 (12.53)	52.3 (7.65)	0.136
Male sex, n (%)	78 (78.0)	56 (81.2)	22 (71.0)	0.3
White race, n (%)	91 (91.0)	62 (89.9)	20 (93.5)	0.498
Type 2 diabetes, n (%)	87 (87.0)	60 (87.0)	27 (87.1)	1
Duration of diabetes (years), mean (SD)	15.2 (11.31)	16.2 (11.55)	12.7 (10.55)	0.147
Baseline HbA1C (%), mean (SD)	8.2 (1.87)	8.32 (1.96)	8.0 (1.67)	0.461
Baseline WBC (mm3), mean (SD)	7950.5 (1905.97)	7751.5 (1916.58)	8387.1 (1837.52)	0.121
C Reactive Protein (mg/L), mean (SD)	2.2 (4.78)	1.7 (3.04)	3.2 (7.25)	0.284
Ulcer duration (weeks), mean (SD)	31.1 (40.22)	33.5 (42.46)	25.90 (34.81)	0.352
Toe/brachial pressure index, mean (SD)	0.9 (0.25)	0.9 (0.27)	0.9 (0.22)	0.803
Ulcer surface area (cm2), mean (SD)	2.4 (3.32)	2.0 (3.01)	3.3 (3.84)	0.101
Ulcer depth (cm), mean (SD)	0.3 (0.33)	0.2 (0.27)	0.4 (0.39)	**0.002***
Ulcer location, n (%)				
Forefoot	73 (73.0)	50 (72.5)	23 (74.2)	0.585
Midfoot	20 (20.0)	13 (18.8)	7 (22.6)	
Heel	7 (7.0)	6 (8.7)	1 (3.2)	
Transcutaneous oxygen level (mmHg), mean (SD)	46.9 (15.11)	49.1 (13.80)	42.2 (17.00)	0.057

Table S1

Patient and ulcer characteristics for the total sample and by complication status.

‡ continuous level characteristics were analyzed with an independent samples t-test; Dichotomous characteristics were analyzed with Fisher's Exact Test; Other categorical characteristics were analyzed with Pearson's Chi-Square. An asterisk (*) indicates p<0.05.

	Combined (n = 348)		Baseline (n = 89)		Rest (n = 259)	
	Samples	**Proportion**	**Samples**	**Proportion**	**Samples**	**Proportion**
Bacterial Taxon						
Staphylococcus	345	0.2277	86	0.2188049	259	0.2317
aureus	308	0.1331	79	0.1559	229	0.1257
pettenkoferi	287	0.0532	60	0.0290	227	0.0617
unclassified	301	0.0402	69	0.0308	232	0.0435
Streptococcus	318	0.1250	81	0.1918	236	0.1025
anginosus	51	0.0052	9	0.0008	42	0.0067
unclassified	317	0.1198	81	0.1910	235	0.0958
Corynebacterium	345	0.1121	86	0.0761	258	0.1249
Anaerococcus	300	0.0700	78	0.0745	222	0.0688
Planococcaceae	221	0.0401	58	0.0457	162	0.0383
Alcaligenaceae	194	0.0379	40	0.0020	153	0.0502
Paenibacillus	293	0.0364	79	0.0429	214	0.0342
Brevibacterium	222	0.0325	44	0.0070	177	0.0414
Comamonadaceae	321	0.0193	84	0.0227	236	0.0178
Finegoldia	245	0.0151	64	0.0111	181	0.0165
Helcococcus	207	0.0125	46	0.0144	160	0.0119
Pseudomonas	110	0.0109	20	0.0014	90	0.0142
Actinomycetales	151	0.0103	33	0.0048	118	0.0123

Table S2

Summary of microbial communities in DFU samples. For each bacterial taxon, the number of

samples in which it was present was tabulated, and the mean relative abundance was calculated.

These values were calculated for all samples, baseline only, and non-baseline samples. Taxa were

filtered to those whose mean abundance was greater than 0.01.

	CT 1	CT 2	CT 3	CT 4
Streptococcus	0.0466	0.0528	0.6175	0.0275
anginosus	0.0048	0.0083	0.0032	0.0000
unclassified	0.0418	0.0445	0.6143	0.0275
Staphylococcus	0.2759	0.1710	0.0975	0.3688
aureus	0.1205	0.1012	0.0918	0.3479
pettenkoferi	0.0880	0.0374	0.0026	0.0152
sciuri	0.0025	0.0001	0.0000	0.0000
haemolyticus	0.0001	0.0004	0.0001	0.0000
unclassified	0.0649	0.0320	0.0030	0.0057
Corynebacterium	0.1586	0.0885	0.0269	0.1191
simulans	0.0024	0.0042	0.0010	0.0001
stationis	0.0000	0.0000	0.0000	0.0000
unclassified	0.1563	0.0843	0.0259	0.1190
Anaerococcus	0.0370	0.0884	0.0623	0.1759
Planococcaceae	0.0539	0.0345	0.0050	0.0442
Brevibacterium	0.0385	0.0346	0.0016	0.0419
Paenibacillus	0.0582	0.0233	0.0058	0.0206
Alcaligenaceae	0.0479	0.0495	0.0061	0.0008
Helcococcus	0.0079	0.0114	0.0079	0.0440
Finegoldia	0.0114	0.0197	0.0095	0.0254
Comamonadaceae	0.0245	0.0246	0.0020	0.0009
Peptoniphilus	0.0054	0.0134	0.0095	0.0204
Actinomycetales	0.0056	0.0185	0.0076	0.0106
Porphyromonas	0.0023	0.0141	0.0123	0.0107
Prevotella	0.0101	0.0032	0.0135	0.0026

Table S3

Summaries of taxonomic composition by community type. The values shown are the mean

relative abundance for each community type. Only the top 25 taxa are shown. Species belonging

to the same genera are combined for convenience.

	Stationary Distribution		Expected Recurrence Time (weeks)	
	<12 weeks	>12 weeks	<12 weeks	>12 weeks
CT1	0.546	0.433	3.66	4.62
CT2	0.324	0.2012	6.17	9.94
CT3	0.0343	0.1341	58.28	14.91
CT4	0.0958	0.2317	20.89	8.63

Table S4

Estimated Markov chain parameters of DFU CT transitions. The values shown are 1) the

stationary distribution, which describes the expected frequencies of CTs to be for a Markov chain,

and 2) the expected recurrence time, which estimates the average time it would take to encounter

the same CT again. Both show marked changes in the stability and frequency of CT3 and CT4

between DFUs that heal within 12 weeks and those that do not.

2.10 References

Bickers DR, Lim HW, Margolis D, Weinstock MA, Goodman C, Faulkner E, et al. The burden of
skin diseases: 2004. Journal of the American Academy of Dermatology. 2006
Sep;55(3):490–500.

Brem H, Tomic-Canic M. Cellular and molecular basis of wound healing in diabetes. J Clin
Invest. 2007 May;117(5):1219–22.

Caporaso JG, Kuczynski J, Stombaugh J, Bittinger K, Bushman FD, Costello EK, et al. QIIME
allows analysis of high-throughput community sequencing data. Nat Meth. 2010
May;7(5):335–6.

Dethlefsen L, Relman DA. Incomplete recovery and individualized responses of the human distal
gut microbiota to repeated antibiotic perturbation. Proceedings of the National Academy of
Sciences of the United States of America. 2011 Mar 15;108 Suppl 1(Supplement_1):4554–
61.

DiGiulio DB, Callahan BJ, McMurdie PJ, Costello EK, Lyell DJ, Robaczewska A, et al.
Temporal and spatial variation of the human microbiota during pregnancy. Proceedings of
the National Academy of Sciences of the United States of America [Internet]. 2015 Aug
17;:201502875. Available from: http://www.pnas.org/lookup/doi/10.1073/pnas.1502875112

Ding T, Schloss PD. Dynamics and associations of microbial community types across the human
body. Nature. 2014 May 15;509(7500):357–60.

Dowd SE, Wolcott RD, Sun Y, McKeehan T, Smith E, Rhoads D. Polymicrobial Nature of
Chronic Diabetic Foot Ulcer Biofilm Infections Determined Using Bacterial Tag Encoded

FLX Amplicon Pyrosequencing (bTEFAP). Egles C, editor. PLoS ONE. Public Library of
Science; 2008 Oct 3;3(10):e3326.

Edgar RC. Search and clustering orders of magnitude faster than BLAST. Bioinformatics. Oxford
University Press; 2010 Oct 1;26(19):2460–1.

Flores GE, Caporaso J, Henley JB, Rideout J, Domogala D, Chase J, et al. Temporal variability is
a personalized feature of the human microbiome. Genome biology. 2014;15(12):531.

Gardner SE, Frantz RA. Wound bioburden and infection-related complications in diabetic foot
ulcers. Biol Res Nurs. SAGE Publications; 2008 Jul;10(1):44–53.

Gardner SE, Hillis SL, Heilmann K, Segre JA, Grice EA. The neuropathic diabetic foot ulcer
microbiome is associated with clinical factors. Diabetes. Am Diabetes Assoc;
2013;62(3):923–30.

Glaudemans AWJM, Uçkay I, Lipsky BA. Challenges in diagnosing infection in the diabetic foot.
Diabet Med. 2015 Jun;32(6):748–59.

Gontcharova V. A Comparison of Bacterial Composition in Diabetic Ulcers and Contralateral
Intact Skin. TOMICROJ. 2010 Aug 31;4(1):8–19.

Guariguata L, Whiting DR, Hambleton I, Beagley J, Linnenkamp U, Shaw JE. Global estimates
of diabetes prevalence for 2013 and projections for 2035. Diabetes Research and Clinical
Practice. 2014 Feb;103(2):137–49.

Holmes I, Harris K, Quince C. Dirichlet Multinomial Mixtures: Generative Models for Microbial
Metagenomics. Gilbert JA, editor. PLoS ONE. 2012 Feb 3;7(2):e30126.

Jenq RR, Ubeda C, Taur Y, Menezes CC, Khanin R, Dudakov JA, et al. Regulation of intestinal inflammation by microbiota following allogeneic bone marrow transplantation. J Exp Med. Rockefeller Univ Press; 2012 May 7;209(5):903–11.

Keeney KM, Yurist-Doutsch S, Arrieta M-C, Finlay BB. Effects of antibiotics on human microbiota and subsequent disease. Annual review of microbiology. 2014;68(1):217–35.

Lefcheck JS. piecewiseSEM: Piecewise structural equation modelling in r for ecology, evolution, and systematics. Methods Ecol Evol. 2015 Dec 1;:n/a–n/a.

Loïez C, Wallet F, Pischedda P, Renaux E, Senneville E, Mehdi N, et al. First case of osteomyelitis caused by "Staphylococcus pettenkoferi". Journal of clinical microbiology. American Society for Microbiology; 2007 Mar;45(3):1069–71.

Margolis DJ, Berlin JA, Strom BL. Interobserver agreement, sensitivity, and specificity of a "healed" chronic wound - Margolis - 2002 - Wound Repair and Regeneration - Wiley Online Library. Wound Repair and …. 1996.

Martinez C, Antolin M, Santos J, Torrejon A, Casellas F, Borruel N, et al. Unstable composition of the fecal microbiota in ulcerative colitis during clinical remission. - PubMed - NCBI. The American Journal of Gastroenterology. 2008 Mar;103(3):643–8.

Mayer BT, Srinivasan S, Fiedler TL, Marrazzo JM, Fredricks DN, Schiffer JT. Rapid and Profound Shifts in the Vaginal Microbiota Following Antibiotic Treatment for Bacterial Vaginosis. Journal of Infectious Diseases. 2015 Aug 6;212(5):793–802.

Meisel JS, Hannigan GD, Tyldsley AS, SanMiguel AJ, Hodkinson BP, Zheng Q, et al. Skin

Microbiome Surveys Are Strongly Influenced by Experimental Design. Journal of Investigative Dermatology. 2016 Jan.

Modi SR, Collins JJ, Relman DA. Antibiotics and the gut microbiota. J Clin Invest. American Society for Clinical Investigation; 2014 Oct 1;124(10):4212–8.

Morgan XC, Kabakchiev B, Waldron L, Tyler AD, Tickle TL, Milgrom R, et al. Associations between host gene expression, the mucosal microbiome, and clinical outcome in the pelvic pouch of patients with inflammatory bowel disease. Genome biology. BioMed Central; 2015;16(1):67.

Pinheiro J, Bates D, DebRoy S, Sarkar D. Linear and nonlinear mixed effects models. R package version. 2007.

Price LB, Liu CM, Melendez JH, Frankel YM, Engelthaler D, Aziz M, et al. Community analysis of chronic wound bacteria using 16S rRNA gene-based pyrosequencing: impact of diabetes and antibiotics on chronic wound microbiota. Ratner AJ, editor. PLoS ONE. 2009;4(7):e6462.

Prompers L, Huijberts M, Apelqvist J, Jude E, Piaggesi A, Bakker K, et al. High prevalence of ischaemia, infection and serious comorbidity in patients with diabetic foot disease in Europe. Baseline results from the Eurodiale study. Diabetologia. 2007 Jan;50(1):18–25.

Ramsey SD, Newton K, Blough D, McCulloch DK, Sandhu N, Reiber GE, et al. Incidence, outcomes, and cost of foot ulcers in patients with diabetes. Diabetes Care. 1999 Mar;22(3):382–7.

Stein RR, Bucci V, Toussaint NC, Buffie CG, Rätsch G, Pamer EG, et al. Ecological Modeling
from Time-Series Inference: Insight into Dynamics and Stability of Intestinal Microbiota.
Mering von C, editor. PLoS computational biology. 2013 Dec 12;9(12):e1003388.

Trülzsch K, Grabein B, Schumann P, Mellmann A, Antonenka U, Heesemann J, et al.
Staphylococcus pettenkoferi sp. nov., a novel coagulase-negative staphylococcal species
isolated from human clinical specimens. Int J Syst Evol Microbiol. 2007 Jul;57(Pt 7):1543–
8.

Valensi P, Girod I, Baron F, Moreau-Defarges T, Guillon P. Quality of life and clinical correlates
in patients with diabetic foot ulcers. Diabetes & Metabolism. 2005 Jun;31(3):263–71.

Wittebole X, De Roock S, Opal SM. A historical overview of bacteriophage therapy as an
alternative to antibiotics for the treatment of bacterial pathogens. Virulence. Landes
Bioscience; 2014 Jan 1;5(1):226–35.

Wolcott RD, Hanson JD, Rees EJ, Koenig LD, Phillips CD, Wolcott RA, et al. Analysis of the
chronic wound microbiota of 2,963 patients by 16S rDNA pyrosequencing. Wound Repair
Regen. 2015 Oct 14;:n/a–n/a.

Zhang M, Jiang Z, Li D, Jiang D, Wu Y, Ren H, et al. Oral Antibiotic Treatment Induces Skin
Microbiota Dysbiosis and Influences Wound Healing. Microb Ecol. 2014 Oct 10;69(2):415–
21.

R Core Team. R: A Language and Environment for Statistical Computing. Vienna, Austria; 2016.
Available from: https://www.R-project.org

CHAPTER 3 – Redefining the Chronic Wound Microbiome: Fungal Communities
Are Prevalent, Dynamic, and Associated with Delayed Healing

3.1 Contributions

The following chapter focuses on a project related to Chapter 2 that I contributed to intellectually
and analytically. Specifically, I assisted in the statistical analyses and generation of figures 1, 4,
S5, and S6.

The contents of this chapter have been accepted for publication as:

3.2 Abstract

Chronic non-healing wounds have been heralded as a silent epidemic, causing significant
morbidity and mortality especially in elderly, diabetic, and obese populations. Polymicrobial
biofilms in the wound bed, are hypothesized to disrupt the highly coordinated and sequential
events of cutaneous healing. Both culture-dependent and -independent studies of the chronic
wound microbiome have almost exclusively focused on bacteria, omitting what we hypothesize
are important fungal contributions to impaired healing and development of complication. Here we
show for the first time that fungal communities (the mycobiome) in chronic wounds are
predictive of healing time, associated with poor outcomes, and form mixed fungal-bacterial

biofilms. We longitudinally profiled 100, non-healing diabetic foot ulcers with high-throughput

sequencing of the pan-fungal internal transcribed spacer 1 (ITS1) locus, estimating that up to 80%

of wounds contain fungi, whereas cultures performed in parallel captured only 5% of colonized

wounds. The 'mycobiome' was highly heterogeneous over time and between subjects. Fungal

diversity increased with antibiotic administration and onset of a clinical complication. Proportions

of the phlyum Ascomycota were significantly greater (p=0.015) at the study onset in wounds that

took >8 weeks to heal. Wound necrosis was distinctly associated with pathogenic fungal species,

while taxa identified as allergenic filamentous fungi, were associated with low levels of systemic

inflammation. Directed culturing of wounds stably colonized by pathogens revealed that inter-

kingdom biofilms formed between yeast and co-isolated bacteria. Combined, our analyses

provide enhanced resolution of the mycobiome during impaired wound healing, its role in chronic

disease, and impact on clinical outcomes.

3.3 Importance

Wounds are an under-appreciated but serious complication for a diverse spectrum of

diseases. High-risk groups, such as persons with diabetes, have a 25% lifetime risk of developing

a wound that can become chronic. The majority of microbiome research related to chronic

wounds is focused on bacteria but the association of fungi with clinical outcomes remains to be

elucidated. Here we describe the dynamic fungal communities in 100 patients with diabetic foot

ulcers. We found that communities are unstable over time, but at the first clinical presentation, the

relative proportions of different phyla predict healing times. Pathogenic fungi not identified by

culture reside in necrotic wounds, and are associated with poor prognosis. In wounds stably

colonized by fungi, we identified yeast capable of forming biofilms in concert with bacteria. Our findings illuminate the associations of the fungal mycobiome with wound prognosis and healing.

3.4 Introduction

In recent years, the implication of microorganisms in complex human processes has begun to come into focus. Negative consequences of these interactions can result in large health-care burdens such as non-healing or chronic wounds (1-5). One example is diabetic foot ulcers (DFUs), which contribute to 80% of non-traumatic lower-extremity amputations and are associated with five-year mortality rates of 43-55%, higher than Hodgkin's disease, breast cancer or prostate cancer(6-8). Chronic wounds are largely believed to be critically colonized by polymicrobial communities that contribute to persistent inflammation and stalled healing processes, significantly reducing the quality of life for those inflicted(9-11). The skin normally harbors diverse communities of microbes(12-17) that can contribute to health, but like other ecosystems, the niche can direct composition and ultimately function(18-20). In tissue injury, microbes enter the wound where the physical environment differs from the skin surface in temperature, pH, nutrient availability, and host immune effectors. Here, microbial metabolism can shift, providing opportunities for commensal microbes to become virulent and community compositions to fluctuate in response to host clinical factors(21-23). It is hypothesized that once colonization occurs these communities form a biofilm within the wound, disrupting the coordinated tissue regeneration process. This is also true in other chronic infections, such as cystic fibrosis (CF) where the environment of the CF lung allows for colonization(24), unlike the healthy lung from which microbes can be cleared .

Prior research has primarily focused on the role of bacterial species in wound healing(10, 23, 25-30); however, the skin is also host to resident fungi and our environment is rich with fungal diversity(31-34). Many human commensal fungi or yeast are also opportunistic pathogens, and many species are known to be prolific biofilm formers(34-38). There are few studies describing the 'mycobiome' portion of the human microbiome and it's relation to health(32, 34, 39-41), while the incidence of fungal colonization in chronic wounds is even less known. A previous cross-sectional study of chronic wounds of mixed etiology and without standardized treatment utilized molecular-based methods to observe that up to 23% of chronic wounds contain fungi (41). Chellan *et al.* studied 518 diabetic lower leg wounds and detected fungi in 27% of samples with culture-based methodology(42). In these studies, several aspects of the cross-sectional study design limit the ability to draw conclusions. These designs preclude longitudinal observation of fungal colonization, and the relationship to clinical outcomes (i.e. rate of healing, infection-related complication), while controlling for clinical variables such as tissue perfusion or blood glucose control.

Here, we add a new perspective to the current models of impaired wound healing with a longitudinal study of 100 DFUs under standardized treatment. High-throughput sequencing of the nuclear ribosomal internal transcribed spacer 1 (ITS1) allowed us to define the dynamic diversity of the mycobiome, its stability in response to host factors, and the association of pathogenic fungi with poor clinical outcomes.

3.5 Results

3.5.1 Study overview

To minimize variability associated with wound etiology, we limited our study to a single wound etiology consisting solely of DFUs. Subjects were enrolled into the study and wound specimens were obtained every two weeks until the wounds healed, another infection occurred, the wounds resulted in amputation, or were not closed after 26 weeks (Visit 0 -12). Table 1 summarizes the cohort where a total of 384 specimens were collected from 100 DFUs in a sample of 100 subjects. Additional clinical factors measured include white blood cell count (WBC), ankle-brachial index (ABI), toe-brachial index (TBPI), hemoglobin A1c, glucose (HgbA1c), C Reactive Protein, and transcutaneous oxygen levels of the wound edge. Monofilament testing confirmed neuropathy in all subjects. Complications were experienced by 31 (31%) subjects defined as: 1) wound deterioration, 2) development of osteomyelitis, and/or 3) amputations.

The fungal component of DFU microbiomes was studied by sequencing the hypervariable internal transcribed spacer 1 (ITS1) region of the eukaryotic ribosomal RNA cistron using the Illumina MiSeq platform (2x300 PE chemistry). The ITS region has been formally recognized as the universal barcode for fungal identification(43) so we elected to use this region and the curated fungal barcode reference database UNITE(44) for operational taxonomic unit (OTU) assignment. We employed the PIPITS pipeline(45) because it extracts the ITS sub-region from raw reads and assigns taxonomy with a trained RDP Classifier(46). Of the 10,673,363 sequences, 10,593,779 sequences were identified as containing an ITS1 subregion. DNA from *Saccharomyces cerevisiae* was detected in the medium in which the wound samples were collected, and therefore all OTUs identified at the genus or species level as *Saccharomyces* were filtered from the data set, resulting in removal of 3 phylotypes. After quality filtering and

58

contaminant removal, 2,842,822 reads remained, resulting in 482 OTUs and taxonomic

identification yielded 284 phylotypes.

3.5.2 Characterization of the DFU Fungal Mycobiome

Seventeen phylotypes were identified in >1% relative abundance across the entire dataset,

all belonging to the phyla Ascomycota or Basidiomycota. The two most abundant taxa were

Ascomycota corresponding to *Cladosporidium herbarum* (teleomorph *Davidiella tassiania*),

present in 41% of the samples and 56% of subjects, followed by *Candida albicans* (22% of

samples; 47% of subjects). Notably, 10 of the 17 most abundant taxa are Ascomycetes

filamentous fungi found ubiquitously in the environment, while the most abundant

Basidiomycota identified were opportunistic yeast pathogens *Trichosporon* and *Rhodosporidium*

spp. (Table 2, Figure 1A).

Malassezia species are reported as a major component of the healthy skin

mycobiome(32) and were detected in >0.05% abundance in 26 subjects in a total of 36

specimens, but only seven specimens had >10% relative abundance of *Malassezia* species. This

observation is not unexpected as *Malassezia* spp. are lipid dependent and the foot is known to

have overall lower abundances of *Malassezia* spp. relative to other body site niches(32, 47), in

part due to absence of sebum in this microenvironment and in the wound itself.

A major current limitation of molecular DNA sequencing based analysis of the

mycobiota is representation of fungal species in available reference databases. It is estimated that

sequence data is available for a mere 1.5% of the estimated 1.5 million fungal species(46).

Indeed, 32% of the DFU samples contained OTUs that could not be assigned beyond the kingdom level and 16% of samples contained OTUs unclassified beyond phylum Ascomycota (Table 2). Limitations of reference databases necessitate the use of reference-independent analyses to characterize diversity and variation of fungal communities. Alpha diversity metrics use reference-independent OTU data to summarize diversity, such as number of OTUs in a sample and their evenness. We analyzed DFU mycobiome alpha diversity with respect to wound health and inflammation factors measured at the patient- and ulcer-level (Supplementary Figure 1 and Supplementary Table 1). At baseline, diversity measured as the number of observed species-level OTUs (median=6; range=1-21) and Faith's PD (median=4.64; range=1.31-14.92) was negatively associated with tissue oxygenation (rho=-0.258, p=0.046; rho=-0.295, p=0.022, respectively) (Supplementary Figure 1), suggesting that high fungal diversity is associated with poor perfusion. As measured by the Shannon Diversity Index, which takes into account both richness and evenness of OTUs, ulcers on the forefoot were more diverse (median=1.03; range=0-3.83) compared to hindfoot ulcers (median=0.51; range=0-1.65; Wilcoxon rank sum test; p=0.02) with midfoot ulcers falling in between (median=0.95; range=0-3.15) to create a gradient of diversity (Figure 1B). The number of observed species-level OTUs did not significantly differ between the forefoot and hindfoot indicating that evenness of differentially abundant OTUs contribute to topographical variability of the mycobiome. Decreased Shannon Diversity appears to be primarily driven by a significant increase in the relative abundance of *C. albicans* in ulcers formed on the hindfoot (Figure 1C; Supplementary Table 2).

At each study visit, wound specimens were also collected for quantitative cultures. Three subjects were culture positive for yeast isolates categorized as "skin flora" or "other" and two subjects were positive for *Candida* sp. at one study visit. In all five cases, the study visit positive

for yeast culture was concurrent with or preceded the study visit of a complication (Supplementary Figure 2). With a culture-independent sequence-based approach, after quality and contaminant filtering, 275 of the 384 samples analyzed, corresponding to 79 subjects, were positive for at least one fungal phylotype (Table 1). The culture positive specimens were confirmed by ITS1 sequencing to contain high relative abundances of *Candida* spp (*C. albicans, C. glabrata*) with the exception of one subject specimen containing primarily *Trichosporon asahii*. Our analysis identified these same species and others in additional study visits (Supplementary Figure 2). For these subjects, we also compared the bacterial communities (obtained by 16S rRNA gene sequencing and reported in(48)) and discovered in some cases, such as subject 194 and 198 (visit 0), fungal identification resulted in the absence of bacterial taxa in the specimen. However, for the majority of wound specimens, mixed fungal-bacterial communities were observed (Supplementary Figures 2,3A).

3.5.3 The DFU Mycobiome Has High Interpersonal and Intrapersonal Variation

A striking feature of DFU fungal community structures was the absence of a core mycobiome or shared taxa across the study cohort (Figure 1A). We assessed the temporal stability of fungal communities over time by calculating the weighted UniFrac distances (WUF) between study visits within a single subject. We compared this to mean interpersonal WUF distances at their baseline visit. Mean interpersonal WUF distances were significantly greater than mean intrapersonal WUF distances (Figure 1D), suggesting that interpersonal variability is greater than intrapersonal variability. However, a high level of dissimilarity occurred in both groups (mean = 0.71 vs 0.67, respectively; Wilcoxon rank sum test; $p<0.0001$). At the taxonomic level, community structure was ephemeral, with taxa sometimes appearing or disappearing within one study visit (Figure 2).

High rates of change between study visits suggest transient colonization or environmental contamination of the wound bed by fungi. Contrary to this hypothesis is the standardized care employed in this study, where a total contact cast (TCC) (n=87) or a DH Boot (n=13) was applied for offloading following wound cleansing and dressing. TCC results in creation of an occlusive environment for the entire foot, minimizing influence from the external environment. We examined the mycobiome community stability of ulcers offloaded with TCC and DH Boot, but did not observe significant differences between the two offloading methods (data not shown).

3.5.4 The DFU Mycobiome is Associated with Clinical Outcomes

We next determined if the DFU mycobiome was associated with clinical outcomes. An ideal biomarker would differentiate wound outcomes at initial patient presentation; therefore, we analyzed the mycobiomes of the baseline study visit (Visit 0) with respect to outcomes, in addition to analyses incorporating all longitudinal data. At the baseline study visit, Ascomycota were present in significantly greater relative abundance in wounds that healed in >8 weeks compared to those that healed in <4 weeks (Tukey post-hoc; p=0.017). This distribution was only significant at the initial presentation and did not significantly differ by healing time of all the later visits combined (Figure 3A). Baseline specimens were taken at the initial clinical presentation and before the wound was surgically debrided of dead tissue and/or biofilms, but the specimens were obtained over viable wound tissue, not necrotic tissue. This suggests that the mycobiome at the presentation visit can be predictive of time to heal.

We also assessed stability of the mycobiome and its association with outcomes. Inter-visit WUF was not associated with healing outcome; healed, unhealed or amputated wounds

62

display high levels of change over time that were not significantly influenced by a clinical complication or administration of an antibiotic (Figure 3B, C). Although the mean WUF values were >0.5, indicating high rates of change, in some cases, a trend was observed in subjects that ultimately required an amputation, where the WUF values were lower, meaning mycobiomes from sequential visits were less dissimilar. This suggests a more stable colonization of the fungal community, and potentially implicates the formation of a biofilm or infection leading to subsequent chronicity. This is exemplified in the bottom panel of Figure 2 (subject 198) where the first three study visits of this particular subject were dominated by *Trichosporon asahii* followed by a shift to a predominant population of *C. herbarum* in the later visits. Conversely, the bacterial community stability in this subject is low during the first three visits, until the fungal community shifts and stability for both groups then follows the same general pattern. Similar trends are observed in other subjects and indicates that the stability of the fungal community structure is not independent from co-habitating bacterial community stability (Supplementary figure 3B).

Antibiotics were administered to 31 of 100 subjects at some point during the course of the study. We hypothesized that antibiotic treatment would influence the fungal portion of the microbiome in response to observed bacterial perturbation and disruption (48). In subjects that received antibiotics, the Shannon diversity indices for all visits combined were significantly higher than those subjects who did not receive an antibiotic (Wilcoxon rank sum test; p=0.029). However, diversity over time did not significantly fluctuate before, during or after antibiotic administration. We also examined the class of antibiotic administered and discovered it was non-discriminating in influencing the overall diversity metrics in these subjects (Supplementary Figure 4). In samples from study visits where a complication occurred, Shannon diversity was

also significantly higher (mean=0.98 vs 1.30; Wilcoxon rank sum test; p<0.001) but visits with complications only co-occurred with visits of antibiotic administration 45% of the time (41/91 total visits).

3.5.5 Pathogens versus allergens in the DFU mycobiome

We elected to bin taxa into the categories "pathogens" or "allergens", because with respect to the skin and cutaneous infection, the majority of taxa identified in our dataset fell into one of these two groups of either known/opportunistic skin pathogens or the filamentous fungi often identified as allergenic molds (Figure 4A). While some members of the "allergens" group, such as *Aspergillus* spp., can also be opportunistic pathogens, this is rare in the context of skin and cutaneous infection so we limited their classification. We first assessed associations between the list of allergen and pathogen phylotypes and the taxa listed in Table 2 using Spearman rank correlations. Taxa correlations were then subjected to hierarchical clustering via hclust. The allergens and pathogens clustered separately, discriminated by their associations with six key taxa (*Aspergillus cibarius, Penicillium bialowiezense, Epicoccum nigrum, Pencillium sp., Trichopsoron asahii and Candida albicans*). Allergens had positive associations with all six, whereas pathogens did not exhibit any strong associations, positive or negative. (Supplementary Figure 5).

With respect to clinical outcomes, a trend emerged where the mean proportions of pathogens were higher in non-healing wounds and those that ultimately resulted in amputation, as compared to wounds that healed, though this trend was not statistically significant (Figure 4B). The mean proportion of allergens was unchanged across all outcome groups (data not shown).

64

We also examined mean relative abundance of allergens and pathogens with respect to necrosis, because the level of necrotic wound tissue may indicate wound health or deterioration. Strikingly, in wounds with 75-100% necrotic tissue the proportion of allergens is reduced and a highly significant increase in the proportions of pathogens is observed ($p<0.001$; analysis of variance and Tukey post-hoc analysis) (Figure 4C). To better visualize this distribution across samples, we constructed an independently calculated weighted UniFrac distance ordination plot overlaid with the relative proportion of allergens, pathogens and the level of necrotic tissue in each sample. Clear separation is observed between the two groups and pathogens are predominantly found in those samples with high levels of necrosis (Figure 4D).

Since pathogens may directly contribute to wound necrosis and negative outcomes, the most severe being amputation, we further examined all possible associations between additional clinical factors and the relative abundance of pathogens and allergens, and the two dominant taxa in each of those groups (*C. albicans* and *C. herbarum* respectively). By Spearman rank correlation, allergens were negatively associated with HgbA1c levels (rho=-0.308, p=0.02) and WBC counts (rho=-0.346, p=0.009), suggesting that glucose control and lower levels of inflammation are consistent with allergen colonization (Supplementary Figure 1). Specifically, *C. herbarum* was negatively associated with HgbA1c (rho=-0.405, p=0.002) but positively associated with the ulcer surface area (rho=0.348, p=0.008) and days in the study (rho=0.279, p=0.038) (Supplementary Figure 1). Because the culture positive samples co-coincided with wound deterioration and the mean proportion of the group "pathogens" is elevated in non-healing wounds and necrosis, we looked for associations between both *Candida* spp. and the pathogens group to clinical factors but no additional significant associations were identified (Supplementary Figure 1).

65

3.5.6 The DFU Mycobiome Forms Multi-Species Biofilms with Bacteria

We hypothesized that biofilm formation occurred in those ulcers where a pathogenic fungal species was detected. Cultures were obtained from samples collected from subjects 145 and 198, representing delayed (>6 weeks) but healed and amputated wounds, respectively (Figure 2). *C. albicans* was isolated from subject 145 and *T. asahii* from subject 198. Samples from these subjects also grew the bacterial isolates *Citrobacter freundii* (subject 145) and *Staphylococcus simulans* (subject 198). The ability for each isolate to form a biofilm as mono-culture or co-culture was assessed and confirmed visually by confocal microscopy. The yeast-bacteria pairs (*C. albicans + C. freundii; T. asahii + S. simulans)* readily grew as co-culture on agar plates. Biofilm growth was observed for mono-culture of each yeast strain with distinct hyphal growth of *C. albicans* and chains or clumping of cells for *T. asahii*. The bacterial strains were also able to grow as biofilms in mono-culture, forming distinct micro-colonies although in a more dispersed and confluent layer than the yeast mono-cultures (Figure 5). Mixed-species biofilms formed within 24 hours and further matured over 48 hours. The co-cultures revealed close interactions between bacterial and yeast cells. The yeast appears to form the 'core' of the colony and bacteria associate around the periphery of the cells, coating yeast cells and hyphae as they grow out of the plate to approximately 30 µM thick for *C. albicans + C. freundii* and 15 µM thick for *T. asahii* and *S. simulans* after 48 hours (Figure 5). These observations coupled with quantitative counts of the planktonic and biofilm mono- or co-cultures (Supplementary Figure 7) suggest that the yeast and bacterial species interact in a non-competitive manner to form mixed biofilms.

To assess fungal-bacterial interactions with a more global view we determined Spearman rank-correlations between the fungal and bacterial taxa found in >1 % abundance in the entire

dataset. *Corynebacterium sp.* in the order Actinomycetales, was significantly negative correlated

with *C. albicans* and *C. parapsilosis*. Members of the Actinomycetales are historically rich

sources of bioactive small molecules. On the other hand, *C. albicans* was significantly positively

correlated with the order Alcaligenaceae, a group of Gram-negative Proteobacteria.

3.6 Discussion

Chronic non-healing wounds are host to polymicrobial communities that can form

biofilms and interfere with healing processes. Here we utilized high-throughput sequencing of the

ribosomal RNA internal transcribed spacer ITS1 amplified from DFU specimens collected

longitudinally to demonstrate that DFUs contain a diverse repertoire of fungi not recognized

clinically or by traditional culture procedures. Our study is the first to identify fungi in a large

proportion (80%) of DFUs surveyed. The longitudinal aspect of our study design and

standardized care protocol establishes that the mycobiome is highly dynamic and transient in

DFUs, with increased fungal diversity in subjects administered antibiotics or experiencing a

complication. While the subset of subjects on antibiotics was not large enough to allow for

detailed investigation into the short- and long-term effects on the mycobiome, future studies are

warranted, incorporating both fungal and bacterial community dynamics in response to antibiotic

perturbation.

Studies of the mycobiome in chronic disease are not abundant. It was striking to us that

C. herbarum was the most abundant species found in ≥ 1 sample from 56% of our subjects.

Although this saprophytic dematiaceous fungus is widespread in the environment, it has been

reported as one of the most common fungal species associated with the human body across

67

different body sites including the oral, nasal, vaginal and gut mycobiomes(31, 34, 49-51). Not only are *Cladosporium* spp. sensitizing agents leading to allergic rhinitis, but they are linked to other human diseases including an outbreak of fungal meningitis in 2012(52), and recently *Cladosporium* spp. were identified in 92 clinical specimens with 28% of those coming from superficial and deep tissues(53). Together, these data indicate that *Cladosporium* spp. should be regarded as a member of the human mycobiome.

Candida albicans was the second most abundant phylotype identified, present in 47 subjects and 21% of samples. Other species identified were *C. parasilopsis* (15%), *C. tropicalis* (9.76%), *C. glabrata* (3.7%), and *C. smithsonii* (2.9%), while *C. boleticola*, *C. dubliniensis*, *C. orthopsilosis*, *C. metapsilosis*, and *C. xylopsoci* were found in less than 3% of the samples. *Candida* abundance can fluctuate during gut microbiome dysbiosis, for instance by antibiotic administration early in life, and has been associated with asthma and allergic airway response to fungal allergens(54-56). Specifically, overgrowth of *Candida albicans* in the gut microbiome of mice can provoke sensitization resulting in a CD4+ T-cell mediated response to mold spores that is not observed in mice without microbiota disruption(57). It is not clear if similar responses occur in other tissues and body sites, or if this response is isolated to the gut-airway axis. The DFU mycobiome is primarily composed of a balance of commensal and pathogenic yeasts (*Candida* spp, *Trichosporon* spp.) and a heterogeneous population of anamorphic fungi recognized as important causes of respiratory allergies(58). Instability in communities both inter- and intra-individually suggests transient or superficial colonization of the DFUs by spores, highlighting an important limitation to sequence based studies: the inability to determine active metabolism. In this context however, it is tempting to imagine a scenario by which exposure to

fungal spores and their antigens is sufficient to provoke an immunological response that contributes to prolonged inflammation and stalled healing.

Poor perfusion is a hallmark of DFUs and can contribute to impaired healing. Increased fungal diversity in DFUs with reduced oxygenation is consistent with our finding that biofilm forming yeasts and opportunistic skin commensal pathogens were highly significantly and strongly associated with wound necrosis and poor outcomes. This association was not driven by a single species but a mixed group of pathogens.

This study provides the foundation for further dissection of microbial interactions and their profound influence on disease progression. Here, we demonstrate the ability of DFU isolated yeast-bacterial pairs to form mixed biofilms. Two pairs were cultured from DFUs identified as having a stable community by our molecular analysis and used to validate fungi-bacteria biofilm formation. To our knowledge there is little information regarding interactions between *C. albicans* and *C. freundii* or *T. asahii* and *S. simulans*. Our *in silico* analysis also suggests that an antagonistic interaction is occurring between *Candida sp.* and *Corynebacterium* sp. Continued exploration to determine the magnitude and mechanisms of microbiome interactions in contributing to impaired healing and skin and soft tissue infection is an important and timely area of research. Observation of diverse fungal communities in chronic non-healing wounds and their ability to form inter-kingdom biofilms with both Gram-negative and Gram-positive bacterial species emphasizes the paramount importance but also complexity of studying whole microbial communities, their inter-species interactions and implications in chronic disease.

3.7 Materials and Methods

3.7.1 Study Design

During September 2008 through October 2012 100 subjects were enrolled in a prospective-cohort to sample the DFU microbiota and measure outcomes. Subjects were recruited through local media advertisements and from outpatient clinics at the University of Iowa Hospitals and Clinics (UIHC) and the Iowa City Veteran's Affairs Medical Center (VA). Samples for microbiota analyses were collected at initial presentation (V0) and every two weeks until the DFU: i) healed; ii) was amputated; or iii) 26 week of follow up elapsed (V1-12). The Institutional Review Boards at the University of Iowa (IRB#200706724) and the University of Pennsylvania approved the study procedures (IRB#815195). Informed consent was obtained from all participants in writing.

Wound management was standardized to aggressive sharp debridement of necrotic tissue in the wound bed at baseline and wound edge callus removal every two weeks followed by non-antimicrobial dressing application (i.e., Lyofoam®, Molnlycke Health Care). Ulcers were offloaded with total contact casts (87 subjects) or DH boots (13 subjects). Topical antimicrobial or system antibiotic administration was not included unless an infection-related complication was present at baseline or occurred within the study period. Data was collected at baseline and longitudinally every two weeks until the wound healed or 26 weeks elapsed.

3.7.2 Study Variables

Clinical factors: Demographic variables were collected at the baseline visit including age, sex, diabetes type and duration and duration of the study ulcer using subject self-report and medical records. At each study visit glycemic control was measured by levels of haemoglobin

70

A1c and blood glucose. Inflammatory (Erythrocyte sedimentation rate (ESR), C-reactive protein) and immune (white blood cell counts) markers were determined with standard laboratory tests. Each subject was also assessed for ischemia using the ankle-brachial and toe-brachial index and for neuropathy using the 5.07 Semmes-Weinstein monofilament test. Transcutaneous oxygen pressure was measured at baseline and at each follow-up visit, using a transcutaneous oxygen monitor (Novametrix 840®, Novametrix Medical Systems Inc.). Ulcer location was categorized as forefoot, midfoot, or hindfoot. The level of necrotic tissue was defined as black, grey or yellow tissue in the wound bed measured using a likert scale as the percentage of the total wound area binned according to 0-25%, 25-50%, 50-75% or 75-100% necrotic tissue.

Outcomes: Healing and infection-related complications were assessed every two weeks. Ulcer closure was determined using the Wound Healing Society's definition of "an acceptably healed wound," a valid and reliable definition(59). "Development of infection-related complications" was defined as wound deterioration, new osteomyelitis, and/or amputations due to DFU infections.

Wound deterioration was defined as the new development of frank erythema and heat, and an increase in size > 50% over baseline. Two members of the research team independently assessed each DFU for erythema and heat. Two members of the research team independently assessed size using the VeVMD® digital software system (Vista Medical, Winnipeg, Manitoba, Canada) and procedures previously described(60). A cotton-tipped swab, placed in the deepest aspect of the DFU, was marked where the swab intersected with the plane of the peri-wound skin. The distance between the tip of the swab and the mark was measured as ulcer depth using a centimeter ruler.

71

Osteomyelitis was assessed using radiographs and MRI at baseline and during follow-up visits when subjects presented with new tracts to bone, wound deterioration, elevated temperature, elevated white count, elevated erythrocyte sedimentation rate, or elevated C-reactive protein. If these indicators were absent at follow-up, radiographs were not retaken. Subjects experiencing new amputations had their medical records reviewed by the research team to ensure amputations were due to DFU infection, and not some other reason.

Sequencing of fungal ITS1 rRNA region: Ulcer specimens were collected using the Levine technique and established protocols(61). DNA was isolated from swab specimens as previously described(21). The ITS1F (CTTGGTCATTTAGAGGAAGTAA) and ITS2R (GCTGCGTTCTTCATCGATGC) primers were used for PCR amplification, each having a linker sequence, a sample specific GoLay12 index, and an Illumina adapter to amplify the ITS1 region of the fungal rRNA region. These indexed primers were used in combinations that made it possible to multiplex up to 576 (24 x 24) samples at a time. Each sample (along with one mock community, three buffer controls and two water controls) was amplified in duplicate, combined, and cleaned using the Agencourt AMPure XP bead-based PCR purification system (Beckman-Coulter). PCR reactions contained 9.65 μL PCR-clean water, 1.25 μL 10X Accuprime Buffer II (Invitrogen), 0.1 μL Accuprime High Fidelity Taq (Invitrogen), 0.25 μL each of the forward and reverse primers (at 10 μM concentration), and 1.0 μL genomic DNA. Reactions were held at 94°C for 3 min to denature the DNA, with amplification proceeding for 35 cycles at 94°C for 45 s, 56°C for 60 s, and 72°C for 90 s; a final extension of 10 min at 72°C was performed. Purified amplicon pools were quantified using the Quant-IT dsDNA High-Sensitivity Assay Kit (Invitrogen) and a microplate reader (Thermo Scientific). A composite sample for sequencing

was made by combining equimolar ratios of amplicons from the samples, followed by gel

purification with a Qiagen MinElute Gel Extraction Kit to remove potential contaminants and

PCR artifacts (the acceptable size window for amplicons was 200-1000 bp in length). The pooled

DNA was quantified using a Qubit Fluorometer (Life Technologies), and PhiX174 genomic DNA

was spiked in to the sample at ~40% prior to sequencing. MiSeq 300 bp paired-end 'V3'

sequencing was performed. Additional negative controls were processed as above, except the

ITS1F and ITS2R primers were used without barcoded adapters and amplicons were sequenced

by standard Sanger sequencing.

The MiSeq ITS libraries were preprocessed using an in-house pipeline that includes read QC,

barcode de-multiplexing, paired-end assembly and linker cleaning steps. The pipeline procedures

are briefly explained below.

1. Read QC. Raw read quality was checked for the average and range of the Phred quality

    scores along the reads (1~300 bp) for both forward and reverse reads independently.

2. Read de-multiplexing. Our MiSeq ITS library construction protocol utilizes a customized

    barcode system with both forward & reverse barcodes embedded near the 5' of both reads;

    thus, the forward and reverse barcodes are first spliced and concatenated from the

    corresponding reads, then read-pairs are de-multiplexed using the Flexbar program (v2.4)(62)

    with default settings.

3. Paired-end assembly. De-multiplexed paired-end reads are assembled (merged) using the

    PEAR (v0.9.0) program(63) with default settings.

4. Barcode/linker cleaning. Our customized barcode/primer system incorporates a linker region between the actual barcodes and PCR primers to increase the heterogeneity of the amplicons for successful Illumina sequencing. These in-line barcode and linker sequences are cleaned from final assembled amplicons by in-house Perl scripts, in a way that is based only on the length of the barcodes/linkers, which guarantees a successful removal.

The PIPITS pipeline was used for ITS1 processing(45). Briefly, the ITS1 region was extracted with ITSx(46), clustered into operational taxonomic unites (OTUs) with VSEARCH(https://github.com/torognes/vsearch) at 97% sequence similarity and chimera removal performed using the UNITE UCHIME reference data set. Representative sequences were assigned taxonomic classification with the RDP classifier against the UNITE fungal ITS reference data set(64) at a confidence threshold of 0.85. Contaminants found in negative controls (corresponding to taxa *Saccharomyces cereviseae* or *Alternaria eichornia*) were removed at the OTU level (4 OTU's removed) followed by subsampling 500 sequences per sample. The Shannon diversity index, Simpson diversity index (1-D), Faith's phylogenetic distance (PD) and number of observed species (richness) were calculated using the QIIME 1.8.0 alpha_diversity.py script(65). Beta-diversity metrics were calculated with the QIIME 1.8.0 beta_diversity.py script.

3.7.3 Fungal and Bacterial Manipulation

Isolation: Yeast and bacterial isolates were grown from wound swabs collated in trypticase soy broth (TSB). Briefly, 100 μL of TSB containing the swab was plated onto yeast-mold (YM; Neogen, Lansing, MI) and incubated at 25°C for up to 7 days. Individual colonies were picked and grown on YM or TSB agar plates to be made into glycerol stocks for long term storage. All strains isolated were identified by amplification of the ITS1 region (primers

described above without adapters) or 16S rRNA gene (16S 27'F and 534'R) and Sanger sequencing. Secondary confirmation was obtained by MALDI TOF mass spectrometry at the Pennsylvania Animal Diagnostic Laboratory System.

The yeast isolate grown from P198 was identified as *Trichosporon asahii* by Sanger sequencing and a BLAST search against the NCBI nt database and UNITE database. The sequence was compared to the OTU identified as *Trichosporon ovoides* as part of the PIPITS pipeline and found to have 100% identity so the OTU was re-classified as *T. asahii*.

Biofilm growth: Isolates were grown overnight at 37°C on YM agar (fungi) or TSA (bacteria). Colonies were scraped into 0.89% NaCl to an OD_{600} nm of 0.08-0.1 with the exception of *T. asahii* (OD_{600nm}=0.17-0.2). Bacterial suspensions were diluted 1/10 into RPMI 1649, GlutaMax media (ThermoFisher Scientific, Waltham, MA). The inoculums were then added in a 1/10 dilution to a final volume of 4 mL RPMI in 35 mm polystyrene plates. Cultures were incubated stationary at 37°C for 24 or 48 hrs to allow adhesion and growth. The media was removed and the biofilms washed with 2 x 1 mL sterile 0.89% NaCl to remove non-adherent cells. The biofilms were stained with the LIVE BacLight Bacterial Gram Stain Kit (ThermoFisher Scientific, Waltham, MA) with SYTO9 (480nm/500nm) and hexidium iodide (480nm/625nm) as a 2 mL solution in water and according to the kit instructions. The stain was removed and deionized water was added to the biofilms prior to imaging on a Leica TCS SP5 microscope with 20x objective. Images were post-processed with Volocity software (PerkinElmer, Waltham, MA, USA). The maximum projection for each image was used to generate figure 5.

Quantitative counts of mono and co-cultures were performed by serial dilution of planktonic cells (media), wash media (2 x 1mL) and 0.89% saline containing adherent cells that were scraped and resuspended (n=2). The dilutions were plated onto non-selective media (YM or TSA) and incubated for 16-18 hrs at 37°C. Colonies were counted and the total CFUs calculated.

3.7.4 Data Analyses

The R Statistical Package (66) was used for all computations unless described elsewhere. The classification of 'Pathogens' or 'Allergens' was performed manually based on classification in literature. Statistical methods are described within the text and figure legends. Correlations between microbiome and clinical features were determined by calculating the Spearman coefficient.

3.8 Data Availability

All sequence data is publicly available on the NCBI Sequence Read Archive with accession number SRP076355 and BioProject Accession number PRJNA324668.

3.9 Funding Information

3.10 Acknowledgements

3.11 Figures

A) Subject at Baseline Visit

B) **C)** **D)**

Figure 1

The DFU mycobiome is diverse and highly heterogeneous. A) Heatmap of fungal community

structure for all subjects at the baseline study visit. Hierarchical clustering was performed for taxa

found in >20% abundance in at least one sample. B) Boxplot showing the Shannon diversity

index (Y-axis) by wound location (X-axis). P-values were calculated by pairwise Wilcoxon rank

sum test and adjusted for multiple comparison by method of Holm. C) Relative abundance plot

showing the mean proportions of taxa found in >1% abundance in all of the samples (Y-axis) by

wound location (X-axis). Taxa found in significantly different abundance between forefoot and

hindfoot wounds are listed in Table S2. D) Boxplot showing the weighted UniFrac distances (Y-

axis) between subjects (baseline study visit only) and within subjects longitudinally (X-axis). The

P-value was calculated by Wilcoxon rank sum test. Notches in boxplots display the 95%

confidence interval around the median.
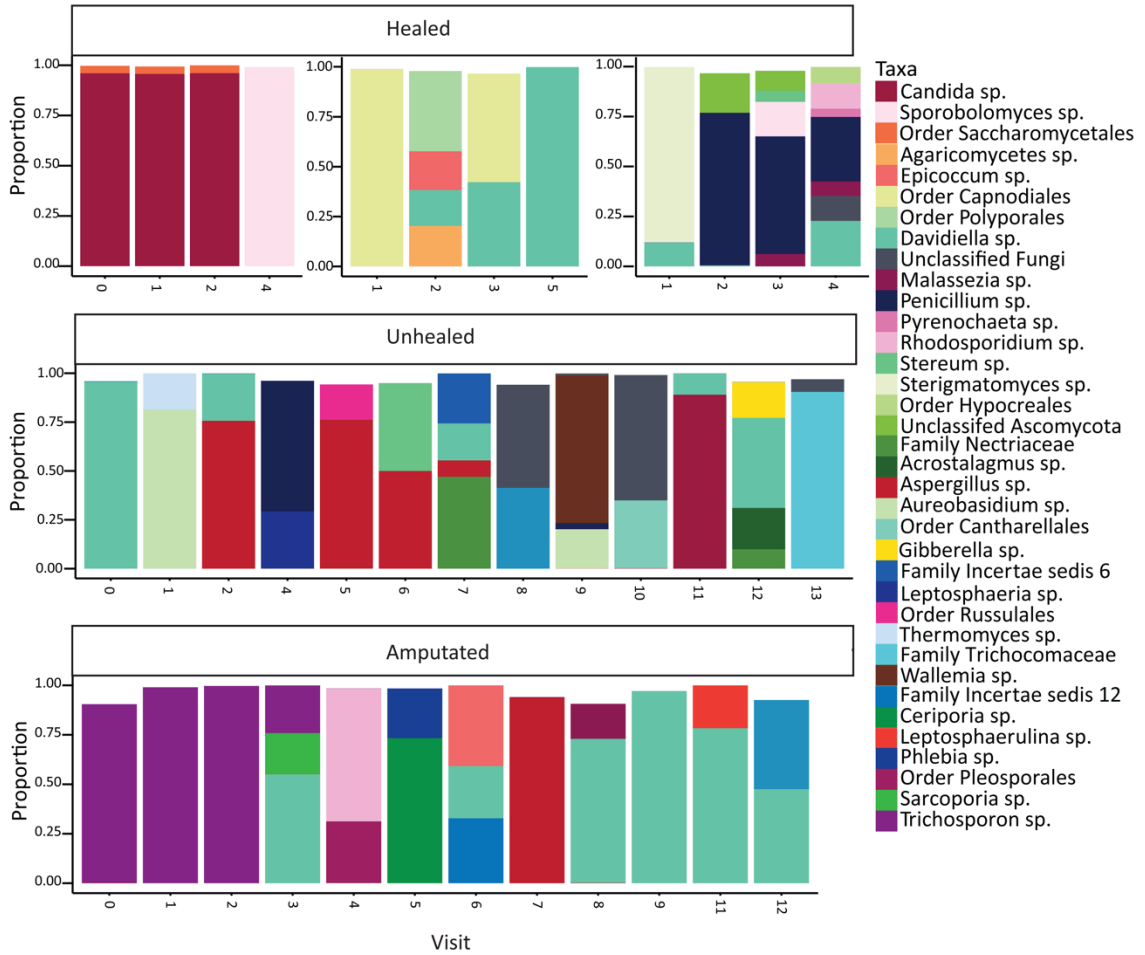
Figure 2

The DFU mycobiome is temporally unstable. Five individual subject timelines showing the relative abundance and structure of fungal communities for DFUs that healed, did not heal within the 26 weeks of the study, or resulted in an amputation. Numbers on the X-axis represent study visit number and Y-axis represents proportion of taxa present.
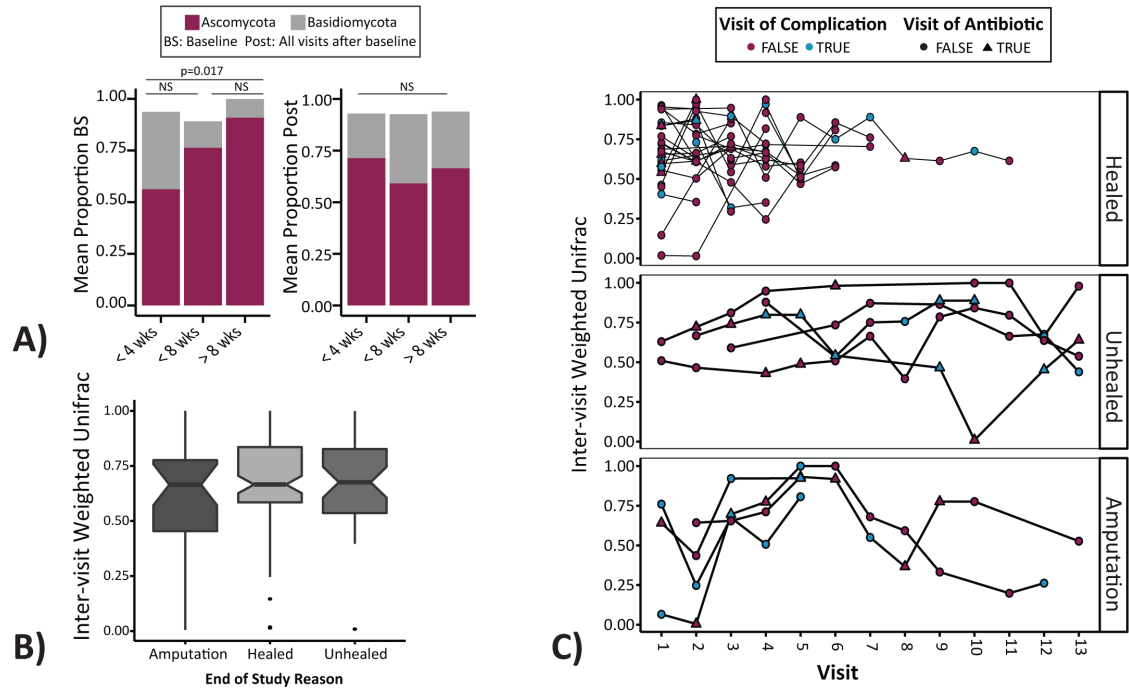
Figure 3

The DFU mycobiome is associated with clinical outcomes. A) Relative distribution of
Ascomycota and Basidiomycota in specimens grouped by time to heal. Baseline specimens (left
panel) were taken from viable wound tissue prior to sharp debridement and cleansing. All study
visits after the baseline study visit are combined (right panel). P-values are calculated with an
analysis of variance model and post-hoc Tukey HSD multiple comparison of means. B) A
boxplot showing inter-visit weighted UniFrac distances (Y-axis) by end of study reason (X-axis)
were not significantly different. Notches display the 95% confidence interval around the median.
C) A timeline of weighted UniFrac distances (Y-axis) plotted by study visit (X-axis) for
individual subjects and grouped by end of study reason (top panel = healed; middle panel =
unhealed after 26 weeks of follow-up; bottom panel = amputated). Blue dots indicate that a
complication was recorded at the study visit. Triangles indicate study visit at which an antibiotic
was administered at or within the previous two-weeks.
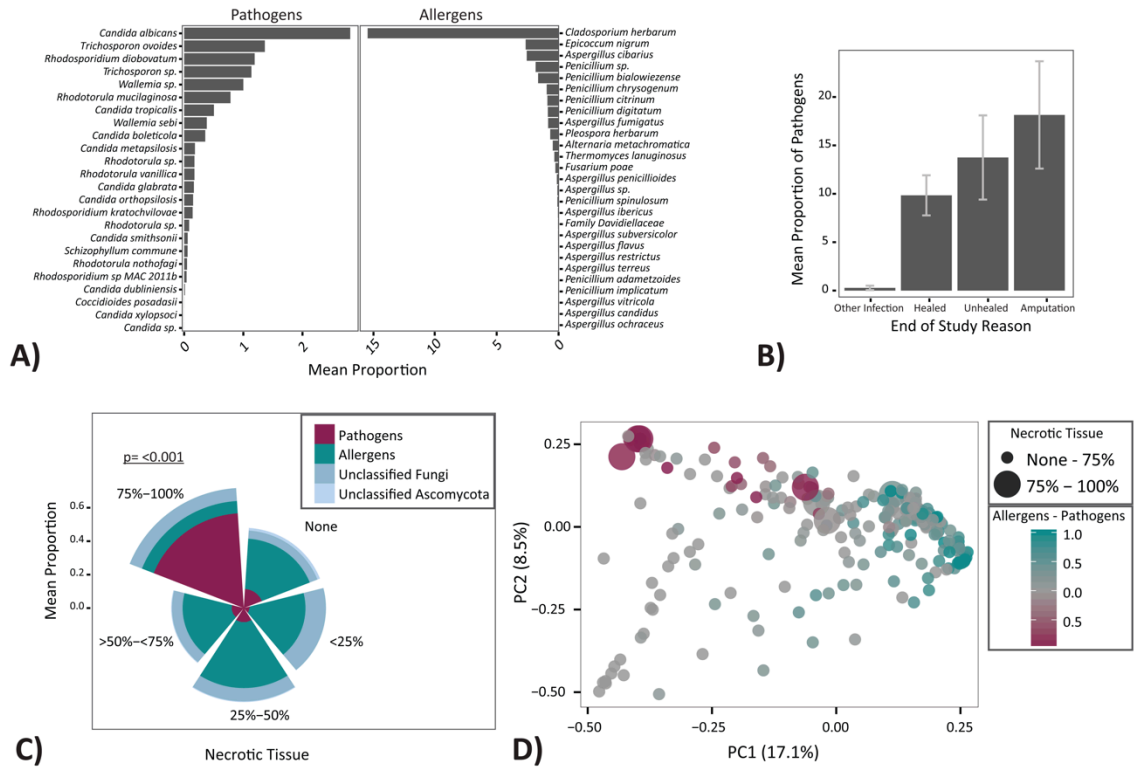
Figure 4

Pathogens are associated with necrotic tissue and poor outcomes. A) Mean proportion (%) (X-axis) of pathogen (Y-axis;left panel) and allergen (Y-axis, right panel) taxa in the data set. B) Mean proportion of pathogens (Y-axis) by end of study reason (X-axis). Error bars indicate standard error of the mean. C) Mean proportion of pathogens, allergens, unclassified Fungi, and unclassified Ascomycota in samples grouped by the level of necrotic tissue present in the wound. The level of pathogens is significantly higher in ulcers with >75% necrotic tissue compared to all other levels of necrosis. P-values are calculated with an analysis of variance model and post-hoc Tukey HSD multiple comparison of means. D) Principal coordinate plot comparing samples by the weighted UniFrac distance. Percent variation explained by each principle coordinate is indicated by % next to each axis. Point size indicates necrotic tissue level, with larger points corresponding to greater amounts of necrotic tissue in the wound from which the sample was

taken. The proportions of allergens and pathogens was calculated by subtracting the proportion of pathogens from the proportion of allergens in each sample resulting in a scale of -1 (dominated by pathogens) to +1 (dominated by allergens). A value of zero indicates either zero or equal proportions of each.
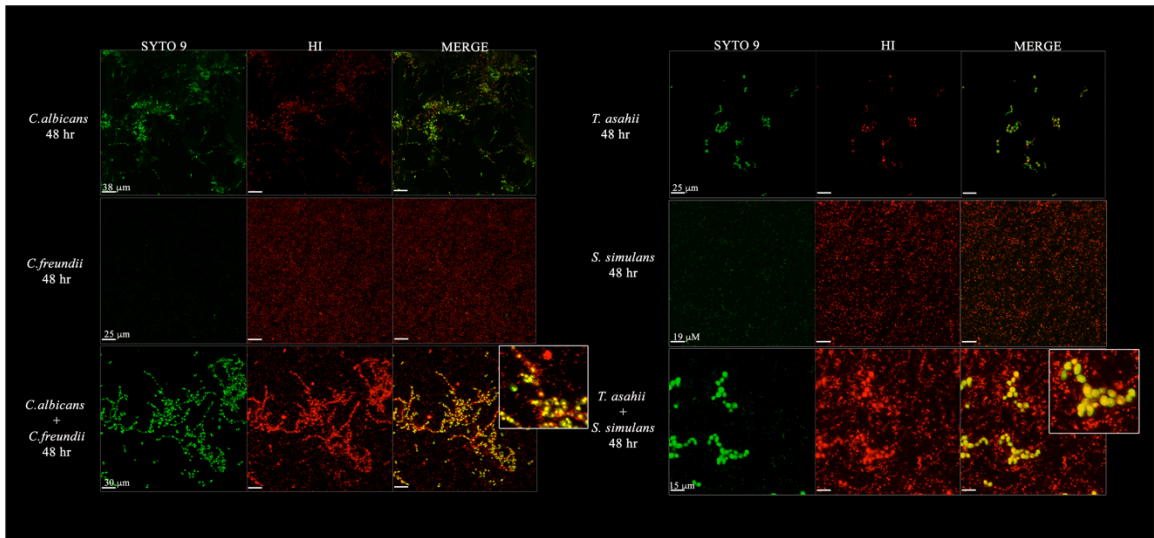
Figure 5

Pathogens form inter-kingdom biofilms. Fluorescent confocal microscope images of mono- or co-culture *Candida albicans* and *Citrobacter freundii* or *Trichosporon asahii* and *Staphlococcus simulans*. Biofilms were grown for 48 hrs. at 37ºC on polystyrene plates in RPMI 1649, GlutaMax media, washed to remove planktonic cells and stained with SYTO 9 and hexidium iodide (HI) prior to imaging. Fungi (large) and bacteria (small) can be distinguished by size. Fungi appear green and bacteria red in the merged images. The size of the scale bar for each row is labelled in the first column (SYTO 9) for each culture. The insets are zoomed in portions of the merged co-culture biofilm images.
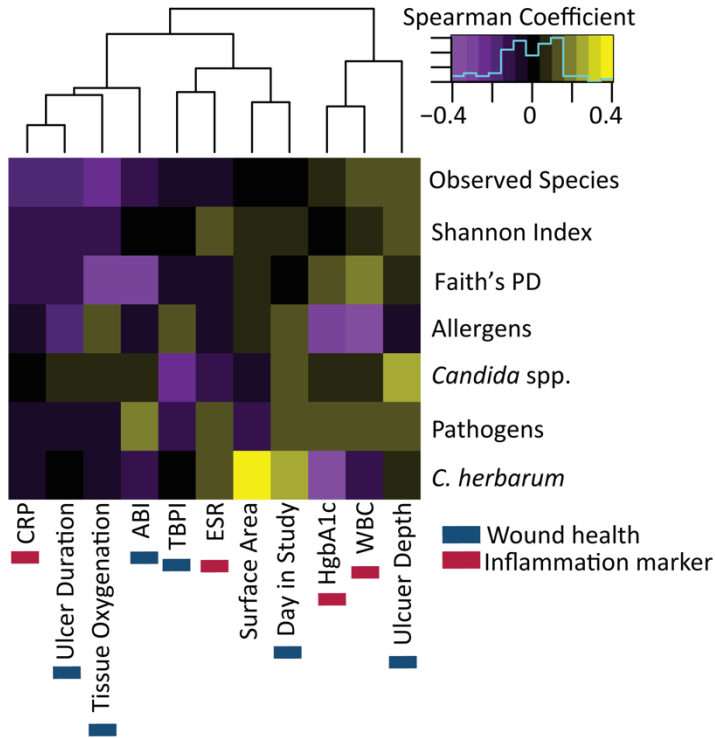
Figure S1

Heatmap illustrating positive (yellow) and negative (purple) correlations between microbiome factors and clinical factors at baseline. Correlations were calculated by the Spearman correlation coefficient. Significant correlations are marked with an asterisk (p=<0.05) and rho and p-values are summarized in Table S1.
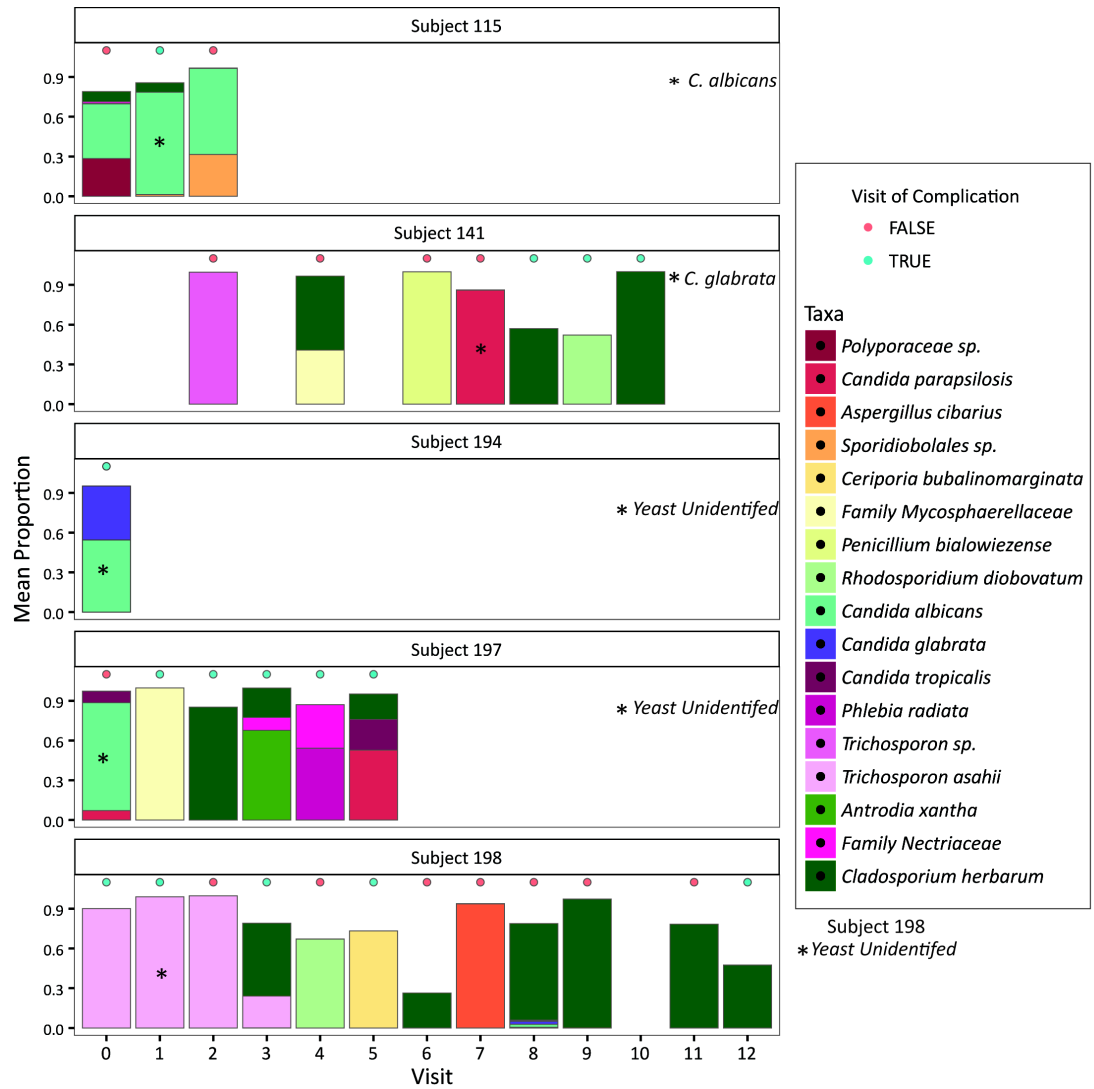
Figure S2

Subjects with positive yeast culture result. The study visit that was culture positive is marked by (*) and the identified species are labelled. Relative abundance plots are shown for taxa identified by ITS1 analysis and found in >5 % abundance in each sample. Numbers on the X-axis represent study visit number and Y-axis represents proportion of taxa.
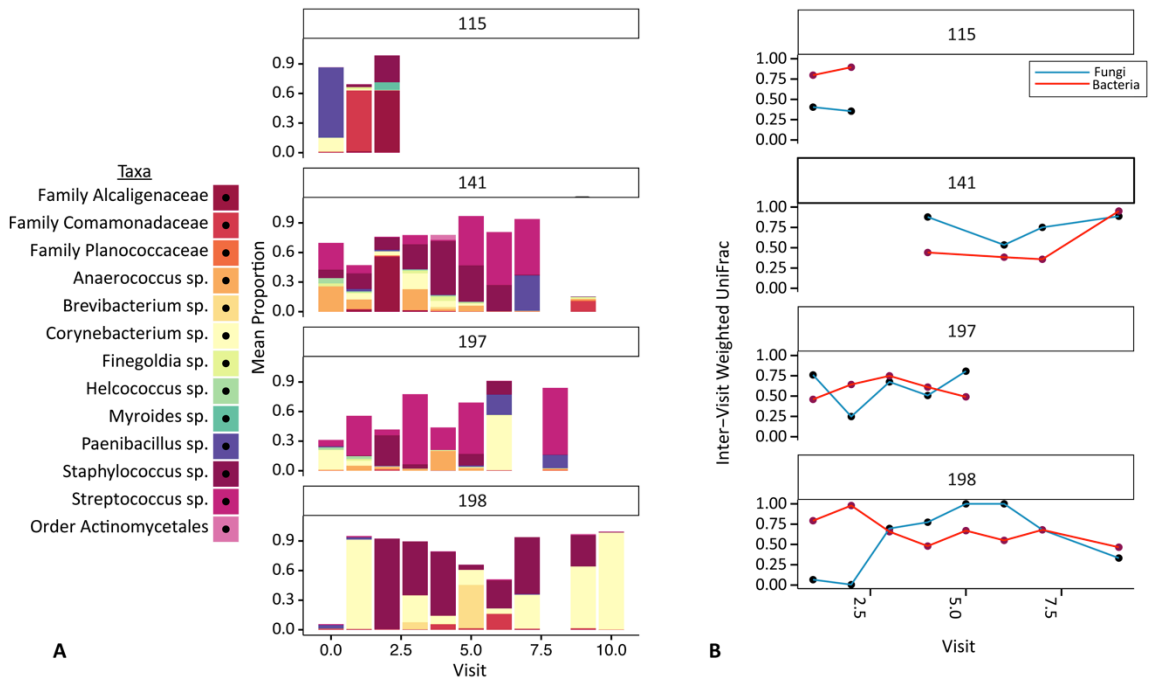
Figure S3

Subjects with positive yeast culture result. A) Relative abundance plots are shown for bacterial taxa identified by 16S rRNA gene analysis and found in >1 % abundance in the entire dataset (384 samples). Numbers on the X-axis represent study visit number and Y-axis represents proportion of taxa. B) A timeline of weighted UniFrac distances (Y-axis) plotted by study visit (X-axis) for individual subjects. Blue lines indicate the fungal wuf distances and the red lines the bacterial wuf distances over time for each subject.
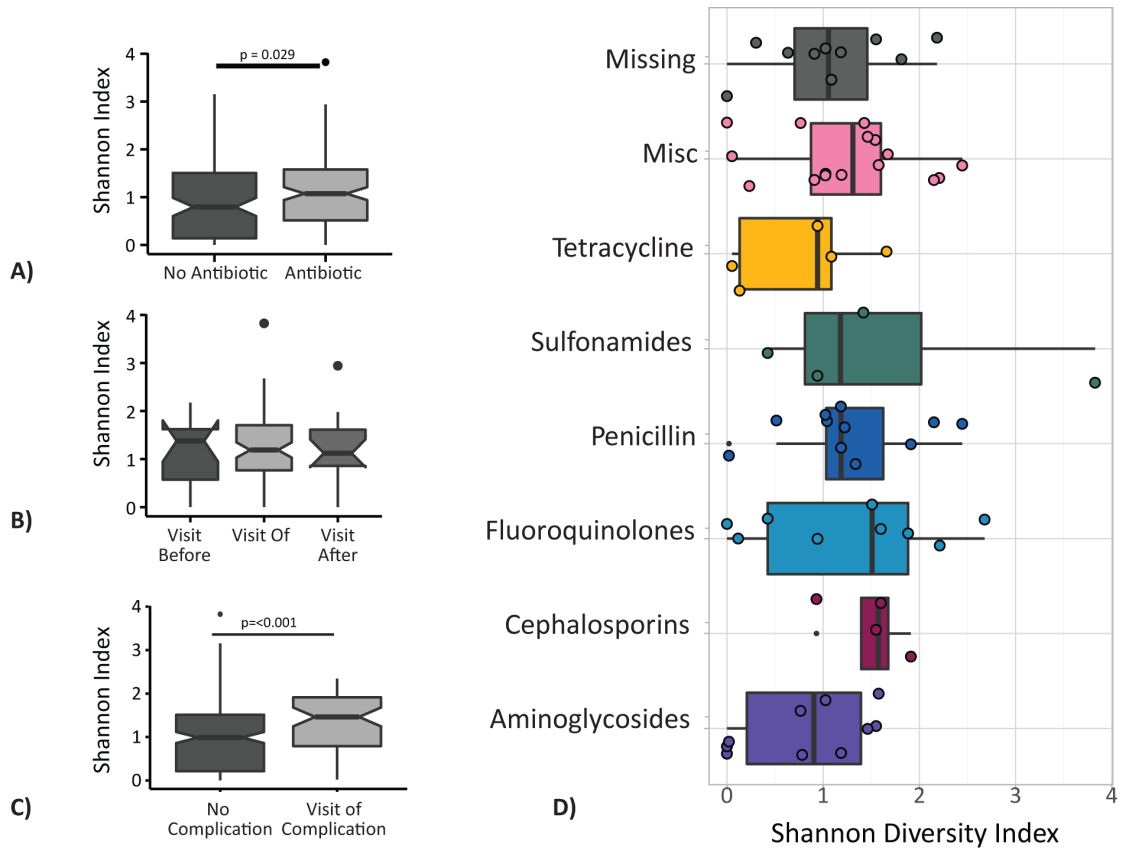
Figure S4

Shannon Diversity Index for subjects administered an antibiotic (n=31) during the course of the study or experienced a complication (n=30) A) All subjects who received an antibiotic at least once during the study period or not at all. B) Shannon Index for samples obtained before, during or following antibiotic administration. C) Shannon Index for visits a complication occurred or did not occur. D) Shannon Index for samples corresponding to different antibiotic classes. Adjusted (Holm) P-values were calculated by pairwise Wilcoxon rank sum test.
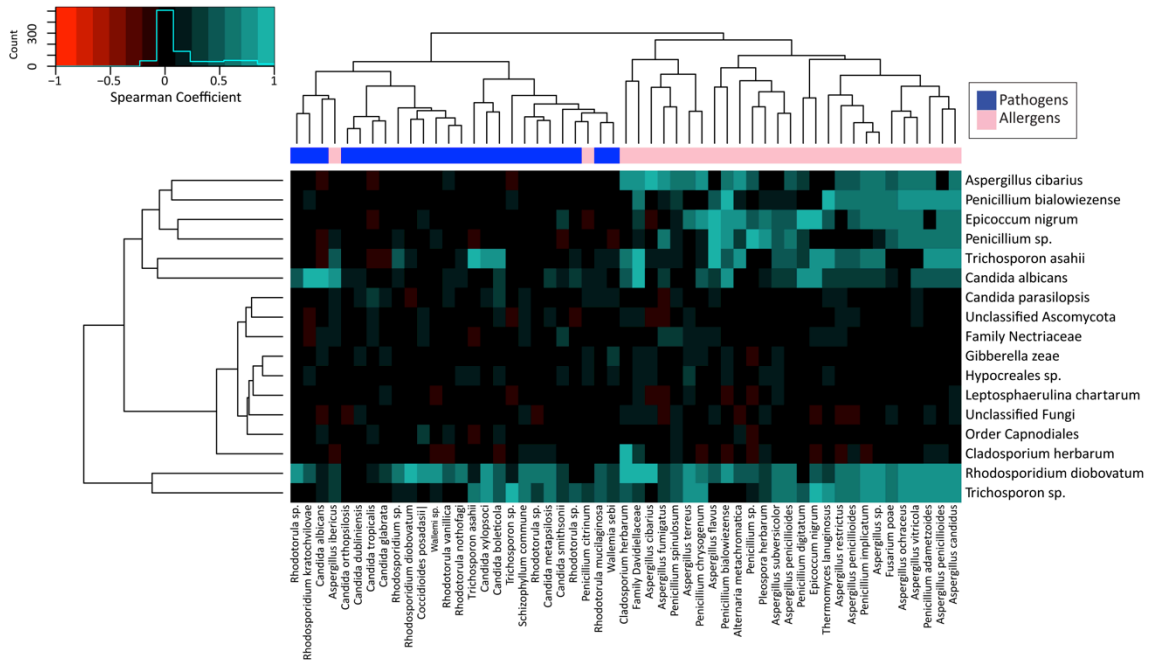
Figure S5

Dendogram and heatmap illustrating positive (blue) and negative (red) correlations between the taxa found in >1% abundance across the entire sample set and the pathogens and allergens groups. Correlations were calculated by the Spearman correlation coefficient. Allergens and pathogens groups are indicated with pink or blue bar, respectively, at the top of the heatmap.
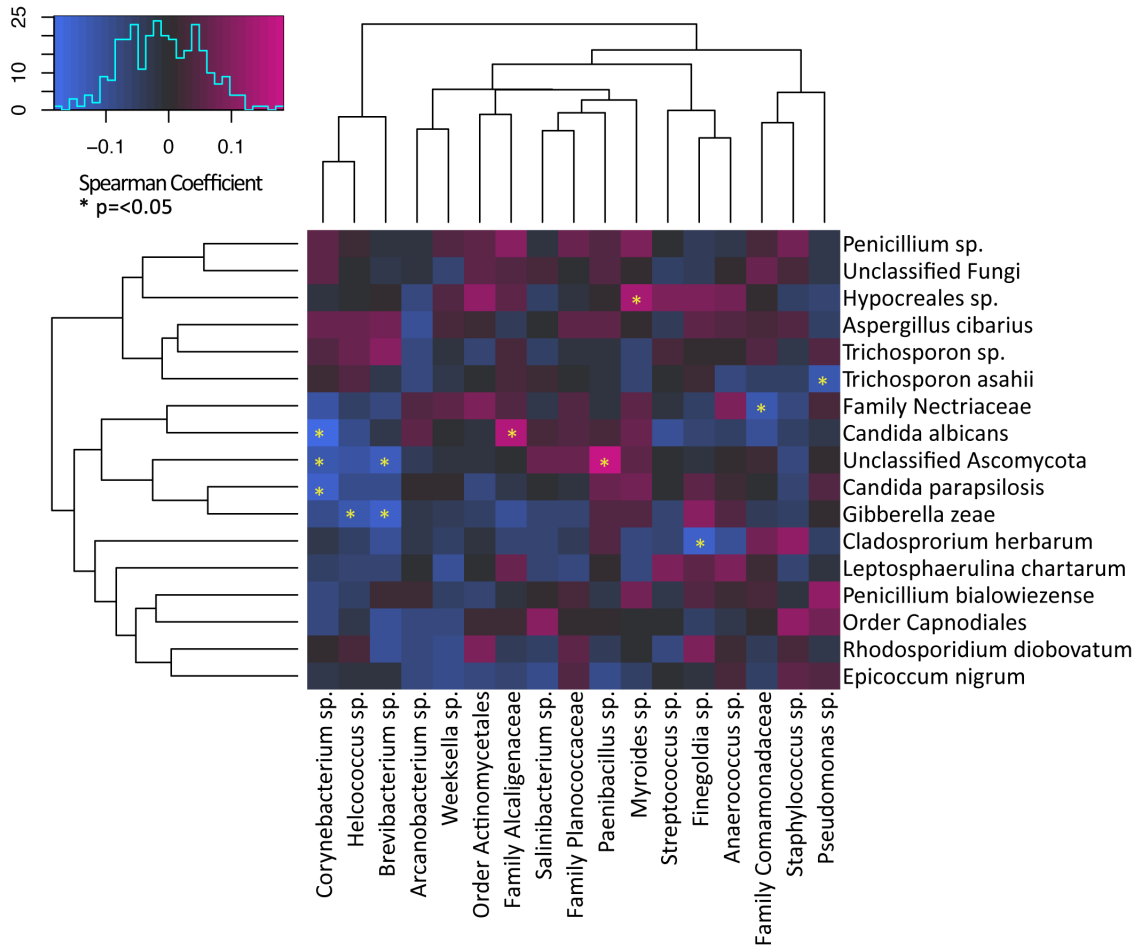
Figure S6

Dendogram and heatmap illustrating positive (pink) and negative (blue) correlations between the fungal and bacterial taxa found in >1% abundance across the entire sample set. Correlations were calculated by the Spearman correlation coefficient. Significant correlations are marked with an asterisk (p<0.05).
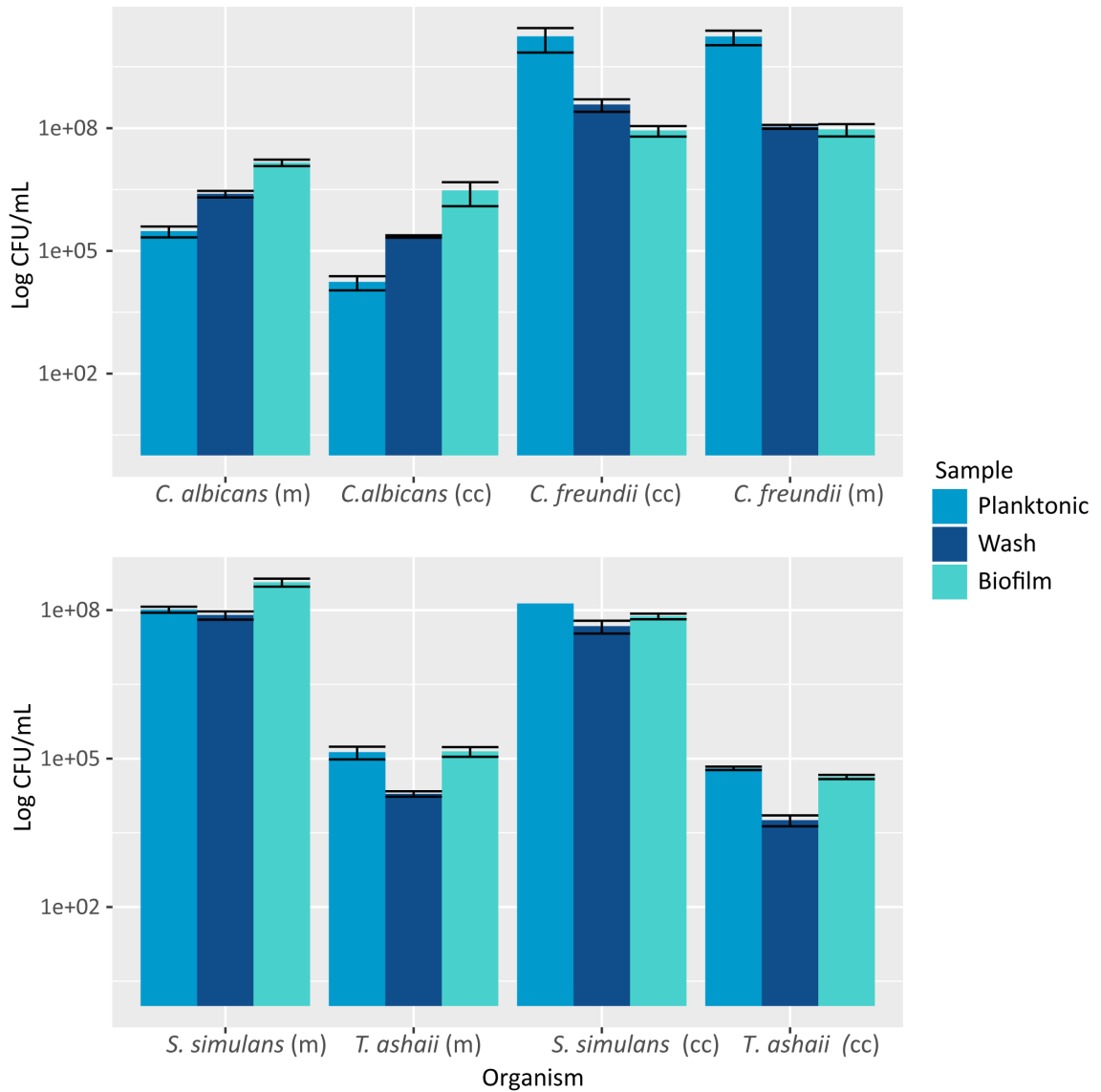
Figure S7

Quantitative culture data. A) Quantitative counts for *C. albicans* and *C. freundii* planktonic and

biofilm populations growing as mono-culture (m) or co-culture (cc). B) Quantitative counts for *T.*

asahii and *S. simulans* planktonic and biofilm populations growing as mono-culture (m) or co-

culture (cc). All biofilm counts were obtained after washing the biofilms 2 x 1 mL of sterile

91

water. Counts are averaged across a minimum of two replicates and two serial dilutions per replicate.

3.12 Tables

	n
Subjects	100
Samples	384
Sex (M/F)	78/22
Type 2 Diabetes	87
Ulcer Duration (wks), mean (SD)	33.1 (41.6)
Ulcer Location	
Forefoot	73
MidFoot	20
Heel	7
End of Study Reason	
Healed	75
Unhealed	5
Amputation	7
Other Infection	3
Dropped Study	10
Subjects with detected ITS1	79
Samples with detected ITS1	275

Table 1

Subject Demographics and wound characteristics

93

Fungal Taxa	% Samples	No. Patients
Ascomycota		
Cladosporium herbarum	41	56
Candida albicans	22	47
Unclassified Ascomycota	16	36
Family Nectriaceae	16	41
Candida parapsilosis	15	37
Aspergillus cibarius	12	30
Epicoccum nigrum	9	27
Penicillium sp	9	26
Leptosphaerulina chartarum	7	23
Penicillium bialowiezense	6	19
Gibberella_zeae	6	18
Hypocreales sp	4	14
Order Capnodiales	4	15
Basidiomycota		
Trichosporon asahii	10	24
Trichosporon sp	4	12
Rhodosporidium diobovatum	5	16
Unclassified fungi	32	55

Table 2

Distribution of the top 1% identified fungal taxa.

94

	HgbA1c		Tissue oxygenation		Ulcer depth		Ulcer duration		Ulcer surface area		WBC	
	rho	p-value	rho	p-value	rho	p-value	rho	p-value	rho	p-value	rho	p-value
Observed species	0.0915	0.4793	-0.2582	**0.0464**	0.1082	0.4026	-0.1843	0.1516	-0.0126	0.9224	0.1013	0.4373
Shannon index	0.0175	0.8923	-0.1284	0.3281	0.1197	0.354	-0.1	0.4394	0.0903	0.4853	0.0521	0.6901
Faith's PD	0.1218	0.3456	-0.2953	**0.022**	0.0415	0.7489	-0.1436	0.2655	0.0649	0.616	0.2094	0.1052
Allergens	-0.308	**0.0198**	0.1371	0.3182	-0.0436	0.7472	-0.1639	0.2233	0.0779	0.5646	-0.3463	**0.0089**
Candida sp.	0.0402	0.7666	0.0465	0.7358	0.2255	0.0917	0.0899	0.506	-0.0387	0.7752	0.0497	0.716
Pathogens	0.0953	0.4808	-0.0781	0.571	0.1517	0.26	-0.0555	0.6818	-0.1281	0.3422	0.1449	0.2866
C. herbarum	-0.4053	**0.0018**	-0.0531	0.7002	0.0346	0.7984	0.0063	0.9631	0.3482	**0.0079**	-0.1452	0.2857

	CRP		TBPI		ABI		Days in study		ESR	
	rho	p-value	rho	p-value	rho	p-value	rho	p-value	rho	p-value
Observed species	-0.1615	0.2099	-0.0453	0.7813	-0.1322	0.5678	0.0185	0.8891	-0.0506	0.6985
Shannon index	-0.1117	0.3874	-0.0305	0.852	-0.008	0.9725	0.0319	0.8103	0.1291	0.3212
Faith's PD	-0.1074	0.4061	-0.0926	0.5697	-0.3254	0.15	-0.0243	0.8552	-0.0705	0.5892
Allergens	-0.0716	0.5965	0.1553	0.3588	-0.05	0.839	0.1096	0.4257	-0.0401	0.7694
Candida sp.	-0.0299	0.8252	-0.2354	0.1608	0.087	0.7231	0.1025	0.4563	-0.113	0.4072
Pathogens	-0.0934	0.4894	-0.1055	0.5342	0.182	0.4559	0.1124	0.4138	0.0956	0.4836
C. herbarum	-0.0361	0.7899	-0.0275	0.8716	-0.1344	0.5832	0.2794	**0.0388**	0.1121	0.4109

Table S1

Summary of Spearman correlation coefficients and p-values for supplementary figure 1.

Taxa	p-value
Order Saccharomycetales	0.024
Mycosphaerellaceae sp.	0.492
Candida albicans	2.19 E-05
Tremellales sp.	0.0191
Sporobolomyces ruberrimus	0.0191
Phlebia radiata	0.0191
Trichosporon sp.	0.870
Kluyveromyces marxianus	0.0191
Antrodia xantha	0.0325
Eurotiales sp.	0.0226
Class Agaricomycetes	0.0226
Candida xylopsoci	0.0191
Ceriporia purpurea	0.0191

Table S2:

Differentially abundant taxa between forefoot and hindfoot wounds (p-values calculated by

analysis of variance and adjusted by the Benjamini & Hochberg method)

3.13 References

1. Sen CK, Gordillo GM, Roy S, Kirsner R, Lambert L, Hunt TK, Gottrup F, Gurtner GC, Longaker MT. 2009. Human skin wounds: a major and snowballing threat to public health and the economy. Wound Repair Regen 17:763–771.

2. Guariguata L, Whiting DR, Hambleton I, Beagley J, Linnenkamp U, Shaw JE. 2014. Global estimates of diabetes prevalence for 2013 and projections for 2035. Diabetes Res Clin Pract 103:137–149.

3. Kerr M, Rayman G, Jeffcoate WJ. 2014. Cost of diabetic foot disease to the National Health Service in England. Diabet Med 31:1498–1504.

4. Hicks CW, Selvarajah S, Mathioudakis N, Perler BA, Freischlag JA, Black JH, Abularrage CJ. 2014. Trends and determinants of costs associated with the inpatient care of diabetic foot ulcers. J Vasc Surg 60:1247–54– 1254.e1–2.

5. Scott RD. 2009. The direct medical costs of healthcare-associated infections in US hospitals and the benefits of prevention.

6. Armstrong DG, Wrobel J, Robbins JM. 2007. Guest editorial: are diabetes-related wounds and amputations worse than cancer. Int Wound J.

7. Robbins JM, Strauss G, Aron D, Long J, Kuba J, Kaplan Y. 2014. Mortality Rates and Diabetic Foot Ulcers. http://dxdoiorg/107547/0980489 98:489–493.

8. Boulton AJ, Vileikyte L, Ragnarson-Tennvall G, Apelqvist J. 2005. The global burden of diabetic foot disease. The Lancet 366:1719–1724.

9.	Dalton T, Dowd SE, Wolcott RD, Sun Y, Watters C, Griswold JA, Rumbaugh KP. 2011. An in vivo polymicrobial biofilm wound infection model to study interspecies interactions. PLoS ONE 6:e27317.

10.	Percival SL, McCarty SM, Lipsky B. 2015. Biofilms and Wounds: An Overview of the Evidence. Adv Wound Care (New Rochelle) 4:373–381.

11.	Rhoads DD, Wolcott RD, Sun Y, Dowd SE. 2012. Comparison of culture and molecular identification of bacteria in chronic wounds. Int J Mol Sci 13:2535–2550.

12.	Grice EA, Kong HH, Renaud G, Young AC, NISC Comparative Sequencing Program, Bouffard GG, Blakesley RW, Wolfsberg TG, Turner ML, Segre JA. 2008. A diversity profile of the human skin microbiota. Genome Res 18:1043–1050.

13.	Grice EA, Kong HH, Conlan S, Deming CB, Davis J, Young AC, NISC Comparative Sequencing Program, Bouffard GG, Blakesley RW, Murray PR, Green ED, Turner ML, Segre JA. 2009. Topographical and temporal diversity of the human skin microbiome. Science 324:1190–1192.

14.	Meisel JS, Hannigan GD, Tyldsley AS, SanMiguel AJ, Hodkinson BP, Zheng Q, Grice EA. 2016. Skin microbiome surveys are strongly influenced by experimental design. J Invest Dermatol.

15.	SanMiguel A, Grice EA. 2015. Interactions between host factors and the skin microbiome. Cell Mol Life Sci 72:1499–1515.

16.	Mathieu A, Delmont TO, Vogel TM, Robe P, Nalin R, Simonet P. 2013. Life on human

surfaces: skin metagenomics. PLoS ONE 8:e65288.

17.   Hannigan GD, Grice EA. 2013. Microbial Ecology of the Skin in the Era of

       Metagenomics and Molecular Microbiology. Cold Spring Harb Perspect Med 3:a015362–

       a015362.

18.   Wiedenbeck J, Cohan FM. 2011. Origins of bacterial diversity through horizontal genetic

       transfer and adaptation to new ecological niches. FEMS Microbiology Reviews 35:957–

       976.

19.   Brock M. 2009. Fungal metabolism in host niches. Curr Opin Microbiol 12:371–376.

20.   Sokurenko EV, Hasty DL, Dykhuizen DE. 1999. Pathoadaptive mutations: gene loss and

       variation in bacterial pathogens. Trends Microbiol 7:191–195.

21.   Gardner SE, Hillis SL, Heilmann K, Segre JA, Grice EA. 2013. The neuropathic diabetic

       foot ulcer microbiome is associated with clinical factors. Diabetes 62:923–930.

22.   Grice EA, Snitkin ES, Yockey LJ, Bermudez DM, NISC Comparative Sequencing

       Program, Liechty KW, Segre JA. 2010. Longitudinal shift in diabetic wound microbiota

       correlates with prolonged skin defense response. Proceedings of the National Academy of

       Sciences 107:14799–14804.

23.   Miller CN, Carville K, Newall N, Kapp S, Lewin G, Karimi L, Santamaria N. 2011.

       Assessing bacterial burden in wounds: comparing clinical observation and wound swabs.

       Int Wound J 8:45–55.

24.   Rogers GB, Hoffman LR, Carroll MP, Bruce KD. 2013. Interpreting infective microbiota:

the importance of an ecological perspective. Trends Microbiol 21:271–276.

25. Grice EA, Segre JA. 2012. Interaction of the microbiome with the innate immune response in chronic wounds. Adv Exp Med Biol 946:55–68.

26. Dhall S, Do D, Garcia M, Wijesinghe DS, Brandon A, Kim J, Sanchez A, Lyubovitsky J, Gallagher S, Nothnagel EA, Chalfant CE, Patel RP, Schiller N, Martins-Green M. 2014. A Novel Model of Chronic Wounds: Importance of Redox Imbalance and Biofilm-Forming Bacteria for Establishment of Chronicity. PLoS ONE 9:e109848–17.

27. Zhao G, Usui ML, Lippman SI, James GA, Stewart PS, Fleckman P, Olerud JE. 2013. Biofilms and Inflammation in Chronic Wounds. Adv Wound Care (New Rochelle) 2:389–399.

28. Edwards R, Harding KG. 2004. Bacteria and wound healing. Curr Opin Infect Dis 17:91–96.

29. Wolcott RD, Gontcharova V, Sun Y, Zischakau A, Dowd SE. 2009. Bacterial diversity in surgical site infections: not just aerobic cocci any more. J Wound Care 18:317–323.

30. Gardner SE, Frantz RA, Saltzman CL, Hillis SL, Park H, Scherubel M. 2006. Diagnostic validity of three swab techniques for identifying chronic wound infection. Wound Repair Regen 14:548–557.

31. Cui L, Morris A, Ghedin E. 2013. The human mycobiome in health and disease. Genome Med.

32. Findley K, Oh J, Yang J, Conlan S, Deming C, Meyer JA, Schoenfeld D, Nomicos E, Park

M, NIH Intramural Sequencing Center Comparative Sequencing Program, Kong HH, Segre JA. 2013. Topographic diversity of fungal and bacterial communities in human skin. Nature 498:367–370.

33. Underhill DM, Iliev ID. 2014. The mycobiota: interactions between commensal fungi and the host immune system. Nature Publishing Group 14:405–416.

34. Ghannoum MA, Jurevic RJ, Mukherjee PK, Cui F, Sikaroodi M, Naqvi A, Gillevet PM. 2010. Characterization of the Oral Fungal Microbiome (Mycobiome) in Healthy Individuals. PLoS Pathog 6:e1000713–8.

35. Di Bonaventura G, Pompilio A, Picciani C, Iezzi M, D'Antonio D, Piccolomini R. 2006. Biofilm formation by the emerging fungal pathogen Trichosporon asahii: development, architecture, and antifungal resistance. Antimicrob Agents Chemother 50:3269–3276.

36. Desai JV, Mitchell AP, Andes DR. 2014. Fungal biofilms, drug resistance, and recurrent infection. Cold Spring Harb Perspect Med 4:a019729–a019729.

37. de Oliveira HC, Assato PA, Marcos CM, Scorzoni L, de Paula E Silva ACA, Da Silva JDF, Singulani J de L, Alarcon KM, Fusco-Almeida AM, Mendes-Giannini MJS. 2015. Paracoccidioides-host Interaction: An Overview on Recent Advances in the Paracoccidioidomycosis. Front Microbiol 6:1319.

38. Nunes JM, Bizerra FC, Ferreira RCE, Colombo AL. 2012. Molecular Identification, Antifungal Susceptibility Profile, and Biofilm Formation of Clinical and Environmental Rhodotorula Species Isolates. Antimicrob Agents Chemother 57:382–389.

39. Kramer R, Sauer-Heilborn A, Welte T, Guzman CA, Abraham W-R, Höfle MG. 2015. Cohort Study of Airway Mycobiome in Adult Cystic Fibrosis Patients: Differences in Community Structure between Fungi and Bacteria Reveal Predominance of Transient Fungal Elements. J Clin Microbiol 53:2900–2907.

40. Guo R, Zheng N, Lu H, Yin H, Yao J, Chen Y. 2012. Increased Diversity of Fungal Flora in the Vagina of Patients with Recurrent Vaginal Candidiasis and Allergic Rhinitis. Microb Ecol 64:918–927.

41. Dowd SE, Delton Hanson J, Rees E, Wolcott RD, Zischau AM, Sun Y, White J, Smith DM, Kennedy J, Jones CE. 2011. Survey of fungi and yeast in polymicrobial infections in chronic wounds. J Wound Care 20:40–47.

42. Chellan G, Shivaprakash S, Karimassery Ramaiyar S, Varma AK, Varma N, Thekkeparambil Sukumaran M, Rohinivilasam Vasukutty J, Bal A, Kumar H. 2010. Spectrum and prevalence of fungi infecting deep tissues of lower-limb wounds in patients with type 2 diabetes. J Clin Microbiol 48:2097–2102.

43. Schoch CL, Seifert KA, Huhndorf S, Robert V, Spouge JL, Levesque CA, Chen W, Fungal Barcoding Consortium, Fungal Barcoding Consortium Author List. 2012. Nuclear ribosomal internal transcribed spacer (ITS) region as a universal DNA barcode marker for Fungi. Proceedings of the National Academy of Sciences 109:6241–6246.

44. Kõljalg U, Nilsson RH, Abarenkov K, Tedersoo L, Taylor AFS, Bahram M, Bates ST, Bruns TD, Bengtsson-Palme J, Callaghan TM, Douglas B, Drenkhan T, Eberhardt U, Dueñas M, Grebenc T, Griffith GW, Hartmann M, Kirk PM, Kohout P, Larsson E,

Lindahl BD, Lücking R, Martín MP, Matheny PB, Nguyen NH, Niskanen T, Oja J, Peay KG, Peintner U, Peterson M, Põldmaa K, Saag L, Saar I, Schüßler A, Scott JA, Senés C, Smith ME, Suija A, Taylor DL, Telleria MT, Weiss M, Larsson K-H. 2013. Towards a unified paradigm for sequence-based identification of fungi. Mol Ecol 22:5271–5277.

45.   Gweon HS, Oliver A, Taylor J, Booth T, Gibbs M, Read DS, Griffiths RI, Schonrogge K. 2015. PIPITS: an automated pipeline for analyses of fungal internal transcribed spacer sequences from the Illumina sequencing platform. Methods Ecol Evol 6:973–980.

46.   Bengtsson-Palme J, Ryberg M, Hartmann M, Branco S, Wang Z, Godhe A, De Wit P, Sánchez-García M, Ebersberger I, de Sousa F, Amend AS, Jumpponen A, Unterseher M, Kristiansson E, Abarenkov K, Bertrand YJK, Sanli K, Eriksson KM, Vik U, Veldre V, Nilsson RH. 2013. Improved software detection and extraction of ITS1 and ITS2 from ribosomal ITS sequences of fungi and other eukaryotes for analysis of environmental sequencing data. Methods Ecol Evol n/a–n/a.

47.   Wu G, Zhao H, Li C, Rajapakse MP, Wong WC, Xu J, Saunders CW, Reeder NL, Reilman RA, Scheynius A, Sun S, Billmyre BR, Li W, Averette AF, Mieczkowski P, Heitman J, Theelen B, Schröder MS, De Sessions PF, Butler G, Maurer-Stroh S, Boekhout T, Nagarajan N, Dawson TL. 2015. Genus-Wide Comparative Genomics of Malassezia Delineates Its Phylogeny, Physiology, and Niche Adaptation on Human Skin. PLoS Genet 11:e1005614–26.

48.   Loesche M, Gardner SE, Kalan L, Horwinski J, Zheng Q, Hodkinson BP, Tyldsley AS, Franciscus C, Hillis SL, Mehta S, Margolis DJ, Grice E. 2016. Temporal stability in chronic wound microbiota is associated with poor healing. J Invest Dermatol. *Under*

49. Drell T, Lillsaar T, Tummeleht L, Simm J, Aaspõllu A, Väin E, Saarma I, Salumets A, Donders GGG, Metsis M. 2013. Characterization of the vaginal micro- and mycobiome in asymptomatic reproductive-age Estonian women. PLoS ONE 8:e54379.

50. Sellart-Altisent M, Torres-Rodríguez JM, Gómez de Ana S, Alvarado-Ramírez E. 2007. [Nasal fungal microbiota in allergic and healthy subjects]. Rev Iberoam Micol 24:125–130.

51. Hoffmann C, Dollive S, Grunberg S, Chen J, Li H, Wu GD, Lewis JD, Bushman FD. 2013. Archaea and fungi of the human gut microbiome: correlations with diet and bacterial residents. PLoS ONE 8:e66019.

52. Smith RM, Schaefer MK, Kainer MA, Wise M, Finks J, Duwve J, Fontaine E, Chu A, Carothers B, Reilly A, Fiedler J, Wiese AD, Feaster C, Gibson L, Griese S, Purfield A, Cleveland AA, Benedict K, Harris JR, Brandt ME, Blau D, Jernigan J, Weber JT, Park BJ. 2013. Fungal Infections Associated with Contaminated Methylprednisolone Injections. N Engl J Med 369:1598–1609.

53. Sandoval-Denis M, Sutton DA, Martin-Vicente A, Cano-Lira JF, Wiederhold N, Guarro J, Gené J. 2015. Cladosporium Species Recovered from Clinical Samples in the United States. J Clin Microbiol 53:2990–3000.

54. Noverr MC, Huffnagle GB. 2005. The "microflora hypothesis" of allergic diseases. Clinical & Experimental Allergy 35:1511–1520.

55.   Forsythe P, Inman MD, Bienenstock J. 2012. Oral Treatment with Live Lactobacillus
        reuteri Inhibits the Allergic Airway Response in Mice. American Journal of Respiratory
        and Critical Care Medicine 175:561–569.

56.   Noverr MC, Noggle RM, Toews GB, Huffnagle GB. 2004. Role of antibiotics and fungal
        microbiota in driving pulmonary allergic responses. Infect Immun 72:4996–5003.

57.   Noverr MC, Falkowski NR, McDonald RA, McKenzie AN, Huffnagle GB. 2005.
        Development of allergic airway disease in mice following antibiotic therapy and fungal
        microbiota increase: role of host genetics, antigen, and interleukin-13. Infect Immun
        73:30–38.

58.   Horner WE, Helbling A, Salvaggio JE, Lehrer SB. 1995. Fungal allergens. Clin Microbiol
        Rev 8:161–179.

59.   Margolis DJ, Berlin JA, Strom BL. 1996. Interobserver agreement, sensitivity, and
        specificity of a "healed" chronic wound. Wound Repair Regen 4:335–338.

60.   Gardner SE, Frantz RA, Hillis SL, Blodgett TJ, Femino LM, Lehman SM. 2012. Volume
        Measures Using a Digital Image Analysis System are Reliable in Diabetic Foot Ulcers.
        Wounds 24:146–151.

61.   Gardner SE, Frantz RA, Saltzman CL, Hillis SL, Park H, Scherubel M. 2006. Diagnostic
        validity of three swab techniques for identifying chronic wound infection. Wound Repair
        Regen 14:548–557.

62.   Dodt M, Roehr J, Ahmed R, Dieterich C. 2012. FLEXBAR—Flexible Barcode and

Adapter Processing for Next-Generation Sequencing Platforms. Biology 2012, Vol 1, Pages 895-905 1:895–905.

63.   Zhang J, Kobert K, Flouri T, Stamatakis A. 2014. PEAR: a fast and accurate Illumina Paired-End reAd mergeR. Bioinformatics 30:614–620.

64.   Nilsson RH, Tedersoo L, Ryberg M, Kristiansson E, Hartmann M, Unterseher M, Porter TM, Bengtsson-Palme J, Walker DM, de Sousa F, Gamper HA, Larsson E, Larsson K-H, Kõljalg U, Edgar RC, Abarenkov K. 2015. A Comprehensive, Automatically Updated Fungal ITS Sequence Dataset for Reference-Based Chimera Control in Environmental Sequencing Efforts. Microbes Environ 30:145–150.

65.   Caporaso JG, Kuczynski J, Stombaugh J, Bittinger K, Bushman FD, Costello EK, Fierer N, Peña AG, Goodrich JK, Gordon JI, Huttley GA, Kelley ST, Knights D, Koenig JE, Ley RE, Lozupone CA, McDonald D, Muegge BD, Pirrung M, Reeder J, Sevinsky JR, Turnbaugh PJ, Walters WA, Widmann J, Yatsunenko T, Zaneveld J, Knight R. 2010. QIIME allows analysis of high-throughput community sequencing data. Nat Methods 7:335–336.

66.   Team RC. 2013. R: A language and environment for statistical computing. R Foundation for Statistical Computing. Vienna.

CHAPTER 4 – Longitudinal study of the psoriasis-associated skin microbiome

during therapy with ustekinumab

The contents of this chapter are being prepared for submission as:

4.1 Abstract

Psoriasis is a chronic autoimmune disease primarily affecting the skin and joints, but may have systemic inflammatory consequences. The worldwide prevalence of psoriasis may be as high as 3%, though this varies by geography and ethnicity. The etiology of psoriasis is currently unknown, but recent studies suggest that the microbiota of the skin may be involved. Despite this, our understanding of the role of the cutaneous microbiota in psoriasis is lacking. Previous studies have suggested that psoriatic lesions harbor a distinct microbiome compared to non-lesion skin, however, these studies are limited by small sample size. Moreover, only one study has provided longitudinal data. Here we present the results of a longitudinal study of the skin microbiome of psoriasis and its response to ustekinumab therapy with 112 weeks of follow-up. We sampled the microbiota of 114 subjects at six body sites, including the arm, axilla, buttock, leg, scalp, and trunk, at contralateral lesion and non-lesion sites. Differences detected between lesion and non-lesion skin at baseline, were mild and body-site specific. After 28 weeks of ustekinumab therapy, specific taxonomic differences between lesion and non-lesion skin were no longer detectable. This was accompanied by a marked increase in sample variance, paradoxically resulting in increased dissimilarity between lesion and non-lesion skin. In addition, ustekinumab therapy induced moderate shifts in community structure, including increases in atypical skin bacteria such

as *Propionibacterium* species, which was shared by multiple body sites regardless of lesion status. After week 28, a subset of subjects were deprived therapy until recurrence of their lesion, after which they received a customized dosing frequency ranging from 12 to 24 weeks. After 112 weeks of follow-up, we noted no differences of the microbiome between subjects receiving normal or tailored dosing frequencies. Our findings suggest that the effect of psoriasis lesions is perhaps secondary to alterations in community immunity on the cutaneous microbiome. Together our results confirm findings from previous studies, but also expand upon and provide nuance to our understanding of the skin microbiota in psoriasis.

4.2 Background

Psoriasis vulgaris ("plaque" psoriasis) is a chronic, immune-mediated disease primarily affecting the skin and joints, though an appreciation of its systemic effects is growing. Psoriasis lesions are classically described as well-demarcated, erythematous plaques covered with a silver scale, however, the severity and distribution of the plaques varies greatly (Nestle et al. 2009). The global prevalence of psoriasis is between 2% and 3% (Perera et al. 2012), though it varies globally, largely as a function of ethnicity and latitude, with higher rates in those of European ancestry and northern latitudes (Parisi et al. 2013). The exact mechanism underlying the pathogenesis of psoriasis remains unclear, though most models incorporate aberrant T cell and keratinocyte responses in addition to a component of genetic susceptibility. Specifically, there is a growing appreciation of the role of the innate immune system in psoriasis pathogenesis, as inflammatory cytokines and cells associated with innate immunity are more prominent in psoriasis (Sweeney et al. 2011).

Because the innate immune system is the first line of defense against invading pathogens, many have questioned whether there is a microbial component contributing to the pathogenesis of psoriasis (Fry et al. 2013). There is a long-standing association between recent Group B Streptococcal infections and exacerbations of psoriasis generally and in particular guttate psoriasis subtype (Telfer et al. 1992; Leung et al. 1995; McFadden et al. 2009), however, anti-streptococcal treatment does not seem to modify disease (Owen et al. 2000). The specific association with *streptococcal* species led to the hypothesis that psoriasis may be an inappropriate reaction to other bacteria colonizing the skin or even entire communities.

Inflammatory bowel disease (IBD; ulcerative colitis and Crohn's disease) is also immune-mediated and clearly associated with microbial dysbiosis in the gut (Kostic et al. 2014). Interestingly, the incidence of psoriasis is nearly five times higher in patients with Crohn's disease and their immediate family (Lee et al. 1990), suggesting a systemic pathological commonality. Comparing the genetics of psoriasis and IBD also reveals recurring themes, implicating a multitude genes associated with the immune system, specifically the Th1 and Th17 axes (Lees et al. 2011). Because clues to the pathogenesis of disease are often revealed in other diseases that similarly behave or overlap epidemiologically, we hypothesize that understanding the skin microbiota of patients with psoriasis is critical to understanding its underlying pathogenesis.

Our understanding of the skin microbiota in psoriasis is in its infancy. Previous studies have consistently identified differences between healthy control skin and psoriatic plaques; however, the specific differences identified have not always been consistent. Moreover, these early studies varied in sample type and sequencing methodology(Gao et al. 2008; Fahlén et al.

2012; Alekseyenko et al. 2013). Notwithstanding these differences, some trends have emerged. Compared to healthy skin, psoriasis lesions trend towards lower Actinobacteria and *Propionibacterium* levels (Gao et al. 2008; Fahlén et al. 2012). A later study by Alekseyenko *et al* also found decreased microbial diversity, decreases in the aggregate composition of common skin commensals such as *Corynebacterium, Propionibacterium, Streptococcus,* and *Staphylococcus,* and increased sample variance in psoriatic subjects versus healthy controls (Alekseyenko et al. 2013). Interestingly, even the unaffected skin of psoriasis subjects is qualitatively different from healthy skin, though less so than lesion skin, as demonstrated by the ability of machine learning algorithms to accurately classify skin microbiome samples (Statnikov et al. 2013).

In the present study, we address several important limitations of previous studies, which have largely aggregated samples from various anatomical skin sites, ignoring the microenvironment specificity of the skin microbiome (Grice et al. 2009) and potential for site-specific trends. In addition, little is known of the longitudinal dynamics of the skin microbiota in response to systemic therapy. Alekseyenko *et al* followed 17 subjects for 36 weeks of treatment, but did not detect any significant changes from baseline (Alekseyenko et al. 2013). However, subjects in this study received a variety of treatments, complicating direct comparisons, further compounded by the naturally high variance of the skin microbiota (Grice et al. 2009). Moreover, this and all previous ones were limited by small sample sizes, which limits the ability to detect subtle differences.

Here we present the results of a longitudinal study where 114 subjects received standardized therapy for their plaque psoriasis with up to 112 weeks of follow up. We present

evidence that confirms findings from previous studies, but also expands upon and provides nuance to our understanding of the skin microbiota in psoriasis. We reveal the body-site specific effects of psoriasis on the skin, with samples across 6 body sites for all subjects. We characterize the response of the skin microbiome to ustekinumab, a biologic therapy targeting IL-12 and IL-23, over 112 weeks of follow-up. Finally, we reveal the effect of lesion recurrence and "subject-tailored" dosing frequencies on the skin microbiota.

4.3 Results: Phase I – Response to Ustekinumab

4.3.1 Characterization of subject demographics and summary of study design

114 subjects with psoriasis vulgaris ("plaque" psoriasis) were enrolled into a sub-study to examine skin microbiome changes with ustekinumab treatment. The sub-study was part of a longitudinal study to explore alternative dosing regimens for ustekinumab treatment. The study is divided into two phases (**Fig 1**, see Methods: *Study Design*). In Phase I, subjects received 28 weeks of standardized treatment with ustekinumab. In Phase II, after 28 weeks of standardized therapy, subjects achieving a therapeutic response (PGA < 2) were randomized to either a standard maintenance regimen of weight-based dosing every 12 weeks (Group 1) or a "subject tailored" off-label dosage regimen (Group 2) (**Fig S1 and S2**). The results of the randomization process are summarized in **Table 1**. Twenty-five subjects failed to achieve a therapeutic response to therapy and were dropped from the study for Phase II analysis. Those that did not achieve PGA < 2 had significantly higher psoriasis severity scores at enrollment and baseline sampling of their microbiota, as measured by the PASI metric and the proportion of body surface area (BSA) affected. Additionally, a greater proportion of those subjects randomized (Groups 1 and 2) were white when compared to the non-randomized group (**Table 1**).

111

4.3.2 Skin microbiome differences between lesion and non-lesion skin are mild and site specific.

We investigated the effect of psoriatic plaques on the composition of the skin microbiota at baseline for each of six body sites including the arm, axilla, buttock, leg, scalp, and trunk. These sites were selected for their predilection for lesions in psoriasis vulgaris. Furthermore, since it has previously been demonstrated that the skin microbiome drastically differs by body sites (REF), we performed all analyses in a site-specific manner, comparing plaque microbiota to that found on the contralateral unaffected site of the same subject ("control"). For the purpose of these analyses, Group 1, Group 2, and non-randomized subjects were included. We first compared relative abundance of taxa at the species level or the highest level of taxonomic classification achieved. Overall, clear and plaque sites were remarkably similar, though some body-site specific differences were detected (**Fig 2A**). In leg lesions, we detected decreases in the relative abundances of both Caulobacteraceae and *Corynebacterium* as compared to control leg sites ($P < 0.05$). In scalp lesions, we found an increase in *Bacilli* and decrease in *Propionibacterium acnes* relative abundance ($P < 0.05$) compared to control sites. At the phylum level, the leg, scalp, and trunk had higher levels of Actinobacteria in the lesions, while Firmicutes was significantly lower in the scalp and trunk lesions ($P < 0.05$) compared to their respective unaffected control sites.

We also identified body-site specific differences in microbial diversity between psoriatic lesions and non-affected skin (**Fig 2B**). The buttock, scalp, and trunk all exhibited increased OTU richness in the lesion skin ($P < 0.05$) while the scalp and trunk also had higher Shannon diversity levels in lesion skin, indicating greater evenness in the microbiota ($P < 0.05$). The psoriatic lesions of the trunk had higher levels of phylogenetic diversity than the normal skin ($P < 0.05$).

112

The trunk demonstrated the most consistent results with all three diversity metrics indicating that lesion sites were more diverse than control non-lesion sites.

Though we detected differences between the lesion and non-lesion skin at certain body sites, we wondered if there were less obvious patterns differentiating the two. We implemented a machine-learning approach to determine whether more subtle patterns of variation in the skin microbiome distinguish lesion from non-lesion sites at the baseline visit. For each body site, a random forest model was trained to identify psoriatic-lesion samples using exclusively OTU relative abundances. The models' accuracy ranged from 60.5-87.8%. In the case of the arm, buttock, and trunk, the classification accuracy was significantly better than chance (**Table 2**). Attempts to accurately classify lesion and non-lesion skin failed at subsequent time points in the study, indicating that differences between lesion and unaffected skin were strongest at baseline prior to treatment. The classification capacities of our models are similar to or in some cases surpasses what has been reported in previous studies (Statnikov et al. 2013). This is likely due to the increased sample size and site specificity of the training data.

4.3.3 Lesion and non-lesion skin microbiota respond similarly to ustekinumab therapy

We next investigated how the microbiota of lesion and non-lesion sites changed as a result of the systemic therapy with ustekinumab. We compared the relative abundances of the major taxa over time at each body site, analyzing lesion and non-lesion control sites separately. We detected significant changes in 11 major taxa in at least one body site (Kruskal-Wallis test; $P < 0.05$, FDR adjusted), the majority of which were shared across more than one body site (**Fig 3A**). Relative levels of *Agrobacterium,* Bradyrhizobiaceae, Caulobacteraceae, and *Pseudomonas*,

exhibited increases in their relative abundance in at least five of the six body sites (**Fig 3B**). *Staphylococcus* and *S. epidermidis* displayed slight decreases in four and five body sites, respectively. *Acinetobacter*, *Bacilli*, *Gemellales*, *Peptoniphilus,* and *P. acnes* demonstrated more body-site specific patterns. The lesion and non-lesion sites experienced similar changes, sharing 22 of the 41 total findings of differential relative abundance. Surprisingly, there were more changes in bacterial taxa in the non-lesion sites than the lesion sites, 14 and 5 respectively (Fig 3B).

Because the control non-lesion sites experienced similar if not greater changes in specific bacterial taxa than lesion sites with treatment, we further investigated how much each site changed respective to its baseline microbiome. We accomplished this by calculating the weighted UniFrac (wUF) distances between baseline samples and samples collected at subsequent study visits. The wUF is a metric used to assess similarity between samples, which incorporates both the abundance and phylogenetic relationships of microbial communities in the calculation (Lozupone et al. 2010). Values of the wUF metric range from 0 to 1, with a score of 0 indicating complete dissimilarity between the samples and a score of 1 indicating complete similarity of the samples being compared. As expected, all body sites exhibited significant dissimilarity from their baseline sample, which ranged from 0.24-0.39 at week 4 and 0.29-0.45 at week 28 (**Fig. 4**). The leg and trunk both exhibited significantly higher rates of change in the lesion sites for the week 4 and week 28 time points ($P < 0.05$). Of the body sites, scalp remained the most stable in both lesion and unaffected control sites. This may be a reflection of the highly sebaceous and haired microenvironment exerting selective pressure on the microbial communities.

4.3.4 Microbiota of lesion and non-lesion skin diverges with treatment

We next evaluated whether differences between lesion and non-lesion skin dissipated with ustekinumab therapy. We first tested the persistence of the taxa that were differentially abundant at baseline (identified above). The baseline differences were no longer detectable by week 28, however, different taxa were identified at later time points that differed in lesion and non-lesion skin (**Fig. 3C**). For the scalp, there were higher levels of *Finegoldia*, *Gemellales*, *Staphylococcus*, and *S. epidermidis* in lesion compared to non-lesion skin at week 4. Lesions in the arm had higher levels of *S. epidermidis* and lower levels of *Pseudomonas* at week 28. The trunk demonstrated higher levels of *Streptococcus* in lesion skin at week 28. Moreover, there were no detectable differences in microbial diversity by week 28, with the exception of the trunk where the lesion sites were more diverse than the non-lesion sites ($P < 0.05$). This led us to conclude that lesion and non-lesion sites were becoming more similar with treatment.

We then evaluated whether the microbial communities from lesion and non-lesion skin had indeed converged with ustekinumab treatment. We used the weighted UniFrac (wUF) dissimilarity metric to generate pairwise-distances between lesion and non-lesion samples. Paradoxically, all body sites exhibited similar trends towards divergence as treatment progresses, with the exception of the scalp (**Fig 5**). This trend was significant in the case of the arm, buttock, and leg ($P < 0.05$). This finding appeared to directly contradict our previous results above. However, these are not mutually exclusive findings as a simultaneous increase in community variance and a resolution of differential selective pressures would yield similar results. The scalp proved to be the exception to general trend, showing significantly less divergence between lesion and non-lesion skin than the arm, buttock, and trunk sites ($P < 0.05$). As discussed before, this

may be due to the presence of hair and sebum on the scalp exerting stronger selective pressures on the microbiota than the effect of lesion or treatment.

4.3.5 Greater heterogeneity within psoriatic lesions than non-lesion skin

We hypothesized that psoriasis lesions may disrupt mechanisms maintaining body-site specific microenvironments, such as sebum or sweat production. To test this, we assessed inter-subject heterogeneity of lesion and non-lesion skin for each body site. We calculated the wUF distance between samples from different subjects at the same body site. At the baseline visit, we found that there was greater heterogeneity in lesion skin compared to non-lesion skin across all body sites except the axilla ($P < 0.05$, **Fig 6A**). With the exception of the arm, this pattern was maintained until week 28, though the magnitude of the difference diminished likely as a result of lesion improvement. Interestingly, as subjects' treatment continues, intra-group heterogeneity continues to increase in all body sites, again indicating that ustekinumab treatment affects the skin microbiota systemically.

We next investigated whether body site niches became more distinct when compared to other body sites. We calculated the mean distance between body sites per subject via the wUF, as a measure of body site dispersion. At all time points, the non-lesion sites exhibited greater dispersion than the lesion sites ($P < 0.05$), though this was not significant during the baseline visit (**Fig. 6B**). However, both lesion and non-lesion body sites became more distinct with treatment, perhaps an indication that psoriasis impacts skin in ways that are subtler than plaques development. Interestingly, the lesion and non-lesion sites did not converge with therapy, possibly suggesting that the prior presence of a plaque has lasting effects. Together, these results suggest that psoriasis lesions diminish the distinctiveness of body site niches.

116

4.4 Results: Phase II – Duration of Ustekinumab Response

4.4.1 The skin microbiome is not predictive of the duration of therapeutic response to ustekinumab

We assessed whether the skin microbiome was indicative of subjects' duration of response to ustekinumab. To do this, we compared multiple features of the skin microbiome between subjects with different therapeutic response durations (12, 16, 20, and 24 weeks) during the randomization visit (week 28). In general, there were no significant differences between these groups in taxonomic composition, community diversity, or similarities between lesion and non-lesion sites. The exception was the non-lesion scalp, which exhibited higher levels of Shannon diversity and OTU richness between the 16-week group and the 20-week groups for non-lesion sites at baseline (data not shown). For the lesion sites, the scalp showed higher levels of Shannon diversity between the 16-week group and the 24-week group during the 28-week time point. However, it is unclear whether this is associated with the underlying biology or a result of noise in a smaller sample set.

We then applied our machine learning approach, as before, to detect more subtle patterns in the microbial composition. We focused on the extremes of the possible therapeutic durations, 12 and 24 weeks. We generated multiple models with three different classification tasks: 1) 12-week group v. the rest, 2) 24-week group v. the rest, and 3) 12-week v. 24-week groups. This method also failed to significantly distinguish the samples in all cases (data not shown). It should be noted that this analysis is limited by our sample size, and true patterns may yet be found with larger data sets.

4.4.2 Recurrent lesions do not resemble original lesions

For subjects randomized to Group 2, the 28-week dose was withheld until their PGA score reached or exceeded 2. This presented us an opportunity to determine if the skin microbiota would return to their baseline state with recurrence of disease. We calculated the wUF distances between the baseline visit (week 0) and both week-28 and recurrence visits. We did not detect any differences between the two time points (**Fig 7**), nor did we find any difference between the lesion and non-lesion skin. This may be further evidence of the non-specific effects of psoriasis lesions on the skin microbiota. Alternatively, ustekinumab may have more subtle effects on the skin microbiota than the formation of skin lesions.

4.4.3 No difference between standard and tailored dosing on effect of skin microbiome

A final sample was collected at week 112, at which point subjects had been on their dosing regimen for at least 70 weeks. We investigated whether different dosing regimens would impact the skin microbiota. We first compared the taxonomic composition of each group for both lesion and non-lesion skin sites. There were no differences detected between the study groups, and this was true of both lesion and non-lesion sites. We also did not find any differences in microbial diversity as measured by OTU richness, Shannon diversity, or phylogenetic diversity. We then used the wUF distances to examine associations between the skin microbiota and their respective treatment group and lesion status (**Fig. 8**). We tested for non-random clustering in these groups via body-site specific ADONIS models, which incorporated terms for lesion status and treatment group. We did not detect any differences for either term in any body site. These results suggest that the dosing regimen does not significantly affect the composition or diversity of microbial communities on the skin.

118

4.5 Discussion

One of the challenges of the presented study is its sheer scale. Our data set includes samples from 114 subjects, five time points, and up to 12 sites per patient per time point, yielding over 4,700 possible samples. We endeavored to provide a comprehensive analysis of the skin microbiome in psoriatic patients, how it evolves with treatment, and how it responds to treatment withdrawal in a body-site specific manner. We built on the foundational work of previous reports and attempted to expand upon and contribute nuance to our understanding of the microbiome and its interactions with psoriasis.

We found that psoriatic lesions exhibited a modified skin microbiome at the baseline study visit, before treatment had commenced. In line with previous studies, the effect of psoriasis lesions on the microbial composition and structure was relatively minor. Even so, the changes identified were specific to the body site, with no bacterial taxa being differentially abundant across more than one body site. Previous work has not commented on differences between body sites. The work presented here represents a significant advancement in our understanding of the psoriasis microbiome and importantly, should inform future study designs.

Though we did not have a healthy control group for comparison, we noted an overall lower abundance of *Propionibacterium* and *Staphylococcus* and increased *Corynebacterium* in lesional skin compared to the healthy skin microbiome reported in Meisel et al, a study from our group that employed the exact same sample collection, processing, and sequencing methodology (Meisel et al. 2016). Moreover, the combined proportion of rare taxa (<1% abundance) made up a

larger fraction of the psoriasis-associated microbial communities than is typical for skin samples. This suggests that the skin of patients with psoriasis is less hospitable to typical skin bacteria, instead being colonized or contaminated by generally rare environmental bacteria.

Unlike the skin disorder atopic dermatitis which has been studied extensively with regard to the skin microbiome and is consistently associated with large increases in *S. aureus* and parallel decreases in microbial diversity(Kong et al. 2012), there is little consensus on the specific bacterial taxa or diversity measures that define psoriasis. This could be a consequence of the diversity of sampling and sequencing methodologies implemented by the various studies, however, it could also be an artifact of the highly variable skin microbiota. Alternatively, psoriatic lesions may have minimal consequences on the microbiota of the skin. Because of the low bioburden of bacteria on human skin and the high exposure to environmental contaminants, the true effect of psoriasis on the skin microbiome may elude even a large study such as ours. A large focus of the work presented here is on exploring the level of heterogeneity in the skin microbiome of psoriasis, which furthers observations first made by Alekseyenko *et al* (Alekseyenko et al. 2013) in psoriasis and our own work on healthy skin (Grice et al. 2009). Lesion and non-lesion samples from the same subject were more similar to each other than either was to the same site in other subjects, which was true even after successful treatment. That is to say that unaffected skin has more in common with affected skin from the same subject than it has with unaffected skin in other subjects. This observation is simultaneously a possible explanation for the discrepancy of previous findings and a hurdle that future studies will need to grapple with when trying to delineate the effects of psoriasis versus the environment.

In the first phase of our study, we characterized the microbiome shifts secondary to a standardized treatment with ustekinumab. Only one study has explored the effect of systemic therapy for psoriasis in a longitudinal setting, though it was limited in sample size and surveyed a wide range of drugs including ustekinumab. The study presented here expands upon it in sample size, but also narrows the focus to ustekinumab. The focus on a single agent reduces the expected variance due to the administered drug; however, it does limit our ability to generalize our findings beyond ustekinumab.

The differences we identified at baseline had all dissipated by the 28th week of treatment, however, other differences emerged transiently and as before were body-site specific. When we quantified the divergence between lesion and non-lesion sites, we found, unexpectedly, that the treatment increased the level of divergence between the two sites. This was an unexpected finding, as one would expect lesion and non-lesion sites to converge as the plaques dissipated. Moreover, the mean variance between samples from the same body site increased with treatment, for both lesion and non-lesion skin. This argues for the existence of some "constraining" factor of psoriasis that limits the variance seen systemically, which is relieved by therapy. A possible explanation for the "constraining" factor is the increased production of antimicrobial peptides in psoriasis, which may provide a strong selective pressure on the microbiota limiting its composition to resistant bacteria. Alternatively, this may be due to behavioral differences, such as scratching or the application of lotions and ointments that may homogenize the skin microbiota within a subject.

We noted that as treatment progressed, the distinction between body sites increased, as measured by their mean wUF distance. Psoriatic lesions are known to impair certain homeostatic

121

functions of the skin, such as sweat production (Cormia and Kuykendall 1955; Johnson and Shuster 1969; Rittié et al. 2016). This may hamper the ability of the skin to create distinct microenvironments, leading to greater similarity between body sites. As treatment progresses and lesions regress, these structures will begin to function more normally and perhaps increase the specificity of body-site niches. It has been documented that these functions return to normal gradually, over the course of at least three months (Suskind 1954), which fits in with the timeline of our findings. Interestingly, lesion sites appeared to have a delayed response to the therapy, which suggests that psoriasis lesions may have lasting effects on the microbiota that are longer lived than deficiencies in sweat production.

A recurring theme was the similar trends detected in lesion and non-lesion skin, perhaps indicating that unaffected skin is not necessarily physiologically normal. When we assayed the longitudinal changes in microbiome composition, we noted that the vast majority of findings were shared between the two. One hypothesis to explain the similarity is the systemic effect of psoriasis. Alternatively, it may be that ustekinumab impacts the skin's microenvironments beyond the amelioration of psoriasis lesions. Regardless, it is interesting to note that ustekinumab treatment broadly affected the skin microbiota beyond lesion sites.

During the second phase of the trial, subjects in Group 2 had therapy withheld until the recurrence of their skin lesions. Interestingly, the recurrence was not associated with a return to the microbiota of the baseline time point. This could be due to the relatively low lesion-scores (PGA > 2) that were used for thresholds or the proximity to ustekinumab dosing. Alternatively, this may be further evidence of the lack of a psoriasis-specific microbiome. We also compared the microbial responses of subjects receiving the standard dosing frequency (Group 1) or the

"tailored" frequency (Group 2). Notably, the skin microbiome was not remarkably different between the groups. Subjects receiving the prolonged 24-week dosing frequency would necessarily have less active drug in their system than those receiving the 12-week frequency, yet we found no differences between these groups. This suggests that the effect of ustekinumab on the skin microbiota has more to do with modulation of their skin phenotype than off-target effects of the drug on the skin microbes.

4.6 Conclusions

Several attempts have been made to characterize the effects of psoriasis on the microbiota of the skin (Fahlén et al. 2012; Alekseyenko et al. 2013; Statnikov et al. 2013; Takemoto et al. 2014; Martin et al. 2015; Drago et al. 2016), though there is little consensus between these studies. Undoubtedly, some fraction of the inconsistency between studies is due to methodological differences in sample collection techniques (skin biopsies, scrapings, swabs), sequencing technologies (Sanger, 454-pyrosequencing, Illumina), and sample size. There is also considerable variation in which and how many body sites were sampled. Moreover, those studies that incorporated multiple body sites provided little if any analyses on the distinction between sites in their analysis. However, where all previous studies agree is that the effect they notice is small. Our results further this line of evidence and expand upon in several important ways.

We demonstrate that the impact on the skin microbiome is body-site specific. This is important in interpreting the results from previous papers that made no distinction, but also will be important to consider in future study designs. We also reaffirm previous studies' findings that the differences in the skin microbiome elicited by psoriasis lesions are small. However, we also

present evidence that may explain the difficulty in differentiating the two. We show that lesions have higher variance between subjects than non-lesion skin at baseline, confirming previous findings (Alekseyenko et al. 2013). This suggests that the effect of psoriatic lesions on the skin may be loosening normal selective pressures, rather than selecting for a different community type. Thus, special care must be applied when identifying differentially abundant bacterial species, so that they aren't confused with stochastic fluctuations.

The skin microbiome was broadly affected by the systemic administration of ustekinumab in both lesion and non-lesion skin. Moreover, lesion status was not associated with the extent of change experienced by the skin. This suggests that the effect of ustekinumab therapy is not limited to amelioration of plaques, but may alter the host-microbiota interactions across all skin sites. Ustekinumab is likely affecting the microbiota indirectly via modulation of inflammation rather than directly through off-target antibody interactions with the microbiota, as dosing frequency did not impact the composition of the skin microbiome.

Our study reaffirms and builds upon previous understandings of the skin microbiome and its interaction with psoriasis in several key areas. Our work is distinguished from previous studies in the scale, attention to body-site specific trends, standardized treatment, and the duration of follow-up. Our cohort nearly doubles the size of the previously largest study, and includes a comprehensive analysis of body-site specific patterns. In contrast to previous longitudinal studies with multiple treatments and only 36 weeks of follow-up, our subjects received the same treatment and were followed for up to 112 weeks. Our results should inform future study design and may have medically relevant implications for diagnostics and therapeutics involving the skin microbiome.

4.7 Methods

4.7.1 Study Design

Subjects enrolled in the study were free of treatment, systemic or topical, for at least 4 weeks (depending on drug class) prior to beginning the study. Subjects were instructed to withhold showering, bathing, and using swimming pools or using topical emollients, soaps, shampoos, deodorants or other treatments and products for a full 24 hours prior to sampling of skin microbiota.

Phase I: The first phase follows subjects' response to ustekinumab therapy over the course of 28 weeks. Subjects received ustekinumab doses at the baseline visit, after 4 weeks, and subsequently in 12-week intervals. Microbiome samples were taken at weeks 0, 4, and 28 at six body sites including the arm, axilla, buttock, leg, scalp, and trunk. Skin swabs were collected in an area clear of lesions and if possible a contralateral site affected by a plaque. At the 28-week time point, those achieving a therapeutic response (PGA < 2) were entered into the Phase II.

Phase II: During the second phase, one third of subjects were randomized to either Group 1 or Group 2. Group 1 received their next ustekinumab dose in accordance with the usual 12-week dosing regimen. Subjects in Group 2 received a "tailored therapy," which entailed withholding their next dose until their PGA score equaled or exceeded 2. We define the visit at which this occurs as the "recurrence" visit. PGA scores were assessed in 4-week intervals at weeks 32, 36, and 40, corresponding 16, 20, and 24 weeks since their last dose. Once a subject experienced a recurrence of their psoriasis, they received their next dose of ustekinumab and subsequent doses at the greatest 4-week interval for which they were asymptomatic (PGA < 2). Thus if a subject

125

developed lesions at week 34 (18 weeks since their last dose), they would be prescribed a 16-week regimen. If a subject's psoriasis did not recur by week 40, they were prescribed a 24-week regimen. Microbiome samples were collected at the "recurrence" time point. If a subject did not develop symptoms by week 40 (24 weeks since last dose), they were prescribed a 24-week dosing regimen. A final time point was collected at week-112 for all randomized subjects.

4.7.2 Sample Sequencing and Processing

Subjects were enrolled at one of 23 clinical sites. Skin swabs were collected at six body sites (arm, axilla, buttock, leg, scalp, and trunk) at both lesion-free sites and contralateral lesion sites, if available. Amplification of the 16S rRNA gene V1-V3 region was performed as previously described (Meisel et al. 2016). Resulting amplicons were sequenced using the Illumina MiSeq platform with paired-end 300 bp 'V3' chemistry. [Sequences were assembled, demultiplexed, and filtered for quality via super secret Qi pipeline] resulting in 109,132,204 sequences, which were then processed with QIIME 1.9.0 (Caporaso et al. 2010).

Sequences were size filtered to be between 460 and 600 nucleotides, which resulted in 88,780,568 reads and a median of 13,120 reads per sample. Because of the size of the data set, sequences were clustered into operational taxonomic units (OTU) with a modified open-reference OTU picking method. The reference set was generated by randomly subsampling 1% of sequences and performing *de novo* OTU picking using the UCLUST algorithm (Edgar 2010) with a 97% sequence-similarity threshold. For each OTU, the most common sequence was selected as its representative sequence. This representative set served as the reference for QIIME's default UCLUST, open-reference OTU picking script, parallel_pick_otus_uclust_ref.py. OTUs were assigned taxonomy using the RDP classifier (Cole et al. 2013) with the Greengenes 97%

126

sequence-similarity database (DeSantis et al. 2006). Singletons, OTUs with only one sequence, were removed. OTU corresponding to *Cyanobacteria*, *Delftia*, or were otherwise unclassifiable were removed as contaminants. The remaining 133,398 OTUs were kept for subsequent analyses.

Samples were then subsampled to 2,000 sequences per sample for estimation of alpha and beta diversity metrics. Microbial diversity was estimated using the following alpha diversity metrics: 1) number of observed OTUs (OTU richness); 2) Shannon diversity; and 3) Faith's phylogenetic diversity. Sample similarity was estimated using the weighted UniFrac (Lozupone et al. 2010) beta diversity metric.

4.7.3 Data Analysis

All analyses were performed using the R statistical package (R Core Team 2016). Comparisons of relative abundance, microbial diversity, or sample similarities were performed using Wilcoxon or Kruskal-Wallis tests where appropriate. *P*-value adjustments for multiple hypotheses testing were performed for the multiple taxonomic comparisons and testing between multiple time points by the false discovery rate method. Adjusted *P*-values less than 0.05 were considered significant. Calculation of NMDS coordinates and ADONIS testing for non-random clustering was performed via the vegan package (Oksanen et al.). We used the *randomForest* package (Liaw and Wiener 2002) in conjunction with *Caret* (Kuhn et al. 2016) to perform the machine learning analyses. The training set was created by randomly sampling 80% of subjects; the remaining 20% were reserved for testing. The number of OTUs was pruned by first removing near-zero variance and highly correlated (rho > 0.7) OTUs. We then performed recursive feature elimination (RFE) with subsets of OTU of 10, 25, 50, 100, and all OTUs combined to identify the ideal number of features to include. The random forest parameter *mtry* was tuned over five

iterations. Both RFE and parameter tuning was evaluated by optimizing the ROC score over 10-fold cross-validation repeated three times. Classification accuracy greater than chance was tested with a Bernoulli binomial test.
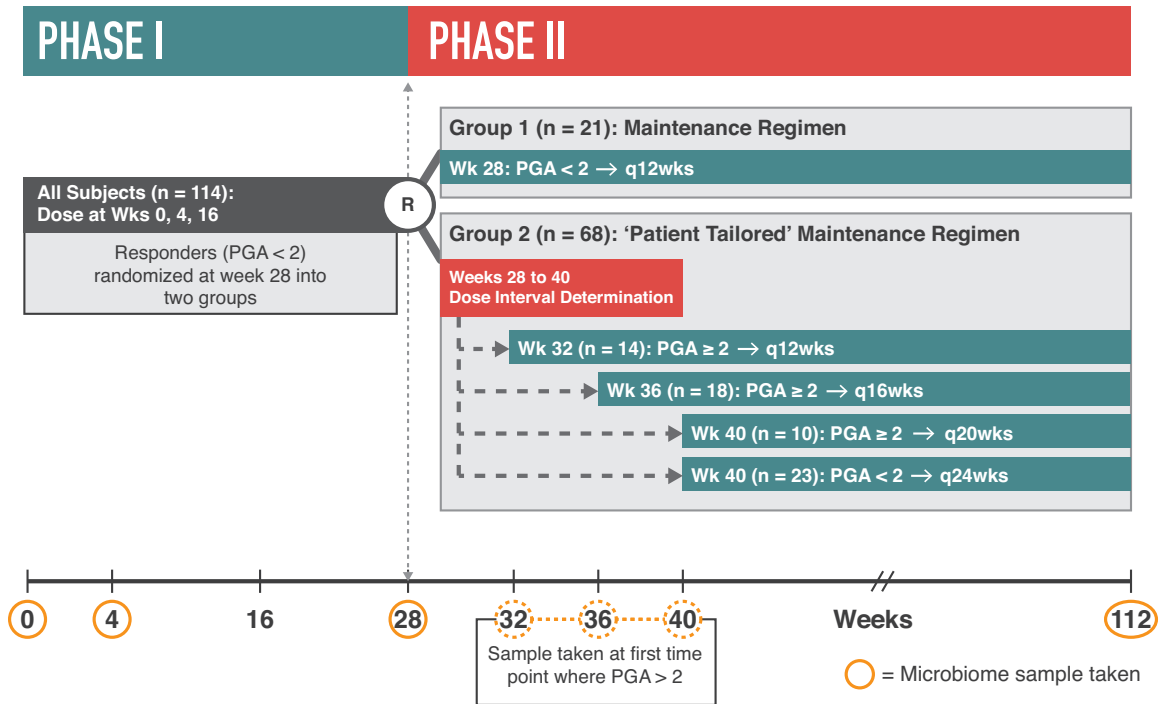
4.9 Figures

Figure 1

Clinical trial design diagram. 114 subjects were enrolled and received standard treatment with ustekinumab at weeks 0, 4, and 16. At week 28, subjects with therapeutic responses (PGA < 2) were randomized to one of two treatment groups. Group 1 received a dose at week 28 and subsequently every 12 weeks. Group 2 subjects did not receive their dose until their PGA score had reached or exceeded 2, measured in 4-week intervals. The longest 4-week interval for which subjects' PGA score was less than 2 defined their subsequent dosing frequency; this constituted their "tailored" regimen. Microbiome samples were taken at multiple time points, indicated by the orange circles on the time line.
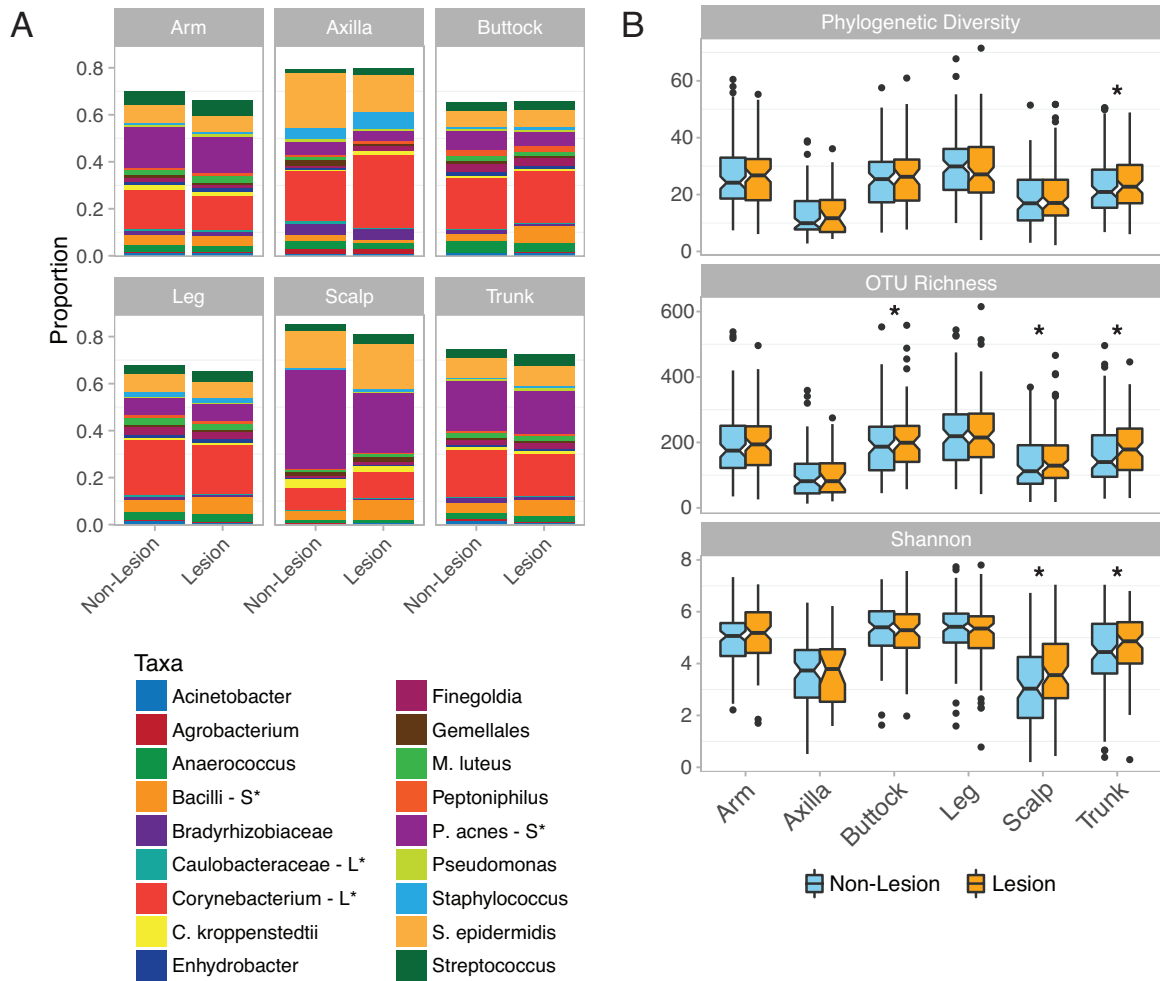
Figure 2

The effect of the psoriatic lesions on the skin microbiota at baseline. A) Stacked bar plot depicting the mean relative abundances of the most abundant taxa of both lesion and non-lesion skin by body site. Colored boxes indicate the mean proportion of specific taxa contributing at least 1% to all samples. Significant differences are denoted by body site labels in the legend – arm (Ar), axilla (Ax), buttock (B), leg (L), scalp (S), and trunk (T). B) Facetted boxplot of sample diversity for both lesion and non-lesion skin split by body site. Facets depict different

alpha diversity metrics including phylogenetic diversity (top), OTU richness (middle), and Shannon diversity (bottom). Significant findings are denoted by asterisk.
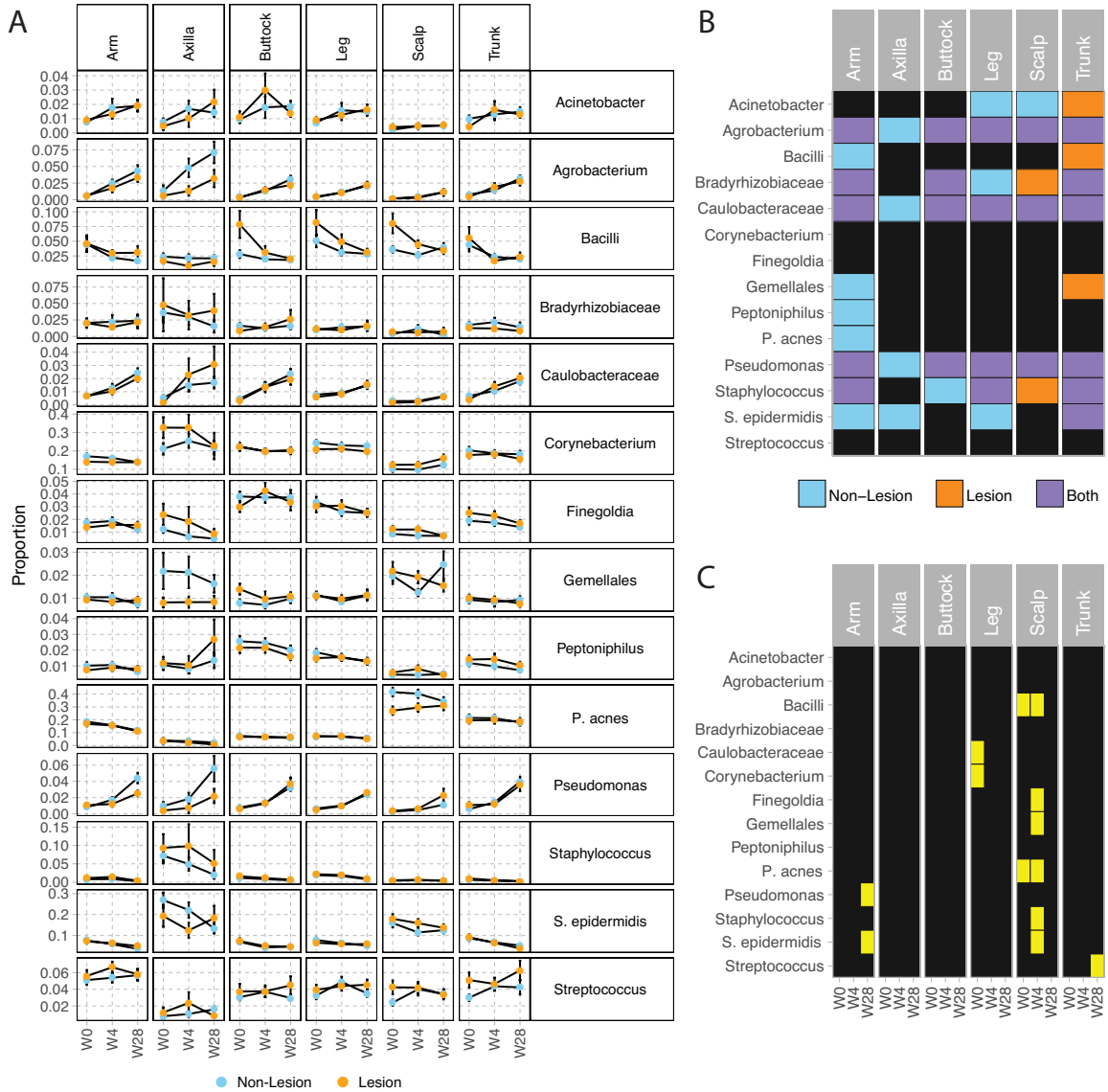

Figure 3

Longitudinal changes in taxonomic composition following ustekinumab treatment. (A) Plot shows the mean relative abundance for taxa identified as changing in at least one body site. Lesion and non-lesion skin are represented by orange and blue dots, respectively. Error bars

131

represent the standard error of the mean. (B) Results of Kruskal-Wallis test for longitudinal changes in relative abundance levels for each of the major taxa by body site. Colored tiles represent significant findings in the non-lesion site only (blue), lesion site only (orange), or both sites (purple). (C) Results of paired-Wilcoxon testing differences between lesion and non-lesion sites at week 0, 4, and 28. Yellow tiles represent significant findings.
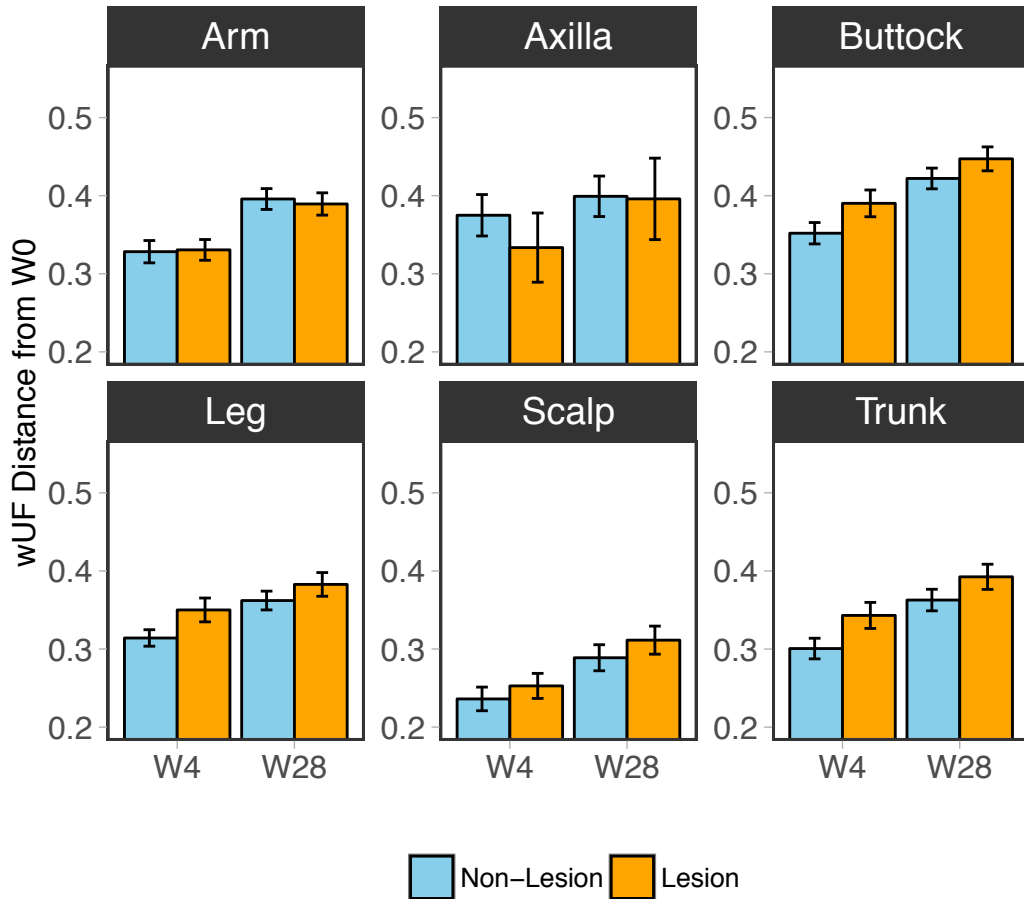
Figure 4

Lesion and non-lesion sites exhibit similar amounts of change due to ustekinumab therapy. Bar plot showing the mean weighted UniFrac distance between baseline (week 0) and subsequent visits (week 4 and 28). Data is split by body site. Non-lesion skin is represented by the blue bars, whereas lesion skin is represented by orange bars. Error bars depict the standard error of the mean.
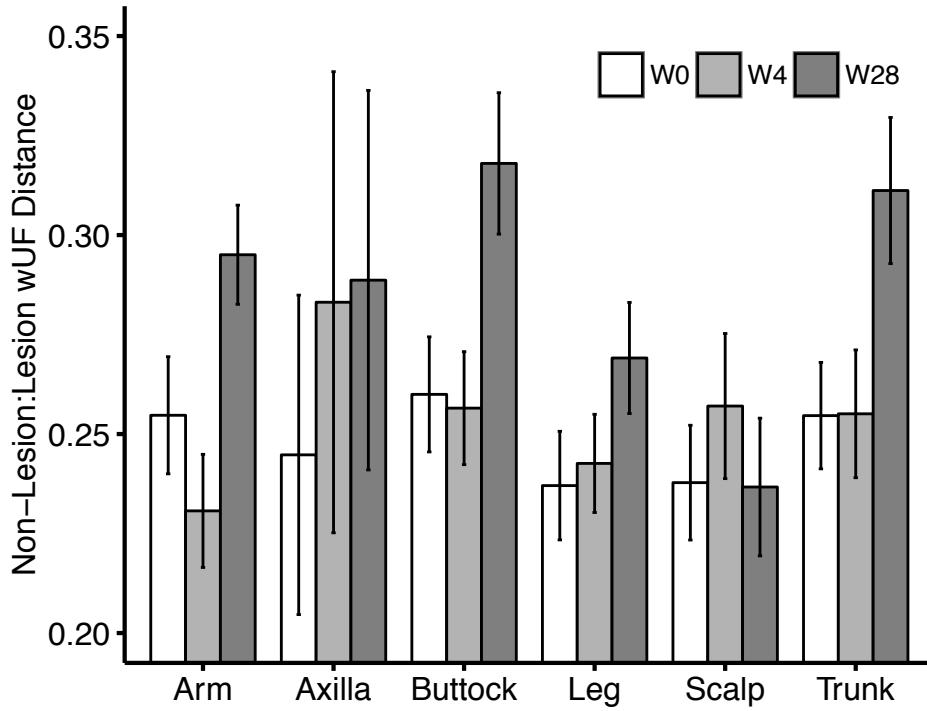
Figure 5

Divergence of lesion and non-lesion skin following treatment. Plot showing the mean weighted UniFrac distance between paired lesion and non-lesion skin samples at multiple time points. Error bars depict the standard error of the mean. Bar shading correspond to time points - week 0 (white), week 4 (gray), and week 28 (dark gray).

Figure 6

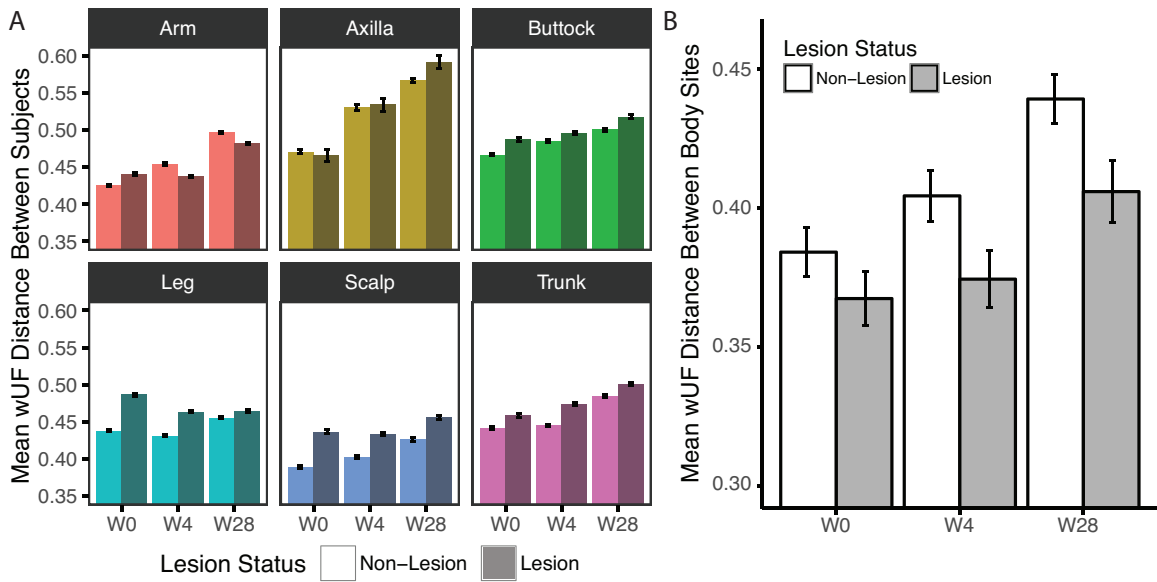Body sites variance and distinctness increases with ustekinumab therapy. (A) Weighted UniFrac distances between subjects by body site and lesion status. Bars are colored by body site and shaded by lesion status. (B) Body site dispersion as measured by the mean weighted UniFrac distances between body sites within subjects. Bars are shaded by lesion status. Error bars depict the standard error of the mean.
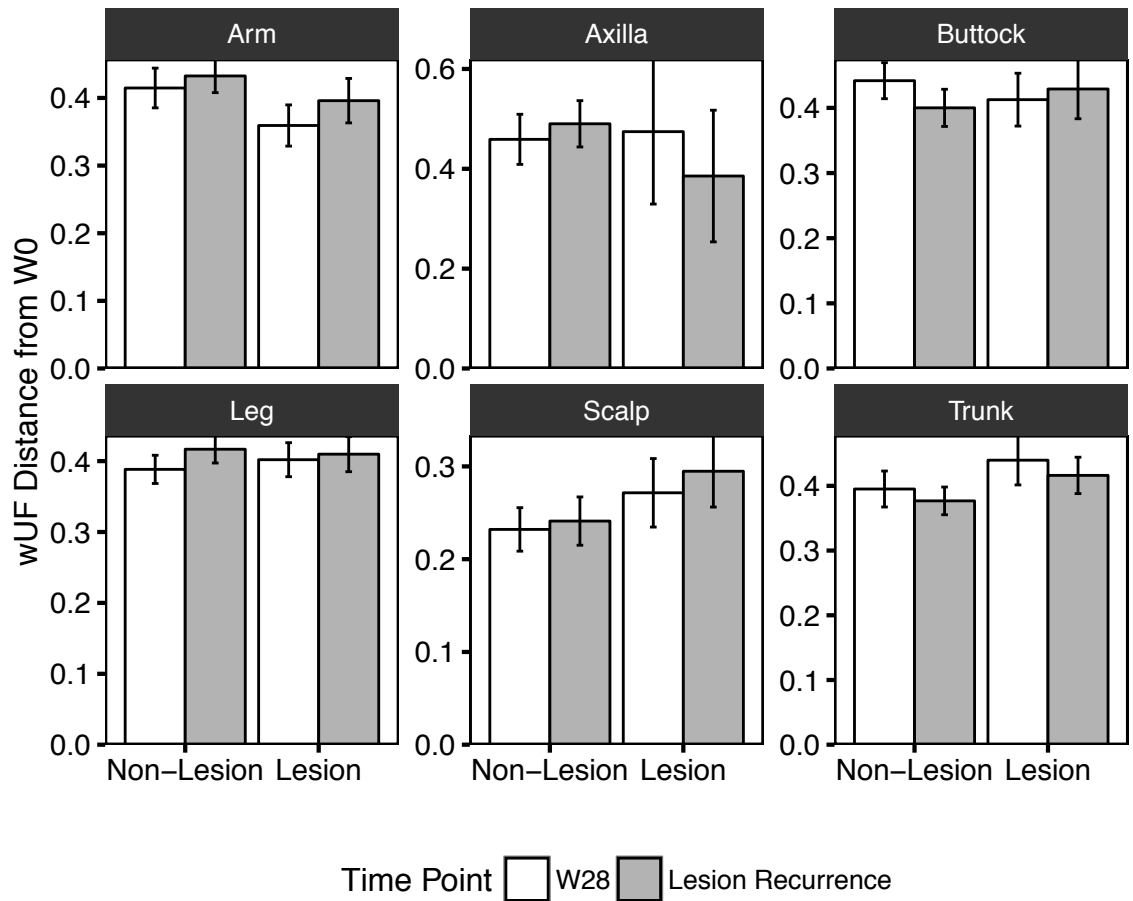
Figure 7

Recurrent lesions do not resemble prior lesions. Weighted UniFrac distances between the baseline samples and either remission (week 28) or recurrence samples. Distances were calculated for both lesion and non-lesion skin. Panels split data by body site. Greater distances indicate greater dissimilarity. Error bars depict the standard error of the mean.
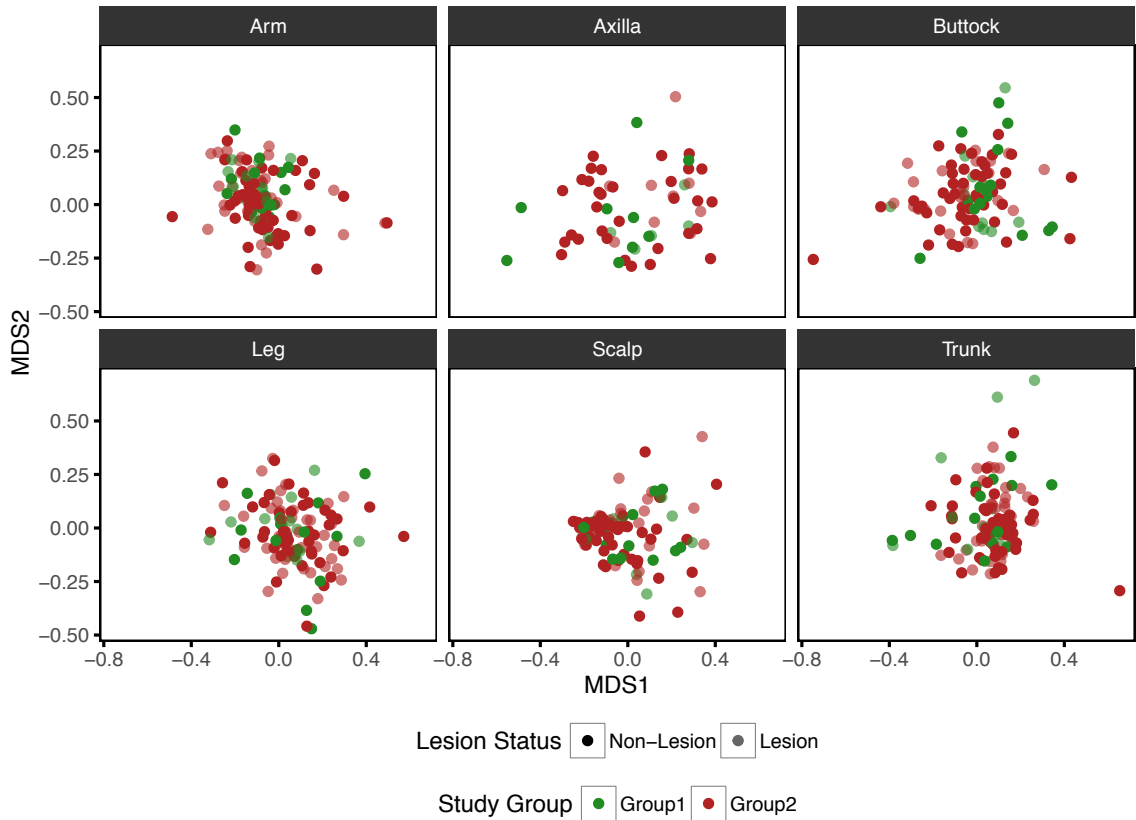
Figure 8

Ustekinumab dosing frequency does not impact the skin microbiota. NMDS plot of weighted

UniFrac distances for each body site at week 112. Samples are represented by points colored by

their treatment group (green – Group 1, red – Group 2) and shaded by lesion status (dark – non-

lesion, light - lesion). Points that are closer together are more similar.
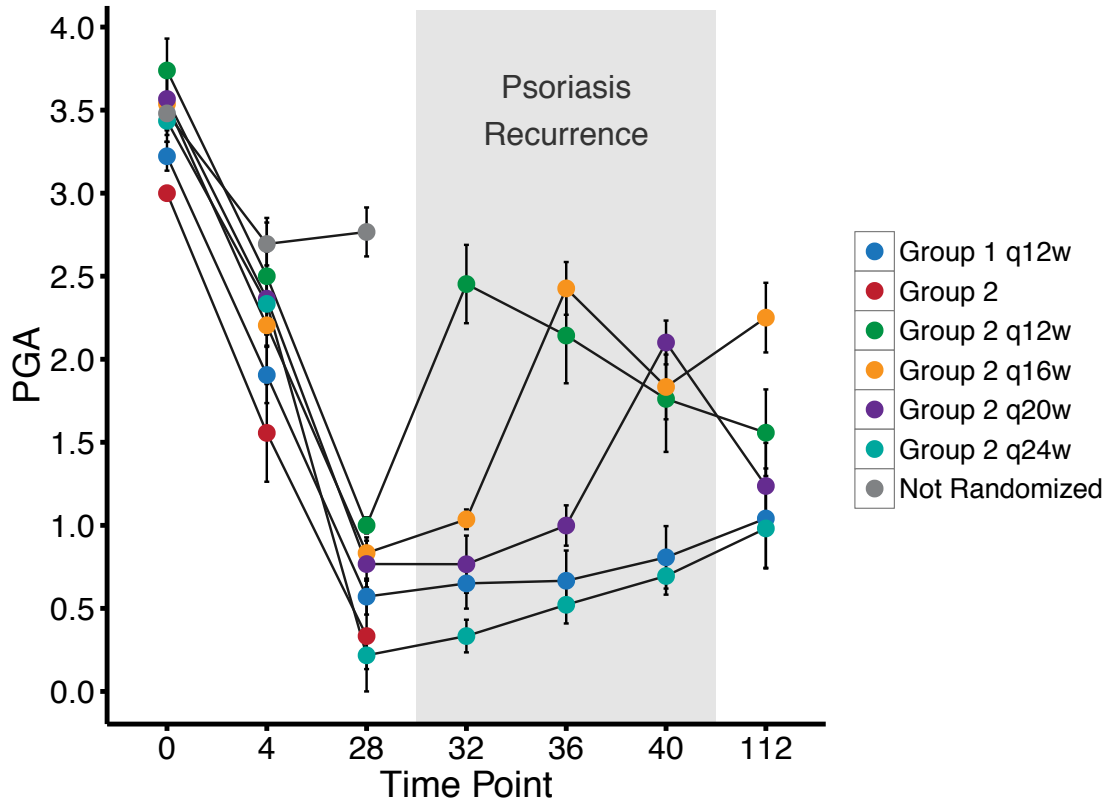
Figure S1

Line plot showing the mean PGA score for each treatment group. Subjects were randomized to group 1 or 2 at week 28. There were 3 subjects that were randomized to group 2, but subsequently left the study. Subjects not achieving a therapeutic response (PGA < 2) were not randomized. Shaded box shows the time points where subjects in group 2 were allowed to develop recurrent lesions. Error bars depict the standard error of the mean.

Figure S2

Subject randomization and dose frequency customization. Flow chart demonstrating how subjects

were randomized and what steps were taken when choosing the 'subject tailored' dosing regimen.

4.10 Tables

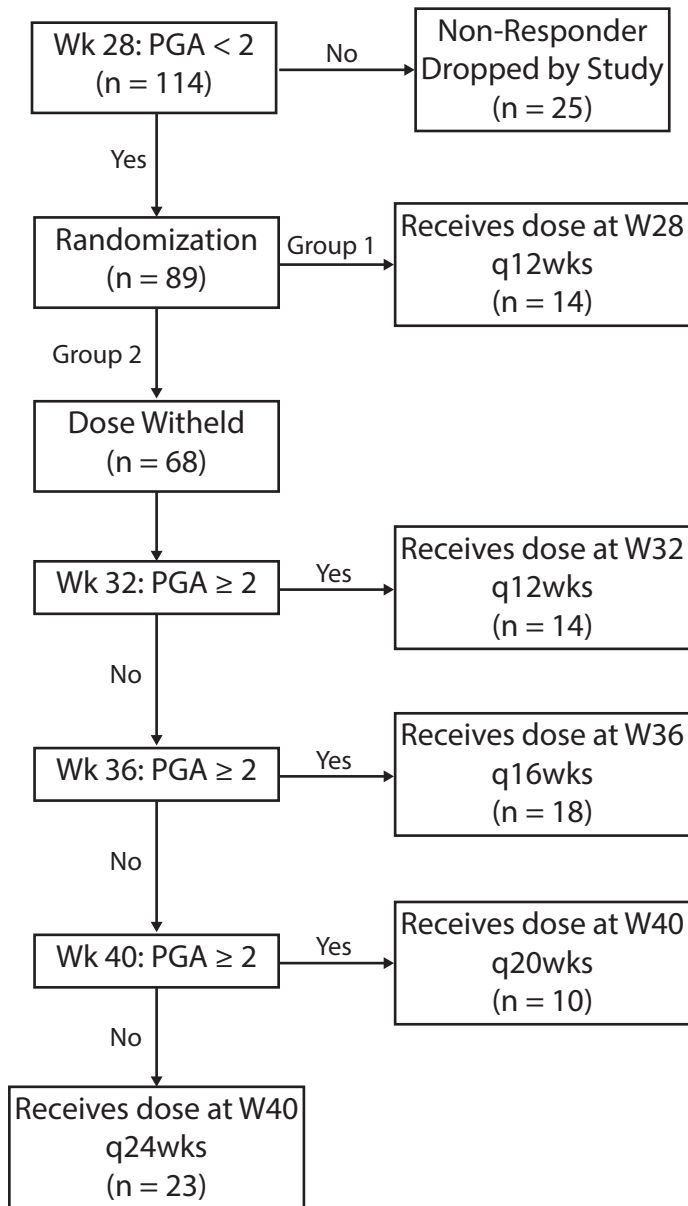|	Group 1	Group 2					Not Randomized
		Overall	*q12w*	*q16w*	*q20w*	*q24w*	
Subjects	21	68	14	18	10	23	25
Age	47.43	44.09	46.71	41.83	44.2	43.74	43.88
BMI	29.65	31.5	35.83	32.25	28.8	28.85	29.1
PGA	3.22	3.52	3.74	3.54	3.57	3.44	3.48
PASI	17.05	18.25	22.36	20.05	15.19	15.96	24.94
BSA	25.24	20.47	25.79	21.19	20.2	17.54	34.44
% Female	0.38	0.32	0.36	0.28	0.2	0.43	0.28
% White	0.81	0.96	0.93	0.94	1	0.96	0.64
% Hispanic	0.1	0.13	0.29	0.11	0.1	0.04	0.16
% Smoking	0.71	0.44	0.43	0.44	0.5	0.39	0.44
% Diabetic	0.1	0.1	0.14	0.11	0.1	0.09	0.04
Sun Exposure	1.86	1.99	1.79	1.94	2.1	1.96	1.96
Outdoor Exposure	2.33	2.29	2.29	2.22	2.2	2.3	2.2

Table 1

Characterization of subjects' demographics and results of randomization process

W0	Accuracy	AUC	p-value	Significance
Arm	87.8%	0.895	8.30E-07	***
Axilla	70.8%	0.547	4.20E-01	
Buttock	77.8%	0.773	2.69E-02	*
Leg	60.5%	0.675	1.43E-01	
Scalp	56.4%	0.693	4.38E-01	
Trunk	78.1%	0.868	3.79E-04	***

Table 2

Psoriatic lesion classification accuracy by body site at the baseline (wk 0) visit.

4.11 References

Alekseyenko AV, Perez-Perez GI, De Souza A, Strober B, Gao Z, Bihan M, et al. Community differentiation of the cutaneous microbiota in psoriasis. Microbiome. 2013;1(1):31.

Caporaso JG, Kuczynski J, Stombaugh J, Bittinger K, Bushman FD, Costello EK, et al. QIIME allows analysis of high-throughput community sequencing data. Nat Meth. 2010 May;7(5):335–6.

Cole JR, Wang Q, Fish JA, Chai B, McGarrell DM, Sun Y, et al. Ribosomal Database Project: data and tools for high throughput rRNA analysis. Nucleic Acids Research. Oxford University Press; 2013 Nov 27;42(D1):gkt1244–D642.

Cormia FE, Kuykendall V. Studies on Sweat Retention in Various Dermatoses. AMA Arch Derm. American Medical Association; 1955 Apr 1;71(4):425–35.

DeSantis TZ, Hugenholtz P, Larsen N. Greengenes, a chimera-checked 16S rRNA gene database and workbench compatible with ARB. Applied and …. 2006.

Drago L, De Grandi R, Altomare G, Pigatto P, Rossi O, Toscano M. Skin microbiota of first cousins affected by psoriasis and atopic dermatitis. Clin Mol Allergy. BioMed Central; 2016;14(1):2.

Edgar RC. Search and clustering orders of magnitude faster than BLAST. Bioinformatics. Oxford University Press; 2010 Oct 1;26(19):2460–1.

Fahlén A, Engstrand L, Baker BS, Powles A, Fry L. Comparison of bacterial microbiota in skin biopsies from normal and psoriatic skin. Arch Dermatol Res. Springer-Verlag;

142

2012;304(1):15–22.

Fry L, Baker BS, Powles AV, Fahlen A, Engstrand L. Is chronic plaque psoriasis triggered by microbiota in the skin? Br J Dermatol. 2013 Jul 8;169(1):47–52.

Gao Z, Tseng C-H, Strober BE, Pei Z, Blaser MJ. Substantial Alterations of the Cutaneous Bacterial Biota in Psoriatic Lesions. Ahmed N, editor. PLoS ONE. 2008 Jul 23;3(7):e2719.

Grice EA, Kong HH, Conlan S, Deming CB, Davis J, Young AC, et al. Topographical and Temporal Diversity of the Human Skin Microbiome. Science (New York, NY). 2009 May 28;324(5931):1190–2.

Johnson O, Shuster S. Eccrine sweating in psoriasis. Br J Dermatol. 1969.

Kong HH, Oh J, Deming C, Conlan S, Grice EA, Beatson MA, et al. Temporal shifts in the skin microbiome associated with disease flares and treatment in children with atopic dermatitis. Genome research. Cold Spring Harbor Lab; 2012 May;22(5):850–9.

Kostic AD, Xavier RJ, Gevers D. The Microbiome in Inflammatory Bowel Disease: Current Status and the Future Ahead. Gastroenterology. 2014 May;146(6):1489–99.

Kuhn M, Wing J, Weston S, Williams A, Keefer C, Engelhardt A, et al. caret: Classification and Regression Training [Internet]. 6 ed. 2016. Available from: https://CRAN.R-project.org/package=caret

Lee FI, Bellary SV, Francis C. Increased occurrence of psoriasis in patients with Crohn's disease and their relatives. American Journal of …. 1990.

Lees CW, Barrett JC, Parkes M, Satsangi J. New IBD genetics: common pathways with other diseases. Gut. BMJ Publishing Group Ltd and British Society of Gastroenterology; 2011 Dec;60(12):1739–53.

Leung DY, Travers JB, Giorno R, Norris DA, Skinner R, Aelion J, et al. Evidence for a streptococcal superantigen-driven process in acute guttate psoriasis. Journal of Clinical Investigation. American Society for Clinical Investigation; 1995 Nov 1;96(5):2106–12.

Liaw A, Wiener M. Classification and Regression by randomForest. R News [Internet]. 2002;2:18–22. Available from: http://CRAN.R-project.org/doc/Rnews/

Lozupone C, Lladser ME, Knights D, Stombaugh J, Knight R. UniFrac: an effective distance metric for microbial community comparison. The ISME Journal. 2010 Sep 9;5(2):169–72.

Martin R, Henley JB, Sarrazin P, Seite S. Skin Microbiome in Patients With Psoriasis Before and After Balneotherapy at the Thermal Care Center of La Roche-Posay. J Drugs Dermatol. 2015 Dec 1;14(12):1400–5.

McFadden JP, Baker BS, Powles AV, Fry L. Psoriasis and streptococci: the natural selection of psoriasis revisited. Br J Dermatol. Blackwell Publishing Ltd; 2009 May;160(5):929–37.

Meisel JS, Hannigan GD, Tyldsley AS, SanMiguel AJ, Hodkinson BP, Zheng Q, et al. Skin Microbiome Surveys Are Strongly Influenced by Experimental Design. J Invest Dermatol. 2016 May;136(5):947–56.

Nestle FO, Kaplan DH, Barker J. Psoriasis. N Engl J Med. 2009 Jul 30;361(5):496–509.

Oksanen J, Blanchet FG, Kindt R, Legendre P, Minchin PR, OHara RB, et al. vegan: Community

144

Ecology Package [Internet]. 2nd ed. Available from: https://CRAN.R-project.org/package=vegan

Owen CM, Chalmers RJ, O'Sullivan T, Griffiths CE. Antistreptococcal interventions for guttate and chronic plaque psoriasis. Cochrane Database Syst Rev. 2000;(2):CD001976.

Parisi R, Symmons DPM, Griffiths CEM, Ashcroft DM, the BO. Global Epidemiology of Psoriasis: A Systematic Review of Incidence and Prevalence. J Invest Dermatol. Elsevier Masson SAS; 2013 Jan 1;133(2):377–85.

Perera GK, Di Meglio P, Nestle FO. Psoriasis. Annu Rev Pathol Mech Dis. 2012 Feb 28;7(1):385–422.

R Core Team. R: A Language and Environment for Statistical Computing. Vienna, Austria; 2016. Available from: https://www.R-project.org

Rittié L, Tejasvi T, Harms PW, Xing X, Nair RP, Gudjonsson JE, et al. Sebaceous gland atrophy in psoriasis: An explanation for psoriatic alopecia? J Invest Dermatol. 2016 Jun 13.

Statnikov A, Alekseyenko AV, Li Z, Henaff M, Perez-Perez GI, Blaser MJ, et al. Microbiomic Signatures of Psoriasis: Feasibility and Methodology Comparison. Scientific reports. 2013 Sep 10;3.

Suskind RR. Eccrine function in psoriasis. J Invest Dermatol. 1954.

Sweeney CM, Tobin A-M, Kirby B. Innate immunity in the pathogenesis of psoriasis. Arch Dermatol Res. Springer-Verlag; 2011;303(10):691–705.

Takemoto A, Cho O, Morohoshi Y, Sugita T, Muto M. Molecular characterization of the skin

    fungal microbiome in patients with psoriasis. J Dermatol. 2014 Dec 15;42(2):166–70.

Telfer NR, Chalmers RJG, Whale K, Colman G. The Role of Streptococcal Infection in the

    Initiation of Guttate Psoriasis. Arch Dermatol. American Medical Association; 1992 Jan

    1;128(1):39–42.

5.1 Conclusions and Future Directions

The work presented in this thesis represents a significant advancement in our understanding of the longitudinal dynamics of the cutaneous microbiota when afflicted by disease. In our studies of chronic wounds, we demonstrate for the first time the intrinsically high levels of microbial flux and their relations to outcomes. Chapter 2 explored the bacterial component, revealing the inverse relationship between community stability and the rate of healing. We also characterize the effects of multiple classes of antibiotics on the bacterial communities colonizing the wound. In Chapter 3, we uncover the fungal contributions to wound healing, their associations with co-resident bacteria, and their ability to form inter-kingdom, cooperative biofilms. Chapter 4 presents the largest and longest longitudinal study of the psoriasis microbiome, revealing how the cutaneous microbiota respond to therapy and lesion recurrence. Together these studies expand upon the foundational work generated by cross-sectional studies and provide a foundation for future longitudinal analyses of the cutaneous microbiome.

We modeled the temporal dynamics of the diabetic foot ulcer (DFU) microbiota using discrete and continuous frameworks. The first approach presumed the presence of distinct bacterial community types, with the potential to direct the clinical course of the ulcer. This idea has been applied in many ecological analyses of microbial communities, and is an attractive approach for several reasons. Sample clustering dramatically reduces the variance and dimensionality of the data, making subsequent analyses more tractable. Clustering algorithms are agnostic to preconceived biases and are capable of detecting patterns often too subtle and complex for human observers. However, approaches to clustering differ in the importance

147

assigned to various community parameters, such as the weighting of sample parameters, ideal

cluster sizes, and calculations for sample inclusion. Clustering results may differ between

approaches, and it is often impossible to validate the results; however, these approaches can be of

great utility in isolating a signal in noisy data. This was the case in our study, where our Markov-

chain analysis revealed the positive association between frequent transitions and healing rates.

Moreover, wounds that became entrenched in community types dominated by *Stahylococcus*

aureus and *Streptococcus* were more likely to experience a negative outcome.

To validate our results, we applied mixed-effect modeling of community stability, which

provided greater resolution than the discrete transitions of our Markov-chain analysis. This

confirmed our findings and revealed an inverse relationship with community stability and healing

rates, which was apparent even after the first visit. Unsurprisingly, antibiotics led to increased

dynamism in the wound. Together these results suggest that a stagnant wound microbiota is

harmful to healing, and may reflect the failure of the wounds defenses to repel infection. This has

significant clinical applications, as DFU do not exhibit the traditional signs of infection, making

diagnosis of infection difficult. Thus, microbial dynamics may offer additional guidance for

clinicians managing chronic wounds.

The fungal communities of the wound may also reflect and contribute to the healing

outcomes of chronic wounds. The work presented here is the first to perform metataxonomic

methodologies to understanding these interactions. The DFU mycobiota was striking for its

interpersonal variation and paradoxically low intra-sample diversity. Moreover, the mycobiota

exhibited high turnover of its constituents visit-to-visit, though the wound was still more similar

to itself over time than to other individuals at the same time. The high level of variance

introduced significant challenges for the analysis and pattern detection. However, patterns emerged once taxa were categorized as either pathogen or allergen. Wounds dominated by pathogens were more likely to have high levels of necrotic tissue and have poor outcomes. We also demonstrated the viability of *Candida albicans* and *Citrobacter freudii*, isolated from a single wound, to form cooperative, inter-kingdom biofilms.

Our work on the chronic wound, from both the bacterial and fungal perspectives, has demonstrated that microbial dynamics can provide predictive power for stratifying patients at risk. These studies would be greatly augmented by the inclusion of metagenomic sequencing, which would reveal the functional capacity of the wound microbiota. The need for such studies is obviated when one considers the tremendous genetic heterogeneity even within members of the same species (Lapierre & Gogarten 2009). The prevalence of specific genes, such as those involved virulence or antibiotic resistance, may increase the predictive power of our models and yield biologically meaningful insight. To this end, we are actively pursing whole metagenome sequencing of the samples included in the presented studies.

Future studies should increase the frequency of sampling to provide greater temporal resolution to the observed phenomenon. We measured the wound microbiota at 2-week sampling intervals, a limitation introduced by the use of total contact casts for offloading therapy. For many body sites, microbial communities tend to maintain relatively stable community structure over time(Ding & Schloss 2014). In addition, microbes in chronic wounds form robust biofilms (James et al. 2008), shielding its members from external perturbations. However, our 2-week sampling frequency may be masking interesting shorter-term dynamics, as the majority of bacteria replicate

on the order of minutes to hours. This may be particularly true of the community responses to antibiotic perturbations.

Our work on the cutaneous microbiome represents the largest longitudinal study on the topic, both by number of subjects involved and the duration of follow-up. Similar to previous studies, we found psoriasis lesions to have mild consequences on the composition of the skin microbiota, however, this effect was body-site specific. One of the strengths of our study was the standardized medical intervention received by all subjects, which reduces the variance introduced by multiple therapies. We identified shifts in various taxa following therapy, but it is impossible to determine whether this is due to amelioration of the lesions or some other effect of ustekinumab. As in previous studies of subjects with primary immunodeficiencies, ustekinumab therapy appeared to make the skin more permissive of atypical skin bacteria, such as *Pseudomonas* species (Oh et al. 2013). In addition, the distinctiveness of body sites increased during the course of therapy, suggesting that the normal physiologic determinants of the skin microbiota were reestablishing themselves.

As before, our understanding of the interactions between the skin microbiota and psoriasis would be enhanced by the addition of metagenomic sequencing. Metagenomic studies have demonstrated that the functional composition of the microbiome is markedly more consistent than the taxonomic composition (Human Microbiome Project Consortium 2012), likely a consequence of the redundancy of genes. In psoriasis, there may be many bacteria capable of filling an ecological niche, opened up by the dysfunctional cutaneous immune system. Metagenomic profiling may also reveal specific metabolic pathways or biosynthetic gene clusters that are associated with the development of or severity of psoriatic lesions.

There is a shortage of statistical frameworks available for researchers to model the dynamics of microbial communities in longitudinal settings. Longitudinal microbiome studies are plagued by few time points and irregular sampling frequencies, making pattern detection difficult. Moreover, studies are often designed to capture the perturbation and recovery of the microbiota to some environmental insult, which often do not follow linear assumptions. This is even more of an issue when experiments are attempting to elucidate the effects of stochastic perturbations. To combat these issues, researchers will often analyze their time points as discrete categories, rather than use a true longitudinal model. Some of these issues may be remedied by the use of additive models, but require more time points than most studies have available.

Previous attempts have been made to combine regression techniques with generalized Lotka-Volterra equations (which model microbial dynamics as a function of competitive interactions) to model microbiota responses to external perturbations (Stein et al. 2013). This group went on to model the effects of stochastic antibiotic exposure on *Clostridium difficile* infection in patients hospitalized for cancer treatment to great success (Buffie et al. 2014). They identified specific bacterial species that reduced the risk of infection, due to metabolic pathways involved in modifying bile acids. Lotak-Voltera dynamics are exquisitely sensitive to initial conditions. Much like a double pendulum, the patterns appear random, though they obey specific rules. There is evidence to suggest that ecological dynamics operate in a non-linear or chaotic manner (Sugihara et al. 2012). This finding may lead to the inclusion of non-linear ecological modeling to the field of microbiome research. Indeed, approaches have been developed to allow the "stitching" together of short time-series to create the long timelines required for non-linear modeling (Hsieh et al. 2008). Such approaches will need to be modified to handle the high-

dimensionality and the compositional nature of microbiome data, but may represent an attractive solution to the challenges faced by those studying microbial dynamics.

5.2 References

Buffie, C.G. et al., 2014. Precision microbiome reconstitution restores bile acid mediated resistance to Clostridium difficile. *Nature*, 517(7533), pp.205–208.

Ding, T. & Schloss, P.D., 2014. Dynamics and associations of microbial community types across the human body. *Nature*, 509(7500), pp.357–360.

Hsieh, C.-H., Anderson, C. & Sugihara, G., 2008. Extending Nonlinear Analysis to Short Ecological Time Series. *The American naturalist*, 171(1), pp.71–80.

Human Microbiome Project Consortium, 2012. Structure, function and diversity of the healthy human microbiome. *Nature*, 486(7402), pp.207–214.

James, G.A. et al., 2008. Biofilms in chronic wounds. *Wound Repair and Regeneration*, 16(1), pp.37–44.

Lapierre, P. & Gogarten, J.P., 2009. Estimating the size of the bacterial pan-genome. *Trends in Genetics*, 25(3), pp.107–110.

Oh, J. et al., 2013. The altered landscape of the human skin microbiome in patients with primary immunodeficiencies. *Genome research*, 23(12), pp.2103–2114.

Stein, R.R. et al., 2013. Ecological Modeling from Time-Series Inference: Insight into Dynamics and Stability of Intestinal Microbiota C. von Mering, ed. *PLoS Computational Biology*,

9(12), p.e1003388.

Sugihara, G. et al., 2012. Detecting Causality in Complex Ecosystems. *Science (New York, N.Y.)*, 338(6106), pp.496–500.